



**HAL**  
open science

# Sub-optimal Energy Management Architecture for Intelligent Hybrid Electric Bus: Deterministic vs. Stochastic DP strategy in Urban Conditions

Rustem Abdrakhmanov

► **To cite this version:**

Rustem Abdrakhmanov. Sub-optimal Energy Management Architecture for Intelligent Hybrid Electric Bus: Deterministic vs. Stochastic DP strategy in Urban Conditions. Electronics. Université Clermont Auvergne [2017-2020], 2019. English. NNT : 2019CLFAC020 . tel-02363880

**HAL Id: tel-02363880**

**<https://theses.hal.science/tel-02363880>**

Submitted on 14 Nov 2019

**HAL** is a multi-disciplinary open access archive for the deposit and dissemination of scientific research documents, whether they are published or not. The documents may come from teaching and research institutions in France or abroad, or from public or private research centers.

L'archive ouverte pluridisciplinaire **HAL**, est destinée au dépôt et à la diffusion de documents scientifiques de niveau recherche, publiés ou non, émanant des établissements d'enseignement et de recherche français ou étrangers, des laboratoires publics ou privés.

UNIVERSITÉ CLERMONT AUVERGNE  
ÉCOLE DOCTORALE  
SCIENCES POUR L'INGÉNIEUR DE CLERMONT-FERRAND

# Thèse

Présentée par

**RUSTEM ABDRAKHMANOV**

Master Robotique

pour obtenir le grade de

**Docteur d'Université**

Spécialité : **Electronique et Systemes**

**Sub-optimal Energy Management Architecture for Intelligent Hybrid Electric  
Bus: Deterministic vs. Stochastic DP strategy in Urban Conditions**

Soutenue publiquement le 27 juin 2019 devant le Jury composé de :

YOUCEF MEZOUAR	Président	Professeur, Université Clermont Auvergne/Sigma
LYDIE NOUVELIERE	Rapporteur	Maître de conférences - HDR, Université d'Evry
BELKACEM OULD BOUAMAMA	Rapporteur	Professeur, Polytech Lille
OLIVIER SIMONIN	Examineur	Professeur, INSA de Lyon
LOUNIS ADOUANE	Directeur de thèse	Maître de conférences - HDR, Polytech Clermont-Ferrand
SAMUEL HIBON	Invité	Rolling Stock Energy Efficiency and Innovation Manager, ALSTOM, Saint-Ouen



# ACKNOWLEDGMENTS

I would like to thank Businova Project, funded by ADEME, for giving me this opportunity to carry out this PhD thesis at Institut Pascal, in the Modeling, Autonomy and Control in Complex system (MACCS) team of ISPR (ImageS, Perception systems and Robotics) group. Businova is an ambitious project that has the goal to bring sustainable solutions to the environmental issues in transportation systems.

I would like to thank my thesis committee: Mme Lydie Nouveliere and Mr Belkacem Ould Bouamama, Mr Olivier Simonin and Mr Samuel Hibon for generously accepting to review this document. Furthermore, I would like to thank Mr. Youcef Mezouar for cordially accepting to be the Chairman of the thesis committee. I wish to express my gratitude for these persons to offer their time, insightful comments and hard questions for this thesis.

I would like to thank my PhD supervisor, Lounis Adouane, for sharing his scientific skills with me, his patience and encouragement. His motivation and support taught me to dig profoundly the ideas, to never give up and believe in myself. He led me through the darkest moments of my PhD thesis by giving valuable pieces of advice, and through the brightest moments by learning to be grateful and learn lessons from any experience. Without him I would not have finished this PhD work.

I would like to thank Gautier Claisse, François de la Bourdonnay, Charles Phillippe and Charles-Antoine Noury for the friendship, support and inviting me to take a rest after a hard workday. My special gratitude goes to Nadir Ouddah, Ekhatib Kamal and Yassir Dahmane for their professionalism, work ethic and amicability.

I would love to express special gratitude to my family in Kazakhstan, especially my mother, who taught me to believe in my dreams and to be sure that I can be anything I want despite the initial conditions.

I would like to thank one of my best friends Vildamir Aimanov in Kazakhstan for being my best life advisor during all my PhD thesis. His patience, kindness to listen to me in the hardest times saved me from giving up many times.

Finally I would like to thank Clermont Ferrand city for I have met a lot of wonderful people here, which I knew during short times, but they have inevitably left their print in my heart. Some of them have influenced me at some extent.



# CONTENTS

<b>General introduction</b>	<b>3</b>
<b>1 Intelligent vehicles: overview</b>	<b>7</b>
1.1 Introduction	7
1.2 Energy and powertrain systems for intelligent vehicles	8
1.2.1 Conventional vehicles	8
1.2.2 Electric vehicles	9
1.2.3 Hybrid vehicles	11
1.2.3.1 Hybrid powertrain configuration	12
1.2.3.2 Degree of hybridization	13
1.3 ADAS for intelligent vehicles	15
1.3.1 Adaptive Cruise Control	17
1.3.2 Stop&Go	18
1.3.3 Collision avoidance	19
1.3.4 Eco-Driving support systems	19
1.4 Conclusion	22
<b>2 Energy Management in Hybrid Vehicles</b>	<b>23</b>
2.1 Modelling of hybrid vehicles	23
2.1.1 Bond Graph	23
2.1.2 Analytical modelling of Businova	24
2.1.2.1 Rolling resistance force	25
2.1.2.2 Aerodynamic drag	26
2.1.2.3 Gravity force	27
2.1.2.4 Powertrain tractive effort	27
2.1.2.5 Vehicle dynamics considering the inertia of the rotating parts of the power plant	29
2.1.2.6 Braking performance	30
2.1.2.7 Electric battery SOC	31
2.2 Speed profile optimization	31

2.3	Power split optimization . . . . .	36
2.4	Conclusion . . . . .	45
<b>3</b>	<b>Global control architecture and main hypothesis</b>	<b>47</b>
3.1	Problem statement . . . . .	47
3.2	Global Control Architecture scheme . . . . .	48
3.3	Businova components . . . . .	48
3.3.1	Powertrain elements . . . . .	49
3.3.2	Energy storage elements . . . . .	53
3.4	SOC reference curve . . . . .	55
3.5	Regenerative Braking Logic for Businova . . . . .	56
3.6	Conclusion . . . . .	59
<b>4</b>	<b>Deterministic Energy Management Strategy</b>	<b>61</b>
4.1	Introduction . . . . .	61
4.2	Offline Dynamic Programming approach . . . . .	62
4.2.1	Optimal control problem formulation . . . . .	62
4.2.2	Control constraint set . . . . .	63
4.2.3	State constraint set . . . . .	64
4.2.4	Boundary conditions . . . . .	64
4.2.5	DP algorithm . . . . .	65
4.2.6	Simulation results and analysis . . . . .	69
4.3	Online Energy Management . . . . .	73
4.3.1	Sub-Optimal profiles database based on Dynamic Programming . . . . .	74
4.3.2	Multi-Dimensional Interpolation Method . . . . .	74
4.3.3	Simulation results . . . . .	78
4.4	Conclusion . . . . .	79
<b>5</b>	<b>Stochastic Energy Management Strategy</b>	<b>81</b>
5.1	Introduction . . . . .	81
5.2	Stochastic MPC . . . . .	82
5.2.1	Stochastic MPC model . . . . .	82
5.2.2	Simulation results . . . . .	85
5.3	Stochastic Dynamic Programming . . . . .	87
5.3.1	Stochastic modeling of driver . . . . .	89
5.3.2	Multi-Objective optimization problem formulation . . . . .	90

5.3.3	Sub-Optimal energy management strategy using Database based on SDP . . . . .	91
5.3.4	Transition Probability Matrices generation . . . . .	94
5.3.5	Simulation results . . . . .	94
5.4	Conclusion . . . . .	96
<b>6</b>	<b>Adaptive Cruise Control with Stop&amp;Go</b>	<b>99</b>
6.1	Introduction . . . . .	99
6.2	Adaptive Cruise Control with Stop&Go algorithm . . . . .	100
6.3	Simulation Results . . . . .	102
6.3.1	Urban environment flow . . . . .	102
6.3.2	Congested environment with frequent stops . . . . .	103
6.3.3	Unrestricted environment flow with leader's speed frequent variation	103
6.3.4	NEDC driving cycle . . . . .	104
6.3.5	Art Urban driving cycle . . . . .	104
6.4	Discussion . . . . .	104
6.5	Conclusion . . . . .	106
<b>7</b>	<b>General conclusion and future works</b>	<b>107</b>
	<b>Annexes</b>	<b>113</b>
<b>A</b>	<b>Introduction to Markov Decision Processes</b>	<b>113</b>



# LIST OF FIGURES

1.1	Single energy source powertrain architecture . . . . .	10
1.2	Fuel Cell Electric Vehicle Powertrain . . . . .	10
1.3	Range Extended Electric Vehicle Powertrain . . . . .	11
1.4	Hybrid Electric Vehicle powertrain architecture types . . . . .	13
1.5	Hybrid classification based on incremental powertrain functionality [Karden et al., 2007] . . . . .	14
1.6	Past and potential future evolution towards automated cooperative driving [Bengler et al., 2014] . . . . .	16
1.7	Adaptive Cruise Control principle . . . . .	17
1.8	The inter-distance control scheme [Martinez et al., 2007] . . . . .	18
1.9	The effects of factors influencing vehicle fuel economy [Sivak et al., 2012] .	20
2.1	The forces acting on the vehicle . . . . .	25
2.2	Bus. Front view . . . . .	26
2.3	Coefficients of aerodynamic resistance [Schaltz, 2011] . . . . .	27
2.4	Forces acting on the wheel . . . . .	28
2.5	Conceptual illustration of an automobile power train [Ehsani et al., 2005] . .	28
2.6	Schematic representation of the DP algorithm [Ozatay et al., 2014a] . . . .	32
2.7	Scheme of the offline assessment, online assessment, and online assis- tance scenarios [Dib et al., 2014] . . . . .	34
2.8	Neural network based velocity prediction algorithm results [Sun et al., 2015a]	35
2.9	Energy Management approaches in hybrid vehicles . . . . .	36
2.10	DP approach flow-chart [Song et al., 2015] . . . . .	38
2.11	Schematic diagram if DPRB [Zhang et al., 2014] . . . . .	39
2.12	Procedure to realize DP [Chen et al., 2014b] . . . . .	40
2.13	N1 and N2 switch algorithm [Chen et al., 2014b] . . . . .	41
2.14	DP processes [Chen et al., 2014a] . . . . .	43
2.15	ICE operating points [Fang et al., 2011] . . . . .	44
3.1	Proposed overall control architecture . . . . .	49
3.2	Businova . . . . .	50

3.3	Businova powertrain architecture . . . . .	50
3.4	Otto cycle [Mollenhauer et al., 2010] . . . . .	53
3.5	Schematic of hydraulic system . . . . .	54
3.6	Spatial bounds of a bus running cycle . . . . .	55
3.7	Relation among average speed/acceleration and $SOC_{bat}$ reference. . . . .	57
3.8	Electric machine quadrant in torque-speed . . . . .	58
3.9	Example of regenerative braking profile according to Torque and vehicle Speed . . . . .	59
4.1	Standard bus trip from one bus stop to another. . . . .	64
4.2	Rooted tree illustration . . . . .	66
4.3	Standard PMSM characteristics . . . . .	68
4.4	Standard engine characteristics . . . . .	68
4.5	Standard engine efficiency map . . . . .	68
4.6	Tree example: position, speed, time, cost, EM torque, HM torque. . . . .	69
4.7	Road profile . . . . .	69
4.8	Optimal DP SSEO solution . . . . .	72
4.9	Non optimal DP SSEO solution . . . . .	72
4.10	Average powersplit for different slopes . . . . .	75
4.11	Average energy consumption for different slopes . . . . .	75
4.12	DP based Optimal Profiles Database (OPD-DP) illustration . . . . .	76
4.13	Linear Multi-dimensional Interpolation method illustration . . . . .	77
4.14	Road slope and bus weight . . . . .	78
4.15	First scenario: a) speed profile b) actual $SOC$ and the desired value in the end of the trip $SOC_{min}$ c) Energy consumption . . . . .	79
4.16	Second scenario: a) speed profile b) actual $SOC$ and the desired value in the end of the trip $SOC_{min}$ c) Energy consumption . . . . .	80
5.1	Reference $SOC$ baseline . . . . .	85
5.2	Speed Profiles for NEDC SDC . . . . .	87
5.3	Powersplit Profile for NEDC SDC . . . . .	87
5.4	SOC and fuel consumption comparison for NEDC SDC . . . . .	88
5.5	Energy Profile for NEDC SDC . . . . .	88
5.6	Pareto Front of the minimization functions . . . . .	91
5.7	Modified Policy Iteration Algorithm Flowchart . . . . .	93

5.8	ArtRoad SDC. Constant Weight. <i>a)</i> Speed Profile, <i>b)</i> Battery SOC curve, <i>c)</i> Fuel consumption curve, <i>d)</i> Powersplit for DDP approach, <i>e)</i> Powersplit for the proposed SDP approach, <i>f)</i> Total Energy Consumption. . . . .	95
5.9	ArtUrban SDC. Variable Weight. <i>a)</i> Speed Profile, <i>b)</i> Battery SOC curve, <i>c)</i> Fuel consumption curve, <i>d)</i> Powersplit for DDP approach, <i>e)</i> Powersplit for the proposed SDP approach, <i>f)</i> Total Energy Consumption. . . . .	96
6.1	Global control scheme in eACCwSG mode on . . . . .	100
6.2	eACCwSG concept . . . . .	101
6.3	eACCwSG parameters . . . . .	102
6.4	ACCwSG in an urban environment flow . . . . .	103
6.5	eACCwSG congested environment with frequent stops . . . . .	103
6.6	eACCwSG in unrestricted environment flow with leader's speed frequent variation . . . . .	104
6.7	Leader vehicle follows NEDC driving cycle . . . . .	105
6.8	Leader vehicle follows Art Urban driving cycle . . . . .	106
A.1	Illustration of epochs and stages (periods) . . . . .	113
A.2	Illustration of states and actions . . . . .	114



# LIST OF TABLES

2.1	Rolling resistance coefficients . . . . .	26
3.1	Actual Businova dynamic model parameters . . . . .	50
3.2	Permanent Magnet Synchronous Machine technical characteristics . . . . .	51
3.3	ICE parameters . . . . .	53
4.1	OPD-DP online strategy: interpolation methods comparison . . . . .	79
5.1	Switching logic for the ICE reference power . . . . .	85
5.2	Comparison of the Rule Based strategy and SMPC strategy . . . . .	86
5.3	Comparison of the SDP w.r.t. DDP based strategies. . . . .	94
5.4	Comparison of DDP based and SDP based approaches . . . . .	97
6.1	Parameter values for $d_{ref}$ calculation . . . . .	101
6.2	Comparison of the eACCwSG (I) w.r.t. ACC (II) [Shakouri et al., 2014] strategies. . . . .	105



# LIST OF DEFINITIONS

1	Definition: An intelligent vehicle . . . . .	8
2	Definition: A powertrain . . . . .	8
3	Definition: Hybrid Vehicle . . . . .	11
4	Definition: ADAS . . . . .	15
5	Definition: Energy Management Strategy . . . . .	36
6	Definition: Dynamic Programming . . . . .	61



# GENERAL INTRODUCTION

Life is too short to be insignificant.

---

Charlie Chaplin

Intelligent vehicles can be defined as systems that make use of various automation technologies in order to enhance safety and/or energy efficiency by reducing energy consumption and environmental impact. Obviously, the vehicle interacts with the driver, environment, and infrastructure. In intelligent vehicles, these interactions are increased by the use of sensing, information exchange, and actuation of various primary or secondary driving tasks. For example, a collision avoidance system can detect obstacles ahead and prevent an imminent crash by automatically braking when the driver fails to do so. Or vehicles' energy consumption can be improved by increased knowledge of terrain or by applying an adequate energy management strategy, etc.

In the scope of transportation systems, alternative energy sources can provide a fuel economy and/or even zero emission performance for pure electric vehicles (EV). In the early 1990s, the worsening of air quality in French urban centers led to substantial activity in the policy and legislative arena in France. The French government has been a key player in the development of electric vehicles so far. An initial protocol, the 1992 Accord-Cadre sur le Développement du Véhicule Electrique, considered EVs a timely instrument to reduce pollution and noise as well as CO<sub>2</sub> emissions in French cities[Calef et al., 2007]. In order to encourage the citizens to buy EVs, government allocated a financial aid.

However, according to [Covert et al., 2016], at least for the next decade or two, electric vehicles face an uphill battle to replace the fuel fossil. Not only large continuing decreases in the price of batteries are necessary, but oil prices would have to increase by more than financial markets currently predict.

For that reason, Hybrid Electric Vehicles (HEV), especially Plug-In Hybrid Electric Vehicle (PHEVs, cf. section 1.2.3.2), is a promising technology to replace fuel consumption elements in the vehicle. PHEVs are very marketable in that they combine the beneficial attributes of HEVs and battery electric vehicles (BEVs) while mitigating their disadvantages. PHEVs are fuel-flexible vehicles that can run on petroleum and/or electrical energy. Studies in [Simpson et al., 2006] have shown that the potential for PHEVs to reduce per-vehicle petroleum consumption is clearly very high. Reductions in excess of 45% are available.

The Businova is an intelligent plugin-hybrid bus (PHEV) designed for high energy and environmental performance. Businova Evolution project has been initiated by the company SAFRA<sup>1</sup>, specialized in the vehicle bodywork, funded by ADEME<sup>2</sup>. In 2009, the company

---

<sup>1</sup>[www.safra.fr](http://www.safra.fr)

<sup>2</sup>Agence de l'environnement et de la maîtrise de l'énergie

launched a strategy to diversify its business in order to embark on the construction of innovative buses. Work carried out as part of a first Businova project on this new type of multi-hybrid power bus, have allowed to develop a first version presented in October 2011 during the national meetings of public transport of Strasbourg. This is a bus mostly electric with two other sources of energy (hydraulic and heat engine) used when needed (high power demand, air conditioning, etc.). The LabEx IMoBS3/Institut Pascal<sup>3</sup> is the leader of consortium created to achieve the set objectives of the project. The role of IMoBS3/Institut Pascal is in developing intelligent hybridization strategy for optimal usage in urban and suburban environment.

Such kind of hybrid systems must deliver an efficient powersplit by means of its Energy Management Strategy (EMS). The hybrid control system must create the most efficient strategy of coordinating the flow of energy between the engine, battery, electrical and hydraulic motors (cf. **Chapter 3**). Intelligent EMS should provide smooth operation avoiding unpleasant jerks, shudders and shakes of the vehicle. The obtained strategy is thus related to a multi-objective optimization problem. The resolution of such a complex multi-tasking problem is the main challenge of the given PhD thesis. This represents the first and the main aspect of the optimization problem.

The second constituent of the optimization problem stems from the fact that the Businova bus is subject to frequent starts and stops in an urban and/or sub-urban environment. Bearing in mind the heavy dynamics of the system, these phases are considerably energy consuming. Beside an efficient powersplit control, a smooth driving velocity transition also ensures a fuel economy, as well as passengers' comfort. However, following an optimal speed profile in a cluttered environment is not always possible due to the interaction of the bus with other vehicles and infrastructure (e.g., traffic jam, traffic lights, pedestrian crossing, etc.). Hence, the hybrid system can be supplied with one more layer of "intelligence" by adding a feature related to an Advanced Driving Assistance System (ADAS) to diminish a human intervention and improve active safety, particularly in complex situations, and/or to enhance the driver's sense of comfort. Nonetheless, the main focus of the PhD research is the development of an optimal EMS for the heavy studied hybrid vehicle. An optimal EMS must ensure that, in spite of the environmental conditions (road slope, wind speed, etc.) and the current bus' weight (which depends on the number of passengers), the bus has to operate in an efficient manner, complied with the energy minimization and comfort criteria. These criteria are subject to different physical constraints and efficiency criteria.

This manuscript is organized in two parts, the first part contains two chapters which correspond to the state of the art and bibliographical review:

- **Chapter 1** contains a summary of the state of the art in intelligent vehicles, with a main focus on hybrid vehicles and ADAS.
- **Chapter 2** contains a summary of the state of the art in modeling methods and energy management strategies for hybrid electric vehicles, focusing on powersplit optimization and speed optimization approaches.

The second part corresponds to the different contributions developed during this PhD thesis. This part contains four chapters:

---

<sup>3</sup>Institut Pascal a part of Laboratoire d'Excellence "Innovative Mobility: Smart and Sustainable Solutions"

- **Chapter 3** describes a global control scheme architecture as well as assumptions made in this work.
- **Chapter 4** is dedicated to the proposed offline and online deterministic algorithms for simultaneous speed profiles and energy management optimization.
- **Chapter 5** is related to stochastic approaches studied in this work. Stochastic MPC and Stochastic Dynamic Programming methods have been used for the multi-criteria energy optimization problem for energy optimization.
- **Chapter 6** presents another block from the global control architecture which corresponds to an Eco Adaptive Cruise Control with Stop & Go (eACCwSG).

This manuscript ends with a general conclusion summarizing the main contributions of this PhD thesis and the future works.

## MAIN CONTRIBUTION OF THE PHD THESIS

- 1. Deterministic Energy Management Strategy:** Compared to the approaches in [Dib et al., 2014] [Kitayama et al., 2015a], a simultaneous speed and powersplit optimization algorithm based on Dynamic Programming (DP) has been first proposed for a given trip (constrained by the traveled distance and time limit). This algorithm turned out to be highly time consuming so it cannot be used in real-time. To overcome this drawback, an Optimal Profiles Database based on DP (OPD-DP) has been constructed. It contains elementary optimal speed profiles and related powersplit for different bus masses, road slopes, speeds and accelerations. As only finite number of values can be stored in the OPD-DP, different multi-dimensional interpolation methods have been proposed to make use of the database in real-time application: MinMax, Average and Multi-Dimensional Linear Interpolation [Abdrakhmanov et al., 2017a] [Abdrakhmanov et al., 2017c].
- 2. Stochastic Dynamic Programming based on Trained Database:** A Stochastic Dynamic Programming technique is used to simultaneously generate an optimal speed profile and related powersplit strategy. The cost function is calculated by taking into account the state propagation, making use of Transition Probability Matrices. For that purpose, the driver's power demand is modeled as a Markov Chain. The formulated energy optimization problem, being intrinsically multi-objective problem, has been transformed into several single-objective ones with constraints using an  $\epsilon$ -constraint method to determine a set of optimal solutions (the Pareto Front). Additionally, a reference battery State of the Charge (SOC) is used as one of the main constraints in the optimization problem. The SOC curve is generated via Artificial Neural Network (ANN) module. It has as an input average speed, average absolute acceleration, traveled and remained distance until the end of working day of the PHEV [Abdrakhmanov et al., 2018].
- 3. Adaptive Cruise Control with Stop&Go:** An Adaptive Cruise Control with Stop&Go (eACCwSG) manoeuvres in order to improve the fuel economy and provide passengers' comfort has been developed. The algorithm takes into account the deceleration capacity of the bus to generate the safety distanced to maintain, therefore soft braking is guaranteed for the passengers' comfort.

Smoothing the acceleration phases impact the passengers' comfort at the vehicle start and contribute to the fuel economy [Abdrakhmanov et al., 2017b].

- 4. Stochastic MPC:** Stochastic MPC has been designed to decrease the energy consumption of the bus in the presence of uncertainties. An original control architecture that combines an Adaptive Cruise Control with Stop&Go (eACCwSG) manoeuvres and predictive stochastic energy management strategy has been proposed for the studied PHEV. The required power is considered as a random Markov process, encompassing uncertainties with regards to the road profile, bus weight, etc. A Stochastic MPC problem has been formulated so that it reduces the fuel consumption and smooths engine's power change rate [Dahmane et al., 2018].

Some less important contributions from my part have been made in global control architecture and EMS based on Neuro-Fuzzy approach [Kamal et al., 2017], as well as in optimal control approach [Ouddah et al., 2017] [Ouddah et al., 2018].

# INTELLIGENT VEHICLES: OVERVIEW

## **Abstract**

---

This chapter gives a brief overview of the constituent of the “intelligent” vehicles. Existing vehicle powertrain configurations are classified and their features are described. Some functionalities related to the Advanced Driving Assistance Systems (ADAS), such as Cruise Control (CC), Adaptive Cruise Control (ACC), Stop&Go and Eco-Driving, are reviewed.

---

## 1.1/ INTRODUCTION

The advent of automobiles has strongly influenced the human mobility. The automobile has become an indispensable part of a modern lifestyle. The progress in mobility has brought its challenges in terms of comfort, safety, pollution, and energy demands. As vehicles have become a necessity for living, specially in urban environment, encompassing almost every aspect of our daily lives, throughout the years various laws and standards have been developed for vehicle design, production, and interface with the environment and the driver. Today the vehicle manufacturers go into the production of the vehicles to ensure the intended vehicular performance. In addition to all of these requirements, a significant aspect of vehicular design concerns the interaction of driver with vehicle. This interaction includes the essential tasks of controlling the vehicle and all the auxiliary tasks normally performed by the driver.

Although the driver is still largely in control of driving vehicles, several systems have been introduced to enhance vehicle response in braking and handling. Advances in microprocessors and computers have had a tremendous impact on vehicle design, but their full potential is yet to be realized. Today, vehicles have many sensors and electronic systems that contribute to automatic control of subsystems for a range of functions from controlling vehicle dynamics (ABS and traction control) to support the driver in trip planning and route selection (e.g., navigation systems). Intelligent vehicles aim to fully utilize available technologies to assist drivers by enhancing handling, safety, efficiency, and the comfort of driving [Eskandarian, 2014b].

Human error contributes to most of the road accidents. Human drivers are limited in terms of reaction time, perception, and control. Factors such as high workload and fatigue can aggravate these limitations. New technologies such as sensing and communication equipment lead to intelligent functions to drive more safely and efficiently. On the other hand, human drivers have the capability of understanding complex situations that they

have not experienced before and to identify intentions of other road users from subtle clues.

## 1.2/ ENERGY AND POWERTRAIN SYSTEMS FOR INTELLIGENT VEHICLES

### **Definition 1: An intelligent vehicle**

An intelligent vehicle is a vehicle that performs certain aspects of driving either autonomously or assists the driver to perform his/her driving functions more effectively, all resulting in enhanced safety, efficiency, and environmental impact [Eskandarian, 2014b].

The scope of our research is focused on an intelligent vehicle which is capable of performing some driving assistance tasks. When we speak about the intelligence in vehicles we refer not only to the tasks in terms of the powertrain (cf. definition 2) architecture and energy source nature, intelligent vehicles can be classified into conventional, electric and hybrid vehicles.

### **Definition 2: A powertrain**

The main components that generate and supply power for vehicle traction. It includes the engine, transmission, drive shafts, differential and final drive.

For this type of hybrid vehicles an “intelligence” is introduced by making use of appropriate ADAS which will be reviewed in section 1.3.

HEVs and EVs are more efficient devices with respect to conventional vehicles in terms of energy utilization mainly due to three characteristics [Cervantes, 2014].

1. The average tank-to-wheels efficiency (i.e., chemical-to-mechanical energy conversion efficiency) is higher. That is, even in the case of HEV, where an internal combustion engine (ICE) is used, the utilization of electric power from an energy-storage system (ESS) leads to an increment of the total average efficiency due to the high ESS efficiency.
2. Regenerative braking. Charging the ESS during the braking phase opens the possibility of recycling mechanical energy that in conventional vehicles dissipates, further increasing the efficiency of the vehicle.
3. The controlled powersplit among the energy sources. By managing such powersplit, a decision can be made on how much fuel is consumed. The more frequent use of the ESS, the more efficient vehicle operation and the less energy lost.

### 1.2.1/ CONVENTIONAL VEHICLES

A conventional vehicle is a vehicle which contains only internal combustion engine (ICE) as the propulsion element in the powertrain. Most typically, ICE can be classified into two types: spark-ignition (SI) engines and compression-ignition (CI) engines [Yan, 2014]. ICE

convert fuel energy into mechanical work through fuel combustion, resulting in a power stroke which provides the mechanical work. A typical ICE vehicle only uses approximately 16% of the liquid fuel energy to move the vehicle [Bailey, 2018]. The heat emitted in the combustion process wastes the majority of the energy while frictional losses from the hundreds of moving parts in the engine, transmission and the mechanical connection to the drive wheels consumes the rest. For a given ICE, the efficiency is not a constant. It depends on the engine operating point in terms of engine speed and engine torque, and it also depends on engine operating conditions that may affect the engine friction, the spark timing, valve timings, and fuel air ratio.

An example of conventional powertrain is shown in Figure 1.1(a). The wheels are connected to the engine by means of the differential and the driving axle.

### 1.2.2/ ELECTRIC VEHICLES

Another type of powertrain contains electric motor as a propulsion element in vehicle. The Electric Vehicle (EV) was invented in 1834. During the last decade of the 19th century, a number of companies produced EVs in America, Britain, and France. In London, there were Electric Cab Company's taxis. However, due to the limitations associated with the batteries and the rapid advancement in ICE vehicles, EVs have almost vanished from the scene since 1930 [Chan, 2007]. Electric battery is used as a source of the energy. Compared with conventional ICEVs, EVs have several advantages such as [Jiang et al., 2014]:

- High electric machine efficiency compared to the internal combustion engine efficiency;
- Low level of environmental pollution, which improves local air quality;
- Lower noise;
- Smoother operation;
- Various electricity sources that can be obtained from renewable energies, such as hydro, nuclear, wind, and solar;
- Various onboard energy storage devices such as batteries, supercapacitors, flywheels, and hydrogen fuel cells;
- Regenerative braking to recover the kinetic energy of the vehicle.

Electric vehicles include battery electric vehicles (BEVs), fuel cell electric vehicles (FCEVs), and range-extended electric vehicles (REEVs).

**Battery electric vehicle** An electric battery is the only source of energy used by BEVs. The powertrain architecture of BEV is similar to a conventional vehicle's powertrain, except for the fact that, instead of ICE, an electric motor is used for traction (cf. Figure 1.1(b)). Electric battery energy is transformed into output mechanical energy of the electric motor. During energy transformation zero emission is produced. Despite all the merits mentioned above, purely electric-powered vehicles currently face significant challenges, including insufficient drive range and high costs. Battery-related challenges such as battery cost, volume and weight, short drive range per charge, and long charging time all present significant hurdles to the wide adoption of electric vehicles. To overcome this

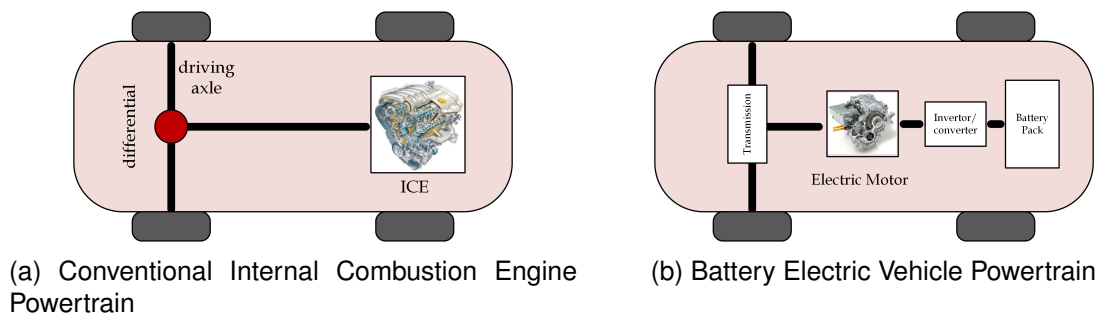


Figure 1.1: Single energy source powertrain architecture

drawback, FCEVs and REEVs have been conceived to extend the range of the battery usage.

**Fuel cell electric vehicles** run on electricity generated by the fuel cells onboard. The fuel cells combine oxygen and hydrogen, in which process electricity and water are generated. The fuel cells are much more efficient than most other types of energy converters, such as internal combustion engines and chemical batteries. Furthermore, the outcome of fuel cells are only water and heat, and depending on the fuel source, very small amount of nitrogen dioxide and other emissions. Figure 1.2 shows a powertrain system for an FCEV. The primary components in the powertrain consist of a fuel tank, a fuel processor, a fuel cell as primary energy source, a battery pack, an electric machine as the traction motor, and so on. The vehicle controller takes command signals from the accelerator pedal and the brake pedal, the speed signal, the fuel cell power signal, and the battery signal, and sends the control signal to the fuel cell system. The power from the fuel cell and the battery pack are combined to provide energy for the electric machine, which propels the vehicle through the transmission system.

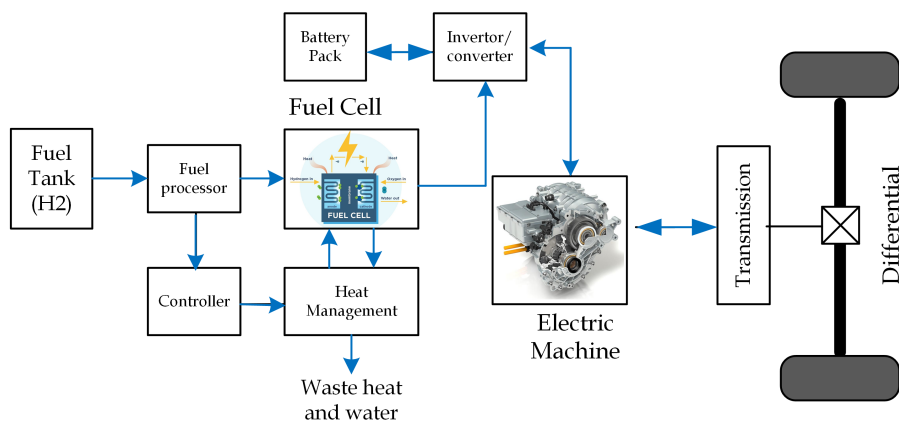


Figure 1.2: Fuel Cell Electric Vehicle Powertrain

**Range-Extended electric vehicle** REEVs increase the driving range of the vehicle by incorporating an auxiliary electrical power source to the propulsion system. As shown in

Figure 1.3, the range extender can be a small internal combustion engine with a generator. Instead of powering the vehicle directly, the engine in a range extender is acting as an electricity generator to recharge the batteries. The battery capacity for a REEV is designed to satisfy a customer's average daily usage, while the range extender allows the vehicle to maintain an acceptable long drive range. The engine-based range extender is commonly designed to be extremely compact, lightweight, and low-cost. The engine is controlled to operate in its economic zone with high efficiency. Often in the literature this type of EV powertrain is referred as Series Hybrid Vehicle (cf. section 1.2.3.1).

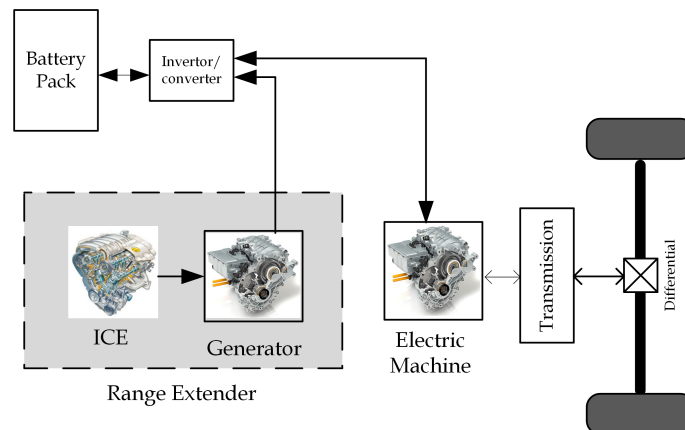


Figure 1.3: Range Extended Electric Vehicle Powertrain

### 1.2.3/ HYBRID VEHICLES

#### Definition 3: Hybrid Vehicle

Hybrid vehicle uses at least two energy sources composing its powertrain.

A hybrid vehicle combines at least two power (energy) sources. Possible combinations include diesel/electric, gasoline/flywheel (mechanical device specifically designed to efficiently store rotational energy), and fuel cell/battery. Hybrid vehicles do not share an electric vehicle's main drawback corresponding to a limited range between charging [Wouk, 1997].

American engineer H. Piper filed for a patent on a hybrid vehicle in 1905. Piper's design called for an electric motor to augment a gasoline engine to let the vehicle accelerate. Hybrid vehicles represents a compromise between the conventional and pure electric vehicle. Involvement of the electric propulsion system in HEV results in four different ways effectively acting to improve the energy efficiency of the vehicle:

- Higher efficiency of electric motor compared to the engine results in higher global operating efficiency;
- Braking kinetic energy regeneration;
- Shutting off the engine during the idling phases;
- Possible zero emissions.

According to the powertrain configuration, HEVs can be classified into (cf. section 1.2.3.1):

- Series Hybrid Electric Vehicles;
- Parallel Hybrid Electric Vehicles;
- Series-Parallel Hybrid Vehicles.

HEVs can be classified according to the degree of hybridization (cf. section 1.2.3.2):

- Micro hybrid;
- Mild hybrid;
- Full hybrid;
- Plug-in hybrid.

### 1.2.3.1/ HYBRID POWERTRAIN CONFIGURATION

**Series hybrid electric vehicles** The series hybrid is the simplest kind of HEV (cf. Figure 1.4(a)). Its engine mechanical output is first converted into electricity using a generator. The converted electricity either charges the battery or can bypass the battery to propel the wheels via the same electric motor and mechanical transmission. Conceptually, it is an engine-assisted EV which aims to extend the driving range to be comparable with that of the REEV (cf. section 1.2.2). Because of the absence of clutches throughout the mechanical link, it has the definite advantage of flexibility for locating the engine-generator set. Although it has an added advantage of simplicity of its drive train, it needs three propulsion devices—the engine, the generator and the electric motor. Another disadvantage is that all these propulsion devices need to be sized for the maximum sustained power if the series HEV is designed to climb a long grade. On the other hand, when it is only needed to serve such short trips as commuting to work and shopping, the corresponding engine-generator set can adopt a lower rating.

**Parallel hybrid electric vehicles** Differing from the series hybrid, the parallel HEV (cf. Figure 1.4(b)) allows both the engine and electric motor to deliver power in parallel to drive the wheels. Since both the engine and electric motor are generally coupled to the drive shaft of the wheels via two clutches, the propulsion power may be supplied by the engine alone, by the electric motor alone or by both. Conceptually, it is inherently an electric assisted Internal Combustion Engine Vehicle for achieving lower emissions and fuel consumption. The electric motor can be used as a generator to charge the battery by regenerative braking or absorbing power from the engine when its output is greater than that required to drive the wheels. Better than the series HEV, the parallel hybrid needs only two propulsion devices—the engine and the electric motor. Another advantage over the series case is that a smaller engine and a smaller electric motor can be used to get the same performance until the battery is depleted. Even for long trip operation, only the engine needs to be rated for the maximum sustained power, while the electric motor may still be about half.

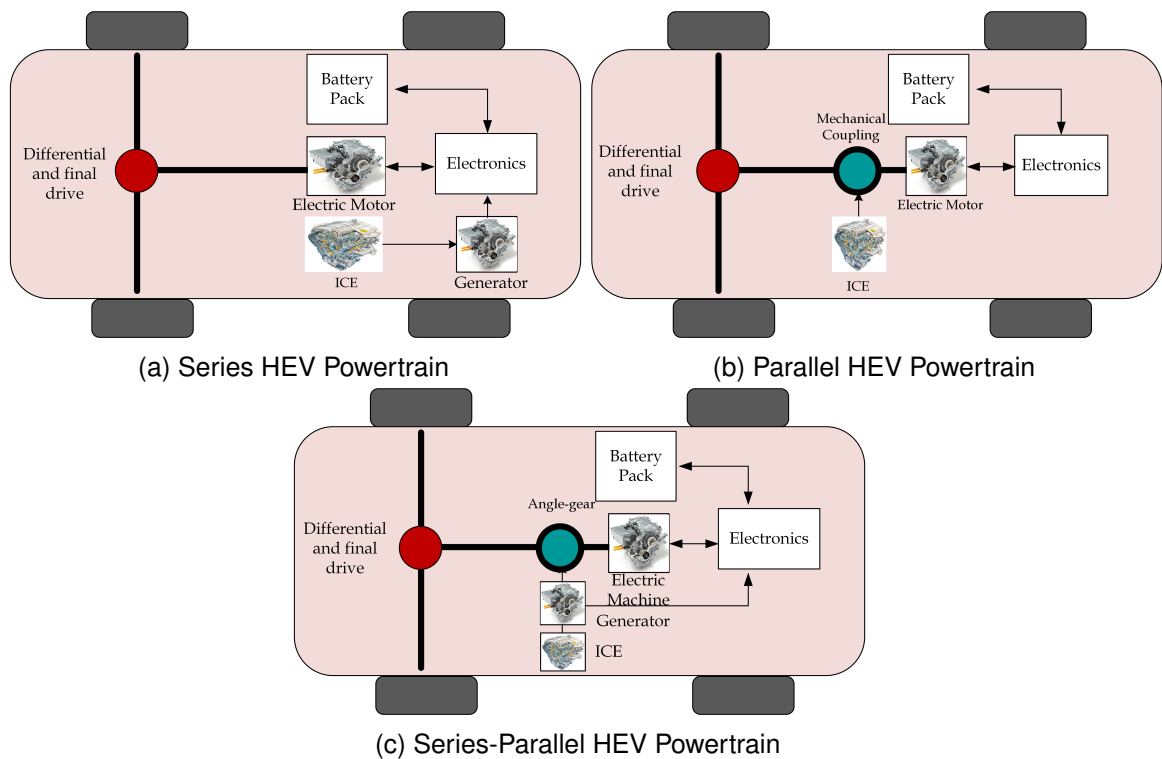


Figure 1.4: Hybrid Electric Vehicle powertrain architecture types

**Series-parallel hybrid electric vehicles** In the series-parallel hybrid (cf. Figure 1.4(c)), the configuration incorporates the features of both the series and parallel HEVs, but involves an additional mechanical link compared with the series hybrid and also an additional generator compared with the parallel hybrid. Although possessing the advantageous features of both the series and parallel HEVs, the series-parallel HEV is relatively more complicated and costly. Nevertheless, with the advances in control and manufacturing technologies, some modern HEVs prefer to adopt this system.

### 1.2.3.2/ DEGREE OF HYBRIDIZATION

In recent years, a number of new hybrid electric vehicle propulsion systems for passenger cars and light trucks have been developed and brought to the market by automotive manufacturers. By adding an electromechanical component to the driveline, improvements in propulsion efficiency and reduced exhaust gas emissions could be shown. Different levels of hybridization can be distinguished, implementing the following hybrid functions to different extents: engine stop/start operation, regenerative braking, modification of engine operating points and various levels of hybrid electric propulsion assist. The classification of the hybrid systems according to the level of hybridization is given in Figure 1.5. The section below details the main differences in the different levels of hybridization.

**Micro and mild hybrid electric vehicles** The lowest level of hybridization, the Micro-HEV, combines automatic engine start-stop operation with regenerative braking [Karden et al., 2007]. Micro hybrids employ a modest electric portion in the power systems. The typical power rating for a micro hybrid sedan is between 3 and 5 kW. Micro

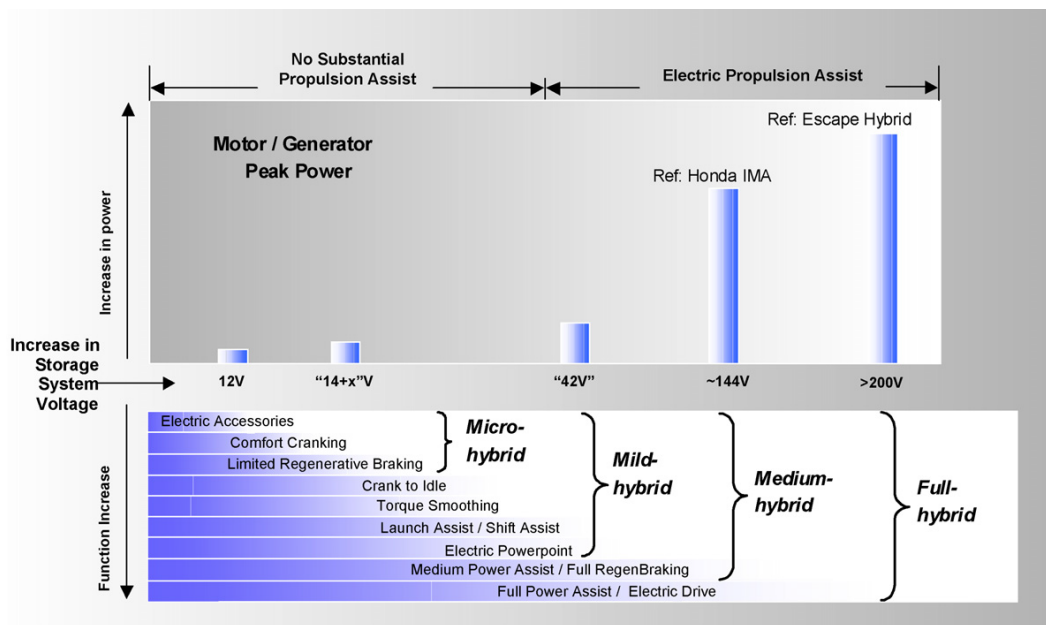


Figure 1.5: Hybrid classification based on incremental powertrain functionality [Karden et al., 2007]

hybrids normally refer to hybrid vehicles with the start–stop or idle–stop systems, which automatically shut down the engines when vehicles are coasting, braking, or stopped according to certain road conditions, and restart the engines when the speed is regained. The added electric power system can also be used to help supply power to driving accessories such as power steering and air conditioning. Some micro hybrids are also capable of certain levels of regenerative braking [Emadi, 2014]. Micro hybrids can provide 1.5–4% [Karden et al., 2007] up to 10% [Emadi, 2014] of fuel economy benefits, especially in urban driving situations, where frequent stop-and-go is inevitable.

Mild hybrids have a higher level of electric power rating, typically ranging from 7 to 15 kW. Consequently, a higher level of fuel economy gain can be achieved, saving up to 20% in fuel compared with conventional combustion vehicles. Propulsion systems in mild hybrids normally consist of electrical motor–generators between the engine crank shafts and the transmission input shafts. The added motor–generators provide the vehicle with the start–stop function, regenerative braking function, and additional electric power to drive the accessories. Some of the mild hybrids can also provide a modest level of power assistance to the engine.

**Full and plug-in hybrid electric vehicles** Full hybrids are defined as those gasoline–electric vehicles that can run on either engine-only mode, battery-only mode, or a combination of the two. In addition to the functions that micro hybrids and mild hybrids are capable of, full hybrids can also operate on an all-electric range where only electric motors are used to propel the vehicle and supply all the internal power loads. However, owing to the limited size of the electric machine and the battery pack, full HEVs normally have a relatively short all-electric range with limited power output. Typically, full hybrids can achieve more than 40% of fuel economy gains in city drives and have more electric power assistance to increase driving performance [Suntharalingam et al., 2014].

Compared with micro and mild hybrids, full hybrids employ the largest electric power portions in the HEV powertrain systems. A larger battery pack is required to achieve the desired electric drive level. Meanwhile, since the motor is directly coupled with the output drive shaft in the electric mode, a robust motor with sufficient speed and enough torque is demanded. Full hybrids also have relatively more complicated configurations. Most full hybrids integrate the electric power path with the mechanical power path by means of powersplit devices such as planetary gear sets [Suntharalingam et al., 2014]. Power split devices serve to divide the power from the onboard power plants, that is, the engine and batteries, and redistribute the power low between the electric path and the mechanical path to achieve optimal fuel efficiency and driving performance. Power split devices and other added mechanical components all add to the complexity of full hybrid systems. Therefore, though the full hybrids achieve significantly higher fuel economy and better performance, the manufacturing costs also increase as larger battery packs, more powerful electric machines, and more complicated configurations are implemented.

Plug-in hybrid electric vehicles are generally either parallel hybrid electric vehicles or series-parallel hybrid electric vehicles. The plug-in hybrid electric vehicle incorporates a bigger electric propulsion system and a smaller IC engine-based propulsion system. Also, the plug-in hybrid electric vehicle incorporates an external charging adopter and it can be used to charge the battery from the grid. Owing to the higher percentage of the electric propulsion system, plug-in HEVs have higher regenerative braking capability compared to traditional HEVs. Plug-in HEVs are highly desirable for city driving cycles.

### 1.3/ ADAS FOR INTELLIGENT VEHICLES

**Definition 4: ADAS**

Advanced Driver Assistance Systems (ADAS) are the systems that help drivers in driving process by increasing safety, comfort and economy.

Recently automobile manufacturers have placed an increasing focus on offering intelligent assistance systems in the vehicle. By delivering targeted information and warnings, by delegation of tasks, or by intervention, these functions aim to improve active safety, particularly in complex situations, and/or to enhance the driver's sense of comfort. One of the purposes of ADAS is to enhance active and integrated safety. The past and a potential future evolution of ADAS is sketched in Figure 1.6 from a technological point of view.

The first generation of the ADAS relates to the epoch before 1995 year. The early technology was based on the proprioceptive sensors, thus sensors measuring an internal state of the vehicle (e.g., velocity, acceleration). The Anti-lock Braking Systems (ABS) and Electronic Stability Control (ESC) relate the first developed ADAS functions.

The second generation of ADAS, based on exteroceptive sensors, focuses on providing information and warnings to the driver, as well as on enhancing the driver comfort. Exteroceptive sensors acquire information from outside the vehicle, including ultrasonic, radar, lidar or video sensors and to some extent Global Navigation Satellite System. These sensors provide information about the road ahead and the presence as well as the driving status of other traffic participants or the vehicle's position in the world.

Parking assistance systems entered the market in the mid-1990s [Bengler et al., 2014].

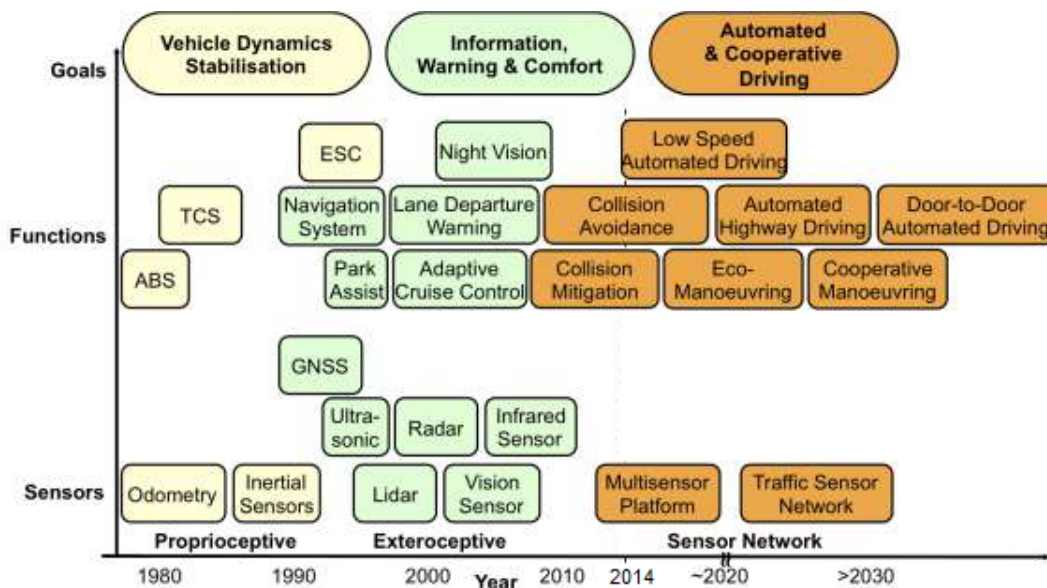


Figure 1.6: Past and potential future evolution towards automated cooperative driving [Bengler et al., 2014]

Ultrasonic sensors are used to detect obstacles in the surrounding environment. Initially, these systems had merely a warning function to help prevent collisions while backing into and out of parking spaces; later, they were complemented by rear-view cameras to better assist the driver with more detailed information.

The development of Adaptive Cruise Control (ACC) is an important step in driving assistance history. Through the implementation of electronic brake and drive control, and the use of previously very expensive radar technology, which in turn became significantly more affordable, partially automated driving was made possible. When ACC was introduced in 1999, these features were initially only usable at speeds greater than 30km/h [Jones, 2001].

Collision avoidance systems using inexpensive low-range and low-resolution versions of lidar sensors are currently being used for low speed applications. By means of increasing warning levels, the driver is made aware of an impending collision. If the driver does not react, the vehicle actively brakes to mitigate accident severity once a collision is no longer avoidable [Maurer, 2014].

The latest class of ADAS selects and controls trajectories beyond the current request of the driver. The high certainty level required for such decisions can only be achieved with an interconnected set of sensors. Radar and camera technologies currently dominate the ADAS sector. Data fusion strategies and joint sensor self-calibration will combine the strengths of both technologies. For example, merging longitudinal and lateral control, these systems are designed for Automated Low Speed Driving on congested highways assuming full lateral and longitudinal vehicle control at low speeds [Bengler et al., 2014].

### 1.3.1/ ADAPTIVE CRUISE CONTROL

In urban environment, due to traffic conditions, traffic lights, a bus encounters frequent Stop&Go situations. This results in augmented fuel consumption during the starts. To reduce the fuel consumption, we can make use of smooth speed profiles. One of the ways to impose the speed profile to the vehicle is implementation of the Adaptive Cruise Control system.

The adaptive cruise control (ACC) system is an enhancement to the conventional cruise control (CC). Compared with conventional cruise control (CC) systems, which regulate vehicle speed only, an ACC system allows drivers to maintain a desired cruise speed as well as a desired following gap  $d_{safe}$  with respect to a preceding vehicle if there is no immediate preceding vehicle (cf. Figure 1.7). The ACC system senses the range (i.e., relative distance) and range rate (i.e., relative speed) to the preceding vehicle with a range sensor (i.e., radar or LIDAR). Such information is used to generate appropriate throttle or brake command to maintain a preset following gap to the preceding vehicle [Bu et al., 2014]. Researches have started to explore the introduction of additional objectives to ACC, e.g.,

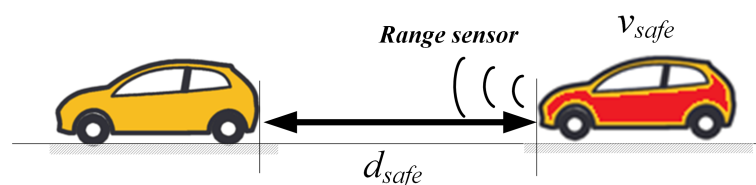


Figure 1.7: Adaptive Cruise Control principle

fuel economy and driver desired response. Ioannou [Ioannou et al., 2005] suggested the use of ITS technologies, including adaptive cruise control, to reduce fuel consumption of vehicles. [Jonsson et al., 2004] proposed a dynamic programming based offline control method. It reduced the fuel consumption while allowing more tracking error. The improvement of fuel consumption usually decreases the acceleration performance and lowers the tracking capability. This will lead to two problems consequently: 1) when the preceding car accelerates, larger inter-vehicular distance occurs due to the deficient acceleration performance, resulting in frequent vehicle cut-ins from adjacent lanes, 2) when the preceding vehicle decelerates, inter-vehicular distance shortens quickly and rear-end collisions happen more easily. On the contrary, if an ACC system pursues good tracking capability only, it leads to unnecessary acceleration and emergency braking, which also deteriorates the fuel economy of vehicle to some extent.

A velocity control system in order to save the fuel consumption by involving traffic signal information was proposed in [Yu et al., 2015]. Model predictive control scheme was used in order to control the velocity predicting states of the vehicle and traffic signal switching. The algorithm judges whether a vehicle should accelerate or not when the vehicle cannot pass the traffic lights during the green phase. In the algorithm, the fuel economy was predicted using traffic signal information.

A vehicle speed and vehicle-to-vehicle distance control algorithm for vehicle stop-and-go cruise control has been proposed in [Yi et al., 2001]. Linear quadratic optimal control theory has been used to develop a vehicle speed and distance control algorithm. A desired acceleration for the vehicle has been designed on the basis of the vehicle speed

and distance control algorithm. [Kim, 2012] formulated the optimization problem to find the optimal relative distance profile during a complete stop and the optimal velocity profile during a starting motion. It suggested that once leader car resumes the motion after a full stop, the host car is not obliged to follow the leader car, instead it can follow an optimal profile.

A generic concept for an autonomous vehicle longitudinal motion control is proposed in [Akhegaonkar et al., 2016]. The final function and its adaption to various power train configurations have been evolved from the basic smart and green ACC which is expanded methodically. It is observed that the smart and green autonomous vehicle (SAGA) function has varied impact on energy saving which is subject to the power train configuration and velocity cycle.

### 1.3.2/ STOP&GO

Stop&Go cruise control is an extension of active cruise control and aims to offer longitudinal support to the driver in an environment characterized by a congested traffic flow on highways and well structured (sub)urban roads at speeds lower than 30-40 km/h. The support function comprises: remaining at a safe distance from preceding vehicles according to the driver's preferences, automatically slowing down and coming to a full stop behind preceding vehicles, and "go" [Venhovens et al., 2000].

[Acarman et al., 2006] present Stop&Go driver assist system with and without wireless communication. They consider both a totally isolated car (without cooperation), as well as the possibility of cooperation through wireless with the cars ahead. A constant time gap control is used as cruise control policy assuring stability of vehicles' string in groups.

In [Martinez et al., 2007] authors have presented a novel reference model based control approach for automotive longitudinal control. The proposed structure (cf. Figure 1.8) combines an exogen reference model with an additional control loop. The former is charged of verify some safety and comfort constraints, while the latter is charged of the model-matching between the model and the actual system, assuring a good tracking of the desired reference inter-distance.

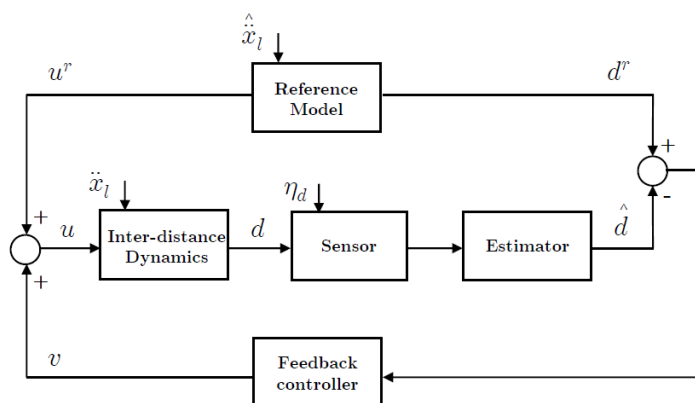


Figure 1.8: The inter-distance control scheme [Martinez et al., 2007]

[Milanés et al., 2012] have presented two control techniques — fuzzy logic and i-PI con-

trollers — with which to solve Stop&Go manoeuvres problem. The i-PI controller, that it is only based on a rough model of the system, provides smoother action on the throttle and brake pedals.

### 1.3.3/ COLLISION AVOIDANCE

The direct safety functions of ADAS aim to mitigate a hazardous situation as best as possible; these are a variety of pre-collision warning, collision avoidance, and collision mitigation systems [Eskandarian, 2014a].

Different factors contribute to vehicle crashes, such as vehicle mechanical problems and bad weather, driver behavior is considered to be the leading cause of more than 90 per cent of all accidents [Biswas et al., 2006]. The inability of drivers to react in time to emergency situations often creates a potential for chain collisions, in which an initial collision between two vehicles is followed by a series of collisions involving the following vehicles.

[Dagan et al., 2004] describes a vision based Forward Collision Warning (FCW) system for highway safety. The algorithm described in this paper computes time to contact (TTC) and possible collision course directly from the size and position of the vehicles in the image - which are the natural measurements for a vision based system - without having to compute a 3D representation of the scene. The use of a single low cost image sensor results in an affordable system which is simple to install. The system has been implemented on real-time hardware and has been test driven on highways. Collision avoidance tests have also been performed on test tracks.

[Jula et al., 2000] analyze the kinematics of the vehicles involved in a lane changing/merging maneuver, and study the conditions under which lane changing/merging crashes can be avoided. That is, given a particular lane change/merge scenario, we calculate the minimum longitudinal spacing which the vehicles involved should initially have so that no collision, of any type, takes place during the maneuver. Simulations of a number of examples of lane changing maneuvers are used in order to demonstrate the results. These results together with appropriate sensors and equipment on board of vehicles could be used to assess the safety of lane changing maneuvers and provide warnings or take evasive actions to avoid collision.

[Coelingh et al., 2010] describes one of the Automatic Emergency Braking systems called Collision Warning with Full Auto Brake and Pedestrian Detection (CWAB-PD). It helps the driver with avoiding both rear-end and pedestrian accidents by providing a warning and, if necessary, automatic braking using full braking power. A limited set of accident scenarios is selected to illustrate the theoretical and practical performance of this system. In this paper it is shown that the CWAB-PD system can avoid accidents up to 35 km/h and can mitigate accidents achieving an impact speed reduction of 35 km/h.

### 1.3.4/ ECO-DRIVING SUPPORT SYSTEMS

The characteristics of eco-driving are generally well defined and easily characterized. They involve such things as accelerating moderately, anticipating traffic flow and signals, thereby avoiding sudden starts and stops; maintaining an even driving pace (using cruise control on the highway where appropriate), driving at or safely below the speed limit; and eliminating excessive idling. The advantages of eco-driving, of course, go beyond

CO<sub>2</sub> reductions. They include reducing the cost of driving to the individual and producing tangible and well-known safety benefits (with fewer accidents and traffic fatalities) [Barkenbus, 2010].

[Sivak et al., 2012] present information about the effects of decisions that a driver can make to influence onroad fuel economy of light-duty vehicles. These include strategic decisions (vehicle selection and maintenance), tactical decisions (route selection and vehicle load), and operational decisions (driver behavior). The effects of factors influencing vehicle fuel economy are summarized in Figure 1.9. According to this summary we can

Level	Factor	Effect
Strategic	Vehicle class	38%
	Vehicle model	800% all cars; 355% cars excluding fully electric; 227% cars excluding fully electric and hybrids; 100% all pickups
	Vehicle configuration	18% cars, 28% pickups
	Out-of-tune engine	4–40%
	Tires with 25% higher rolling resistance	3–5%
	Tires underinflated by 5 psi	1.5%
Tactical	Improper engine oil	1–2%
	Route selection: road type	Variable
	Route selection: grade profile	15–20%
	Route selection: congestion	20–40%
Operational	Carrying extra 100 lb	≤ 2%
	Idling	Variable
	Driving at very high speeds	30%
	Not using cruise control	7% (while at highway speeds)
	Using air conditioner	5–25%
	Aggressive driving	20–30%

Figure 1.9: The effects of factors influencing vehicle fuel economy [Sivak et al., 2012]

see that aggressive driving and not use of cruise control can increase the fuel consumption up to 30% and 7%, consequently.

The research presented in [Rakha et al., 2011] develops a framework to enhance vehicle fuel consumption efficiency while approaching a signalized intersection through the provision of signal phase and timing information that may be available through vehicle-to-infrastructure communication. The paper mainly focused on developing a strategy which yields the most fuel-optimal speed profile for a vehicle approaching a signalized intersection using V2I communication capabilities.

[Wada et al., 2011] develop an eco-driving assist system that is adaptive to a driver's skill and to demonstrate its effectiveness. The eco-driving assist system consists of a visual

indicator illustrating the eco-driving. In the proposed adaptive system, the resolution of the indicator and the threshold of eco-driving are changed to adapt to the driver's skill. Changes in driving behavior and the corresponding eco-driving scores, measured over five days, were investigated. The score with the adaptive system increased through the trial days, while no clear tendency was found with the non-adaptive system.

[Cheng et al., 2013] present a new method to model and optimize the vehicle fuel consumption and its speed in the design of an eco-driving assistance system (EDAS) developed within the EU ecoDriver project. The main objective of this EDAS is to combine a precise fuel consumption model with a robust optimization module. An optimal speed profile is obtained to reduce the energy consumption. The gear management is also included in this procedure. The instantaneous fuel consumption rate is expressed as a piecewise polynomial of the instantaneous engine speed and engine torque. A dynamic programming technique is used to optimize the vehicle fuel consumption considering the safety requirements.

The paper of [De Nunzio et al., 2016] focuses on the possibility of further improvements when information about many successive signalized intersections is available. The presented algorithm is capable of finding the energy-efficient path among all the available ones, and returning the speed advisory to the drivers, in a sub-optimal way. However, for the already complex scenario analyzed in this study, the computation time required by the algorithm is very appealing for online implementation purposes. Experiments in a microscopic traffic simulator demonstrated that the proposed algorithms is able to cope with perturbations and to drastically reduce the traffic energy consumption without affecting travel time.

## 1.4/ CONCLUSION

This chapter provided an overall review of intelligent vehicle systems, including intelligent vehicle classification and ADAS. Due to the large amount of works, only some relevant works, concerning Adaptive Cruise Control, Collision Avoidance, Eco-Driving Systems for fuel economy are described. This description aims to present related works and justify the choice of the proposed global control architecture. The next chapter will present a review of the energy management strategies existing in hybrid vehicles.

# ENERGY MANAGEMENT IN HYBRID VEHICLES

## **Abstract**

---

This chapter is dedicated to the overview of the modeling techniques for a hybrid vehicle and its components. Some research advances in energy management (cf. definition 5) for Hybrid Electric Vehicles (HEV) are presented. Globally, all the reviewed techniques can be classified into speed optimization and powersplit optimization approaches. This chapter also speaks briefly about regenerative braking feature that HEV have.

---

## 2.1/ MODELLING OF HYBRID VEHICLES

The vehicle performance (its motion, acceleration, deceleration) is the response to the applied forces. To evaluate the performance, we must know their nature, how and why the forces are produced.

Understanding of the vehicle dynamics can be accomplished in two levels - the empirical and analytical [D.Guillespie, 1992]. The empirical levels includes the data obtained as a result of the sequence of experiments. However this method may lead to failure, as extrapolation of the past experiences to the new conditions includes new factors, which lead to the other results. The analytical method attempts to show the mechanical relations based on the known laws of physics to obtain the analytical model. The model is usually presented in the form of algebraic or differential equations. These equations allow to identify the factors mostly influencing the vehicle dynamics.

In this PhD work, we apply the analytical level of modelling. Basically, the analytical model based on physical equations has been used in order to describe the Businova dynamics. This chapter starts with a brief description of Bond Graph, a way of modeling based on energy exchange. Afterwards, a detailed model of Businova based on classical mechanics laws is presented.

### 2.1.1/ BOND GRAPH

Any physical process is an exchange of energy. Either the energy is consumed, or it is emitted. An energy flux can be transformed into different forms: thermal, electrical, mechanical, hydraulic, etc. Bond graphs are a domain-independent graphical description

of dynamic behavior of physical systems. This means that systems from different domains (e.g., electrical, mechanical, hydraulic, acoustical, thermodynamic, material) are described in the same way. The basis is that bond graphs are based on energy and energy exchange. Analogies between domains are more than just equations being analogous: the used physical concepts are analogous.

Bond graphs are labelled and directed graphs, in which the vertices represent submodels and the edges represent an ideal energy connection between power ports. The vertices are idealized descriptions of physical phenomena: they are concepts, denoting the relevant (i.e. dominant and interesting) aspects of the dynamic behaviour of the system. It can be bond graphs itself, thus allowing hierarchical models, or it can be a set of equations in the variables of the ports (two at each port). The edges are called bonds.

The concept of bond graphs was originated by [Paynter, 1961]. The idea was further developed by [Karnopp et al., 1968], such that it could be used in practice ([Thoma et al., 1976] [van Dixhoorn, 1980]). Bond-graph model description evolved to a systems theory.

The fundamentals of this approach are given in the Annex ??.

[Bera et al., 2012] deals with modeling of an intelligent autonomous vehicle with four traction wheels, four braking wheels and four-wheel steering system. The bond graph model of the integrated vehicle dynamic system is developed in a modular and hierarchical modeling environment. The intellectual decomposition of a system uses the view of an exchange of energy between subsystems and that there are elementary physical processes on the bottom of the model hierarchy for which fundamental balances.

Since the conceptual starting point of bond graph modelling is the energy exchange between subsystems, this modelling approach is particularly suited for multidisciplinary dynamic systems in which several energy domains are involved. The choice of effort and flow variables is based on an analogy between mechanical and electrical quantities.

### 2.1.2/ ANALYTICAL MODELLING OF BUSINOVA

The first step in modeling a vehicle is to produce the equations of the vehicle dynamics. The forces acting on the vehicle of a mass  $m$  moving with a linear acceleration  $\vec{a}$  are expressed by the Second Newton's Law:

$$\sum_i \vec{F}_i = m\vec{a} \quad (2.1)$$

where  $\vec{F}_i$  corresponds to the different forces acting on the vehicle.

They are given by (cf. Figure 2.1):

- the tractive force  $\vec{F}_t$ ;
- the rolling resistance  $\vec{F}_{rr}$  ;
- aerodynamic drag  $\vec{F}_{ad}$ ;
- the gravity force  $\vec{F}_g$ .

To describe a generic case, let us assume that the vehicle is moving up the slope of  $\theta$  degree (cf. Figure 2.1). The origin of the coordinates is situated in the center of mass

(CoM). We suppose that CoM of the bus is in its geometric center. So the equation 2.1 can be re-written in scalar form:

$$m\vec{a} = \vec{F}_t + \vec{F}_{rr} + \vec{F}_{ad} + \vec{F}_g \quad (2.2)$$

Now let's regard each force in details.

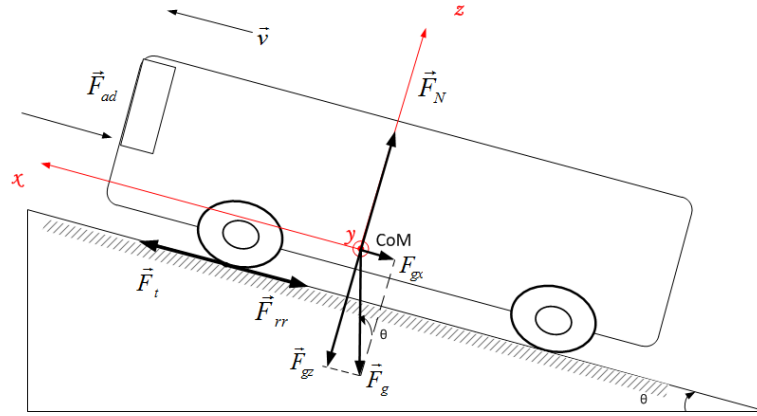


Figure 2.1: The forces acting on the vehicle

### 2.1.2.1/ ROLLING RESISTANCE FORCE

The rolling resistance appears mainly due to the friction of the vehicle tyre on the road. The rolling resistance is approximately constant, hardly depends on vehicle speed. It is proportional to the vehicle weight [Larminie et al., 2003]. It yields the following equation:

$$F_{rr} = \mu_{rr}mg \quad (2.3)$$

where  $\mu$  rolling resistance coefficient, and  $g = 9.81m/s^2$  gravity acceleration.

Typical values of  $\mu_{rr}$  are 0.015 for a <sup>1</sup>radial ply tyre, down to about 0.005 for tyres developed specially for electric vehicles [Larminie et al., 2003].

The expression for the rolling resistance developed in [Astrom et al., 2009] adds the sign of the vehicle velocity, implying that when  $v = 0$ ,  $F_{rr} = 0$  as well:

$$F_{rr} = mg\mu_{rr}sign(v) \quad (2.4)$$

The equations 2.3 and 2.5 imply that the vehicle is moving along an even surface. To take into account the slope along which the vehicle is moving, in [Schaltz, 2011] the following equation for the rolling resistance is given:

$$F_{rr} = \mu_{rr}F_Nsign(v) \quad (2.5)$$

where  $F_N = mg \cos(\theta)$  the normal force of the vehicle (Figure 2.1),  $\theta$  the angle of a slope,  $v$  the velocity of the vehicle, and  $\mu_{rr} = 0.01(1 + \frac{3.6}{100}v)$ , this equation predicts the values of  $\mu_{rr}$  with acceptable accuracy up to 128 km/h [Ehsani et al., 2005]

In [Ehsani et al., 2005] they provide the values for the rolling resistance coefficient  $\mu_{rr}$  (table 2.1), which do not take into account the variation of the speed

<sup>1</sup>a particular design of vehicular tire. In this design, the cord plies are arranged at 90 degrees to the direction of travel, or radially (from the center of the tire)

Table 2.1: Rolling resistance coefficients

Conditions	$\mu_{rr}$ rolling resistance coefficient
Car tires on concrete or asphalt	0.013
Car tires on rolled gravel	0.02
Tar macadam	0.025
Unpaved road	0.05
Field	0.1-0.35
Truck tires on concrete or asphalt	0.006-0.01
Wheels on rail	0.001-0.002

### 2.1.2.2/ AERODYNAMIC DRAG

Aerodynamic force is the part of the force due to the friction of the vehicle body moving through the air. It is a function of the frontal area, shape, <sup>2</sup>protrusions such as side mirrors, ducts and air passages, and many other factors. It is calculated as [Larminie et al., 2003]:

$$F_{ad} = \frac{1}{2} \rho A C_d v^2 \quad (2.6)$$

where  $\rho$  the density of the air,  $A$  is the frontal area ( $H \times W$  cf. Figure 2.2), and  $v$  the velocity.  $C_d$  the constant called drag coefficient that depends on the shape of the vehicle. The wind speed  $v_w$  is added to the equation 2.6 in [Schaltz, 2011] and [Ehsani et al., 2005] yielding the following formula for aerodynamic drag:

$$F_{ad} = \frac{1}{2} \rho A C_d (v + v_w)^2 \quad (2.7)$$

The typical values for the air drag (aerodynamic resistance) coefficient are presented in

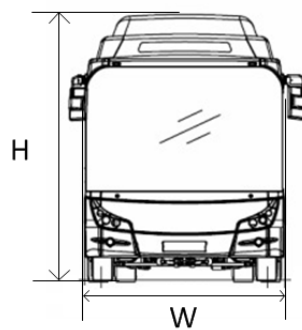


Figure 2.2: Bus. Front view

table 2.3 [Ehsani et al., 2005]. According to this table, the value of  $C_d$  for a bus varies from 0.6 to 0.7.

Though the density of the air varies with temperature, altitude and humidity, a value of 1.25 kg.m/s is a reasonable value to use in most of the cases.

<sup>2</sup>something that sticks out from something

Picture	Vehicle Type	$C_d$
	Open convertible	0.5-0.7
	Van body	0.5-0.7
	Ponton body	0.4-0.55
	Wedge-shaped body; headlamps and bumpers are integrated into the body, covered underbody, optimized cooling air flow	0.3-0.4
	Headlamp and all wheels in body, covered underbody	0.2-0.25
	K-shaped (small breakway section)	0.23
	Optimum streamlined design	0.15-0.20
	Trucks, road trains	0.8-1.5
	<b>Buses</b>	<b>0.6-0.7</b>
	Streamlined buses	0.3-0.4
	Motorcycles	0.6-0.7

Figure 2.3: Coefficients of aerodynamic resistance [Schaltz, 2011]

### 2.1.2.3/ GRAVITY FORCE

The gravity force is the weight of the vehicle defined as:

$$\vec{F}_g = m\vec{g} \quad (2.8)$$

For the case when vehicle is moving upon the slope, the projections of the gravity force to the  $x$  and  $z$  axis are given as:

$$F_{gx} = -mg \sin(\theta) \quad (2.9)$$

$$F_{gz} = -mg \cos(\theta) \quad (2.10)$$

### 2.1.2.4/ POWERTRAIN TRACTIVE EFFORT

The force propelling the vehicle forward is called tractive effort  $F_t$ . It is produced by the power train torque (engine or motor) and is transferred through transmission and final drive to the drive wheels.

Traction is defined as friction between a wheel and the surface it moves upon. It is the amount of force a wheel can apply to a surface before it slips. In order the wheel to roll, it must always be in contact with the ground to exert a force opposite to the force applied. So a rolling wheel is in static contact with the ground if it is not slipping. The instantaneous velocity of the contact point with the ground is equal to zero (non-slipping condition). As seen in the Figure 2.4, when a torque is applied to a wheel, it results in an applied force along the ground. If there is friction between the wheel and the ground, an equal and opposite force called the tractive force pushes back against the wheel. The applied force

is the force of the wheel on the surface. The tractive force is the force of the surface on the wheel.

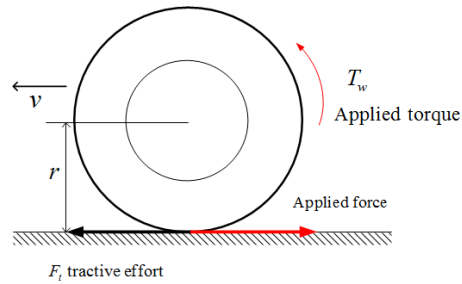


Figure 2.4: Forces acting on the wheel

An automotive power train consists of a power train (engine or electric motor), a clutch in manual transmission or a torque converter in automatic transmission, a gearbox (transmission), final drive, differential, drive shaft, and driven wheels (cf. Figure 2.5). The torque and rotating speed of the power plant output shaft are transmitted to the drive wheels through the clutch or torque converter, gearbox, final drive, differential, and drive shaft. The clutch is used in manual transmission to couple the gearbox to or decouple it from the power plant. The gearbox supplies a few gear ratios from its input shaft to its output shaft for the power plant torque–speed profile to match the requirements of the load. The final drive is usually a pair of gears that supply a further speed reduction and distribute the torque to each wheel through the differential.

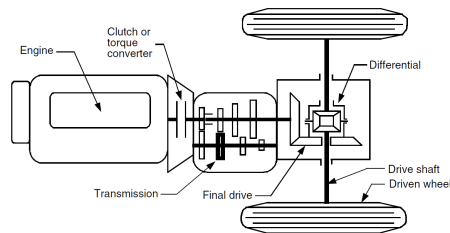


Figure 2.5: Conceptual illustration of an automobile power train [Ehsani et al., 2005]

The torque transmitted on the driven wheels, transmitted from the power plant, is expressed as:

$$T_w = i_g i_0 \eta_t T_m \quad (2.11)$$

where  $i_g$  is the gear ratio of the transmission,  $i_0$  is the gear ratio of the final drive,  $\eta_t$  efficiency of the driveline from the powerplant to the driven wheels,  $T_m$  the torque output from the power plant (engine or electric motor).

The friction the gear teeth and the friction in the bearings create losses in mechanical gear transmission. The following are representative values of the mechanical efficiency of various components [Ehsani et al., 2005]:

- Clutch: 99%
- Each pair of gears: 95 – 97%

- Bearing and joint: 98 – 99%

The total mechanical efficiency of the transmission  $\eta_t$  between the engine output shaft and drive wheels is the product of the efficiencies of all the components of the drive line. So the approximate average value of  $\eta_t$  that may be used is 90 %. The tractive effort on the driven wheels can be expressed as (cf. Figure 2.4):

$$F_t = \frac{T_w}{r} \quad (2.12)$$

where  $r$  is the radius of the wheel.

Substituting 2.11 into 2.12 yields the following:

$$F_t = \frac{i_g i_0 \eta_t T_m}{r} \quad (2.13)$$

### 2.1.2.5/ VEHICLE DYNAMICS CONSIDERING THE INERTIA OF THE ROTATING PARTS OF THE POWER PLANT

The Newton's Second law for rotational dynamics states that rotational acceleration  $\vec{\omega}$  is directly proportional to net torque  $\sum \vec{T}_i$  and inversely proportional to moment of inertia  $J$  or:

$$\sum_i \vec{T}_i = J \vec{\omega} \quad (2.14)$$

So to consider the inertia of the rotating parts of the power train (motor), we make use of this relation and deduce that the torque on the rotor of the motor is:

$$T_m = J_m \dot{\omega}_m \quad (2.15)$$

where  $J_m$  is the moment of inertia of the motor,  $\dot{\omega}_m$  angular acceleration of the motor.

For the vehicle the relation between the linear speed  $v$  and the rotational velocity of the wheel  $\omega_w$  is expressed as:

$$\omega_w = \frac{v}{r} \quad (2.16)$$

Angular velocity of the motor is equal:

$$\omega_m = i_g i_0 \omega_w \quad (2.17)$$

Combining the equations 2.16 and 2.17 we obtain:

$$\omega_m = i_g i_0 \frac{v}{r} \quad (2.18)$$

Similarly for the motor angular acceleration:

$$\dot{\omega}_m = i_g i_0 \frac{a}{r} \quad (2.19)$$

Substituting  $\dot{\omega}_m$  to the equation 2.15 we obtain:

$$T_m = J_m i_g i_0 \frac{a}{r} \quad (2.20)$$

Referring to the expression 2.11 (suppose  $\eta = 1$ ), we substitute  $T_m$  by the expression developed above and get:

$$T_w = i_g^2 i_0^2 J_m \frac{a}{r} \quad (2.21)$$

From the Figure 2.4 we see that force applied on the wheels is given:

$$F_w = \frac{T_w}{r} = i_g^2 i_0^2 J_m \frac{a}{r^2} \quad (2.22)$$

we add this component to the equation 2.2

$$\left(m + \frac{i_g^2 i_0^2 J_m}{r^2}\right)a = F_t - F_{rr} - F_{ad} - F_g \sin(\theta) \quad (2.23)$$

So the final expression for the vehicle dynamics is:

$$a = \frac{dv}{dt} = \frac{F_t - F_{rr} - F_{ad} - F_g \sin(\theta)}{\sigma m} \quad (2.24)$$

where  $\sigma$  is called the mass factor, considering the equivalent mass increase due to the angular moments of the rotating components. The mass factor is defined as:

$$\sigma = 1 + \frac{i_0^2 i_g^2 J_m}{mr^2} \quad (2.25)$$

#### 2.1.2.6/ BRAKING PERFORMANCE

The nonlinear dynamic model in [Shakouri et al., 2014] includes the braking torque  $T_b$  and looks as:

$$ma = \frac{1}{r}[T_t - T_b] - \frac{1}{2}\rho AC_d(v + v_w)^2 - \mu_{rr}mg \cos(\theta) - mg \sin(\theta) \quad (2.26)$$

The braking torque  $T_b$  can be calculated as:

$$T_b = K_b P_b \quad (2.27)$$

$K_b$  is the lumped gain for the entire brake system,  $P_b$  denotes the amount of pressure produced behind the brake disk. The pressure is described by the following dynamic equation:

$$P_b = 150K_c u_b - \tau_b \dot{P}_b \quad (2.28)$$

where  $K_c$  is the pressure gain,  $\tau_b$  is the lumped lag obtained by combining two lags relating to the dynamic of the servo valve and the hydraulic system and  $u_b$  is the brake position within the range  $[-1, 0]$ .

The braking performance is one of the most important characteristics of the vehicle. The braking force  $F_b$  originated from the brake system and developed on the tire-road interface is the primary retarding force [J.Y.Wong, 2008].

### 2.1.2.7/ ELECTRIC BATTERY SOC

The capacity of a battery  $Q$ , expressed in Ah, is the integral of the current that can be delivered under certain conditions. The capacity of the Businova battery is 110 Ah.

The state of the charge ( $SOC$ ) describes the amount of charge remaining in the battery and it is expressed as the percentage of its nominal capacity. The  $SOC$  rate at the discharge or charge current  $i$  during a time interval  $dt$  is expressed as follows:

$$\Delta SOC = \frac{idt}{Q(i)} \quad (2.29)$$

where  $Q(i)$  is capacity of the battery in Ah.

The current  $SOC$  of the battery is expressed as follows:

$$SOC = SOC_0 - \int \frac{idt}{Q(i)} \quad (2.30)$$

where  $SOC_0$  is initial value of the  $SOC$ .

As it is mentioned above, the number of charge/discharge cycles influences the lifespan of the battery. That's why is not sensible to completely charge and discharge the battery. However, in this case, in order to have the same battery duration, it is necessary to increase the capacity of the battery. There is a compromise to commit. For the Businova the operating  $SOC$  range is considered between 90% and 20%.

## 2.2/ SPEED PROFILE OPTIMIZATION

This section presents a review of the recent works who study the problem of finding optimal speed profiles in the vehicles, in order to minimize the fuel or battery consumption. The techniques discussed later can be applied either online or offline.

[Ozatay et al., 2014a] propose an optimization of the speed trajectory to minimize the fuel consumption and communicate it to the driver. The calculation is performed on a distinct computing platform called "cloud". In their approach driver sends the information of the intended travel destination to the cloud. In the cloud, the server generates a route, collects the associated traffic and geographical information, and solves the optimization problem by a spatial domain DP algorithm that utilizes accurate vehicle and fuel consumption models to determine the optimal speed trajectory along the route. Then, the server sends the speed trajectory to the vehicle where it is communicated to the driver.

The objective is to find the optimal velocity profile that minimizes the fuel consumption on over a travel distance  $D_f$ . For that, the optimization is performed in the spatial domain by means of the following transformation:

$$\dot{v} = \frac{dv}{dt} = \frac{dv}{dD} \cdot \frac{dD}{dt} = v \cdot \frac{dv}{dD} \quad (2.31)$$

The cost function is:

$$J_D = \int_0^{D_f} \frac{\dot{m}_{fuel}(T_e(D), \omega_e(D))}{v(D)} \cdot dD \quad (2.32)$$

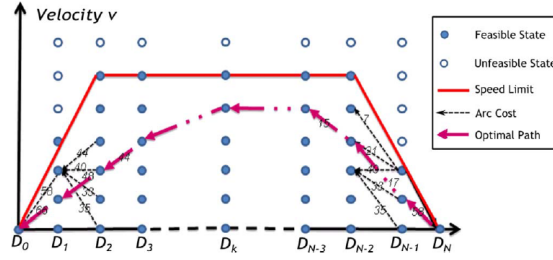


Figure 2.6: Schematic representation of the DP algorithm [Ozatay et al., 2014a]

The state variable is velocity  $v$ . The control variables are engine torque  $T_e$  and braking force  $F_{brake}$ . The schematic representation of the DP is presented in Figure 2.6. This paper is interesting in many aspects:

- A use of DP to obtain an optimal velocity profile. Knowing that DP provides a global optimal solution [Panday et al., 2014], this method ensures the *real* optimal velocity profile
- Communication of an optimal velocity profile to a driver
- Although the technique is tested on the conventional vehicle, it can be interesting to implement it to the hybrid one.

[Tokekar et al., 2014] studied the problem of finding velocity profiles for a car-like robots so as to minimize the energy consumed while traveling along a given path, whereas [Dib et al., 2014] treats an energy management problem for an electric vehicle compliant with online requirements for “eco-driving application”. The difference between two papers is that the robot is fully autonomous, and the electric vehicle is controlled by a driver, but he receives the velocity profile proposed by an eco-driving system. The energy consumption in the vehicle is strongly depended on the driver’s behavior (driving style), which can be formulated as the optimal control problem. This problem consists of the minimization of the vehicle energy consumption (which can be considered as the battery energy  $E_{bat}$ ) over a time and a distance horizon, by acting on the driver’s outputs. We need to find the control policy  $u(t) := (\tau(t), F_{brk}(t)) \in \mathbb{U}(t) \subset \mathbb{R}$

$$\min E_{bat} = \int_0^T P_{bat}(u(t), v(t), x(t)) dt \quad (2.33)$$

under the system dynamics:

$$\begin{aligned} \dot{v}(t) &= f(v(t), u(t), t) - G(x(t)), \\ \dot{x} &= v(t) \end{aligned}$$

and the following constraints:

$$\begin{aligned} x(0) &= v_i, v(T) = v_f, \\ x(0) &= 0, x(T) = D, \\ v_{min}(x(t)) &< v(t) < v_{max}(x(t)), x(t) \in [0, D] \end{aligned}$$

where  $x(t)$  is the traveled distance and  $v(t)$  is the speed of the vehicle, respectively. The functions  $P_{bat}(\cdot)$  and  $f(\cdot)$ , as well as the set  $\mathbb{U}(t)$ , depend on the vehicle and the powertrain characteristics. The parameters  $T$  (final time),  $D$  (distance),  $v_i$  (initial speed),  $v_f$  (final speed) define the particular segment, together with the function  $G(x(t))$  (gravitational force) and the speed limits  $v_{min}, v_{max}$ .

The motion of the vehicle can be described by the equation :

$$f(v(t), u(t), t) = \frac{\gamma\tau(t)\eta^{sign(\tau(t))}}{mR_t} - \frac{\rho_a A_f C_d}{2m} v(t)^2 - gc_r - \frac{F_{brk}(t)}{m} \quad (2.34)$$

$$G(x(t)) = g \sin(\alpha(x(t))) \quad (2.35)$$

where  $m$  is the vehicle mass (curb weight<sup>3</sup> with a driver),  $\eta$  and  $\gamma$  are the efficiency and the constant ratio of the transmission respectively,  $\rho_a$  external air density,  $A_f$  the vehicle frontal area,  $C_d$  is the aerodynamic drag coefficient,  $c_r$  the rolling resistance,  $R_t$  the wheel radius,  $\alpha(x)$  the road slope, and  $g$  is the acceleration of the gravity.

We re-write the equation 2.34 as follows:

$$\dot{x} = v(t) \quad (2.36)$$

$$\dot{v} = h_1 \tau(t) \eta^{sign(\tau(t))} - h_2 v(t)^2 - h_0 - w(t) \quad (2.37)$$

where

$$h_1 := \frac{\gamma}{mR_t}, h_2 := \frac{\rho_a A_f C_d}{2m},$$

$$h_0 := g \sin(\alpha(x(t))) + gc_r, w(t) := \frac{F_{brk}(t)}{m}$$

The power consumption is defined as:

$$P_{bat}(\tau(t), v(t)) = b_1 \tau(t) v(t) + b_2 \tau(t)^2 \quad (2.38)$$

Finally the optimal control problem to find optimal  $(\tau(t), w(t))$  is formulated as follows:

$$\begin{cases} \min \int_0^T (b_1 \tau(t) v(t) + b_2 \tau(t)^2) dt \\ \dot{v} = h_1 \tau(t) \eta^{sign(\tau(t))} - h_2 v(t)^2 - h_0 - w(t) \\ \dot{x} = v(t) \\ x(0) = v_i, & v(T) = v_f, \\ x(T) = 0, & x(T) = D, \\ \tau_m(v(t)) \leq \tau(t) \leq \tau_M(v(t)) 0 \leq w(t) \leq W \end{cases} \quad (2.39)$$

where  $W$  is the upper limit of the deceleration  $w$ ,  $\tau_m$  and  $\tau_M$  minimum and maximum value of the motor torque. This approach permits to obtain the optimal velocity profiles which minimizes the energy consumption of the electric battery. This idea resonates with the initial aim of our optimization problem: obtain the optimal velocity profile. Furthermore, the problem may be treated online and/or offline. Some ideas were proposed by [Dib et al., 2014] which are discussed below.

<sup>3</sup>Curb weight is the total weight of a vehicle with standard equipment, all necessary operating consumables such as motor oil, transmission oil, coolant, air conditioning refrigerant, and a full tank of fuel, while not loaded with either passengers or cargo.

The optimal problem can be solved either offline or online. In offline case, a complete trip is completely identified by their respective parameters  $T_k$ ,  $D_k$ , etc. These data is normally given by the driving cycle profile (the vehicle speed  $v(t)$ ). An offline optimization can be used to *assess* or *qualify* the recorded driving behavior by comparing its energy consumption  $E_{bat}$  with the minimum energy consumption  $E_{bat,min}$  that would have been necessary to complete the trip under *the same* constraints. An eco-driving indicator (EDI) [Dib et al., 2012]:

$$EDI = \frac{E_{bat,min}}{E_{bat}} \quad (2.40)$$

A similar optimization can be also performed online during the vehicle trip, keeping in

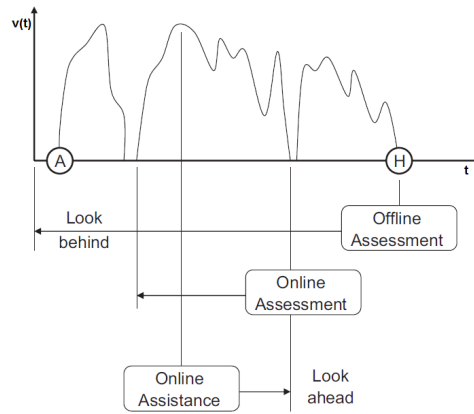


Figure 2.7: Scheme of the offline assessment, online assessment, and online assistance scenarios [Dib et al., 2014]

mind the trip characteristics are not known in advance. The first approach is *online assessment*, when the indicator informs the driver about his behavior after a segment (a part) of the trip is completed. Another scenario is called *online assistance to the driver*, where the optimization is performed continuously in time. At time  $t$ , the optimization is performed for a segment defined by  $v_i = v(t)$  and  $T$ ,  $D$ ,  $v_f$  as a function of the next breakpoint. The latter must be estimated using geo-localization, other environmental information (traffic, signals), and possibly route planning by the driver himself.

[Ozatay et al., 2014b] proposed an analytical solution for a search of the optimal speed profiles in order to minimize energy consumption for trajectory with variable road grade using Hamiltonian function which is defined as:

$$H_i(z(t), u(t), \lambda(t)) = L(z(t), u(t)) + \lambda^T f_i(z(t), u(t)) \quad (2.41)$$

where,  $z$  system states,  $L(z, u)$  is the cost function to be minimized (in the given case, fuel consumption),  $\lambda$  Lagrange multipliers,  $i = 1, 2, \dots, M - 1$ , where  $M$  is the number of different grade regions. The results of this optimization were compared to the results obtained by Dynamic Programming (DP). The results have shown that the analytical and DP solutions generate very close velocity trajectories. However, the calculation time of analytical solution is 560x times faster than the DP solution, and makes possible its real time implementation.

[Sun et al., 2015a] propose a velocity prediction strategy. The prediction process is performed over each receding horizon, and the predicted velocities are used for fuel economy

optimization of a power-split HEV. The velocity prediction approach makes use of a neural network technique. The eight driving cycle samples (four highway types and four urban types) are used for training the neural network. Considering a 1 s time step, at time step  $k$ , the cost function  $J_k$  is formulated as follows:

$$J_k = \int_{k\Delta t}^{(k+H_p)\Delta t} ([\dot{m}_{fuel}(u(t))]^2 + \lambda O(t)) dt \quad (2.42)$$

where  $H_p$  is the prediction horizon length, which is herein equal to the control horizon length;  $O(t)$  is the engine ON/OFF switching time, and  $\lambda$  is the penalty for engine ON/OFF switching. The control procedure is described as follows:

1. A horizon velocity predictor is used to estimate the control horizon driving profile, based on current velocity request  $V_k$  and historical velocities. Assume  $f_p$  is the velocity prediction function

$$V_{predict} = f_p(\dots, V_{k-3}, V_{k-2}, V_{k-1}, V_k) = [V_{k+1}, V_{k+2}, \dots, V_{k+H_p-1}]. \quad (2.43)$$

2. Given  $V_{predict}$ , calculate the optimal control policy minimizing the objective function
3. Apply the first element of the control policy. Feedback states, and repeat the control procedure.

For their experiments they consider that the vehicle is not equipped with any radar or GPS. the road grade is zero and future driving profiles are completely unknown. The results of a neural network based velocity prediction algorithm is demonstrated in Figure 2.8.

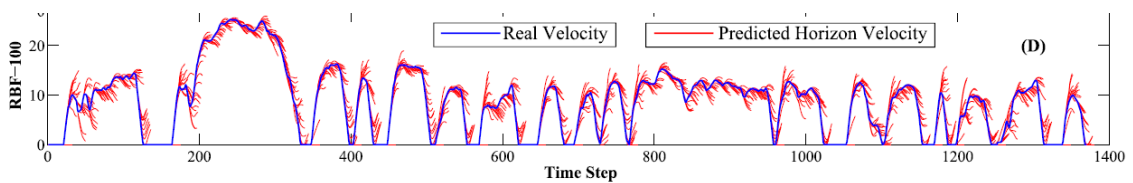


Figure 2.8: Neural network based velocity prediction algorithm results [Sun et al., 2015a]

[Kim et al., 2009] use model predictive control for the velocity and powersplit optimization in HEVs. A given velocity profile is optimized by setting the constraints on the velocity and the acceleration of the vehicle. This allows to smooth the current velocity profile without generating a new one. The authors [Van Keulen et al., 2010a] proposed a method that solves the velocity optimization problem for HEVs, based upon information from Global Navigation Satellite-based Systems, assuming that the velocity trajectory has a predefined shape. Although this method is used for HEVs, the authors do not deal with the energy management optimization aspect.

## 2.3/ POWER SPLIT OPTIMIZATION

### Definition 5: Energy Management Strategy

Energy Management Strategy (EMS) for HEV is a control algorithm or a set of control algorithms, based on either deterministic rules, or optimization, or heuristic approaches, or others, that aims to provide an appropriate power/torque split complied with the energy minimization/optimization objectives and constraints of the system.

The objective of the section is to review the techniques of the energy management of hybrid vehicles and the definition of the most used optimization criteria used recently in the scientific literature.

In [Murphey, 2008a], the author overviews the vehicle power management technologies. He claims that the application of the optimal control theory to power management on hybrid electric vehicles has been the most popular approach, which includes linear programming, optimal control and especially dynamic programming (DP) [Pei et al., 2013][Rousseau, 2008][Chen et al., 2014a][Song et al., 2015] have been widely studied and applied to a broad range of vehicles. However, in general, these techniques don't offer the on-line solution, because they assume that the future driving cycle is entirely known. Some authors propose the fuzzy logic rules based on the results of DP optimization [Schouten et al., 2002][Guemri et al., 2014][Zhang et al., 2014]. Other papers [Zhang et al., 2014] [Chen et al., 2014b] suggest take into account the road type and the driver behavior. Notably, they propose using the neural networks to learn different road profile in order to be able to apply the most suitable one for online optimization. Some interesting ideas from the mentioned references will be discussed in what follows below. Several energy management strategies have been suggested to manage the distribution of power between two sources [Kamal et al., 2017] [Ouddah et al., 2017] [Abdrakhmanov et al., 2017a].

According to the bibliographical review, the energy management strategies can be generally, classified into two categories (cf. Figure 2.9)[Wirasingha et al., 2011], [Salmasi, 2007] : heuristic approaches (algorithms based on the defined rules) and optimal approaches.

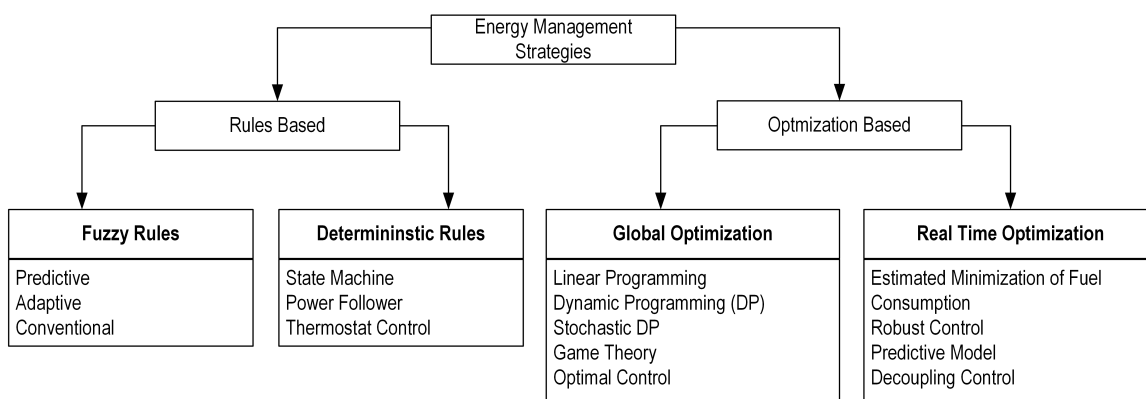


Figure 2.9: Energy Management approaches in hybrid vehicles

[Schouten et al., 2002] designed a fuzzy controller that is built based on the driver command, the state of the charge of the battery, and the motor/generator speed. A set of nine fuzzy rules was derived from the analysis of static engine (internal combustion engine) efficiency map and electric motor efficiency map with input of vehicle current state such as *SOC* and driver's command. This technique is interesting from the real-time implementation point of view. The disadvantage is that it is solely based on the static efficiency maps, which can be not optimal in the realistic dynamic environment.

[Kitayama et al., 2015b] propose a torque control strategy coupled with optimization for a parallel hybrid electric vehicle (HEV). A function to control the driving modes is introduced. This function controls the driving modes (electric motor (EM) driving, ICE driving, and ICE assisted by EM) for reducing fuel consumption and exhaust emissions. This function depends on the several variables that should be optimized (engine/motor speeds, engine/motor torques and demanded torque). This work reveals an interesting idea of torque distribution: the motor torque and speed thresholds are defined in order to switch from one mode to another.

[Rousseau, 2008] treat the energy optimization in the HEV with parallel architecture that has 2 sources of propulsion: electric motor and heat engine.

The motor torque  $T_m$  is controlled by the voltage  $U_c$ , which is regulated by the proportional gain of the tension of inverter  $\lambda(t)$ . For the minimization of instantaneous consumption of the fuel  $L$  during the time  $t \in \{0, T\}$  the optimization problem is formulated as follows:

$$\min_{u \in U} J(u) := \int_0^T L(t, \lambda(t), T_m(t)) dt + \phi(U_c(T), T) \quad (2.44)$$

with

$$U_c(t) = \begin{cases} f_1(U_c(t)), \lambda(t), t, & \text{if } T_m(t) > 0 \\ f_2(U_c(t), T_m, t), & \text{if } T_m(t) < 0 \end{cases} \quad (2.45)$$

$$T_m^{\min} \leq T_m \leq T_m^{\max} \quad (2.46)$$

$$U_c^{\min} \leq U_c \leq U_c^{\max} \quad (2.47)$$

$\phi$  is the constraint function. The electric engine is controlled either by  $\lambda(t)$  for the positive torque (motoring mode of the electric machine), or by  $T_m$  for the negative torque (for the regeneration mode). The functions  $f_1$  and  $f_2$  may be described by the dynamic equations of the electric motor.

D. Pei [Pei et al., 2013] proposed an approach for determining the SOC-dependent equivalent cost factor in HEV supervisory control problems using globally optimal DP. The authors in [Song et al., 2015] use the DP approach to deal with the global optimization problem for deriving the best configuration and energy split strategies of a hybrid energy storage system (HESS), including a battery and a supercapacitor (SC), for an electric city bus. The SC voltage  $V_{SC}$  is the primary state in the DP process, and  $V_{SC}$  is discretized to 250 states in its operation range (from  $0.5V_{SC,max}$  to  $V_{SC,max}$ ) as it's shown in Figure 2.10. The cost function  $J_{bat,loss}$  is the battery capacity loss at any discrete time  $k$ , derived from the dynamic degradation model of the *LiFePO<sub>4</sub>* battery:

$$\min \{ J_{bat,loss}(k) = \frac{|I_{bat}(k)| T_s}{3600} z A^{\frac{1}{z}} e^{-\left(\frac{E_a + B \cdot C_{Rate}(k)}{z R T_{bat}}\right)} Q_{loss}(k-1)^{\frac{z-1}{z}} \} \quad (2.48)$$

where  $T_s$  is the sample time,  $I_{bat}$  battery current,  $A$  pre-exponential factor,  $E_a$  activation energy,  $R$  gas constant,  $T_{bat}$  absolute temperature (K),  $C_{Rate}$  is the battery discharge rate,  $z$  the time factor,  $Q_{loss}$  the percentage of the battery capacity loss.

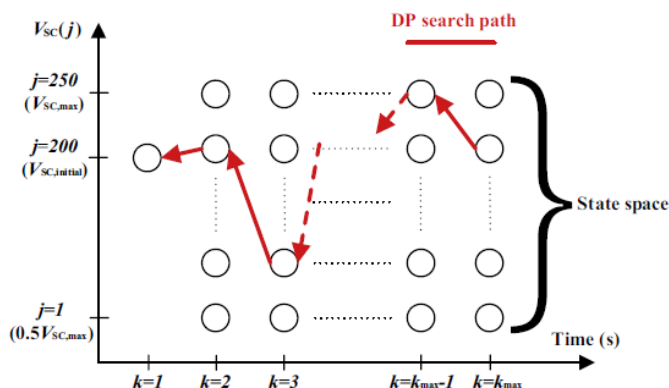


Figure 2.10: DP approach flow-chart [Song et al., 2015]

Although the dynamic programming can find the global optimization solution, it is still difficult to be implemented in practical applications due to its high computational cost. However, the DP results can provide a good intuitive guidance and help us to propose a near-optimal energy management strategy. Therefore, some authors, e.g., in [Zhang et al., 2014] and [Chen et al., 2014b], use the optimal solution of the offline dynamic programming strategy in order to build an intelligent energy management strategy based on fuzzy logic rules or neural networks that can be implemented online.

[Zhang et al., 2014] proposed a dynamic programming-rule based (DPRB) algorithm to solve the global energy optimization problem in a real time controller of a plug-in hybrid electric bus (PHEB). The whole diagram of the DPRB scheme is presented on the Figure 2.11. Part I:

- For a rule-based (RB) control strategy control parameters are selected according to the position and battery  $SOC$  of PHEB;
- The trajectory is divided into  $N$  segments;
- Control parameters between station  $st_n$  and station  $st_{n+1}$  are selected as  $Rule^n$ , which is determined by the  $SOC S^n$  at station  $st_n$ .

In Part II:

- A control grid is build for a typical city route according to the station locations and discrete  $SOC$  levels, and an off-line DP with historical running information of the driving cycle is used to deduce optimal control parameters of RB on all points of the control grid;
- Genetic algorithm is used to replace the quantization process of DP permissible control set.

A bus route is divided into  $N$  sections according to the bus station locations. The state variable is defined as follows:

$$x(st_n) = SOC(st_n) \quad (2.49)$$

where  $SOC(st_n)$  is the battery  $SOC$  at station  $st_n$ . According to the battery characteristics it is not desirable to charge it above 90% and discharge lower than 30%.

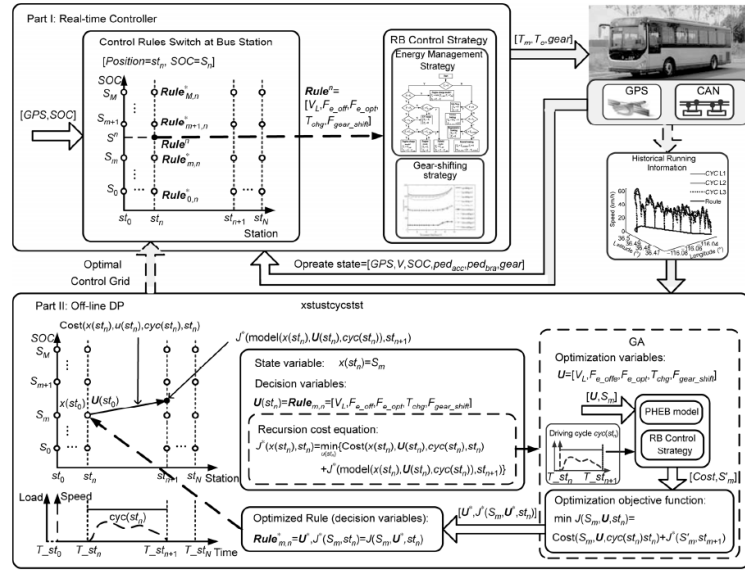


Figure 2.11: Schematic diagram of DPRB [Zhang et al., 2014]

The integral energy consumption cost function  $J$  expressed in yuan:

$$J = \sum_{n=0}^{N-1} Cost(x(st_n), u(st_n), cyc(st_n), st_n) \quad (2.50)$$

where  $Cost(\cdot)$  represents the energy consumption cost of PHEB running on the section between station  $st_n$  and station  $st_{n+1}$ , and it is determined by the decision variables  $u(st_n)$  and the driving cycle  $cyc(st_n)$ . The cost is expressed as follows:

$$\begin{aligned} Cost(x(st_n), u, cyc(st_n), st_n) = & \\ & p_f \int_{T_{st_n}}^{T_{st_{n+1}}} \frac{1}{10^6} Q_g dt + \frac{p_e}{\eta_{elec}} \int_{T_{st_n}}^{T_{st_{n+1}}} \frac{1}{3.6 \times 10^6} P_{ess} dt = \\ & \frac{p_f}{10^6} \int_{T_{st_n}}^{T_{st_{n+1}}} \frac{T_e \omega_e b}{367.1 \rho_g g} dt + \frac{p_e}{3.6 \times \eta_{elec}} \int_{T_{st_n}}^{T_{st_{n+1}}} V_{OC} I dt \end{aligned} \quad (2.51)$$

where  $p_f$  and  $p_e$  are the market price of compressed natural gas (CNG) and electricity respectively,  $Q_g$  consumption rate of CNG engine,  $V_{OC}$  and  $I$  are open-circuit voltage and battery internal current, respectively,  $P_{ess}$  power of energy storage system,  $\eta_{elec}$  power grid efficiency.

According to the authors, the given algorithm can save from 5.30% to 7.87%. This paper regard the case of the urban bus, which close to our topic with respect to Busnova project. For a longtime distance (a whole day trajectory) the path is divided by the sections, corresponding to the distances between the bus stations. However, the main idea is the use of DP optimization results as the base for the setting the near-optimal control based on fuzzy logic rules.

[Chen et al., 2014b], by-turn, proposes a real-time intelligent energy management controller to improve the fuel economy of a power-split plug-in hybrid electric vehicle (PHEV). It consists of two neural network (NN) modules that are trained based on the optimization

results obtained by DP methods, considering the trip length and duration. Three types of driving cycles are classified: highway, urban, and urban-congested. Based on whether the trip length and duration are known or unknown, the controller will choose the corresponding NN module to output the effective battery current commands to realize the energy management.

The objective of their optimization is to minimize the fuel consumption of a power-split PHEV during a certain trip, which is expressed as follows:

$$\min F = \min \sum_{t=0}^{t=n} m_f(t, v) \quad (2.52)$$

where  $F$  is the total fuel consumption,  $n$  is the trip duration, and  $m_f$  is the fuel rate determined by engine speed  $\omega_e$  and engine torque  $T_e$  as follows:

$$m_f = f(T_e, \omega_e) \quad (2.53)$$

To realize DP, some constraints should be considered, such as engine maximum power  $P_e$ , engine maximum and minimum speed  $\omega_e$ , battery maximum charge and discharge current, and a motors maximum and minimum power  $P_{mot}$  as follows:

$$\begin{cases} 0 \leq P_e \leq P_{max}, \omega_{min} \leq \omega_e \leq \omega_{max} \\ P_{mot1-min} \leq P_{mot1} \leq P_{mot1-max} \\ P_{mot2-min} \leq P_{mot2} \leq P_{mot2-max} \\ P_{b-min} \leq P_b \leq P_{b-max} \\ C_{b-min} \leq C_b \leq C_{b-max} \end{cases} \quad (2.54)$$

where  $C_b$  is the battery capacity in ampere-second. The steps to realize DP are shown in Figure 2.12. The results obtained owing to DP are used in order to train two neural

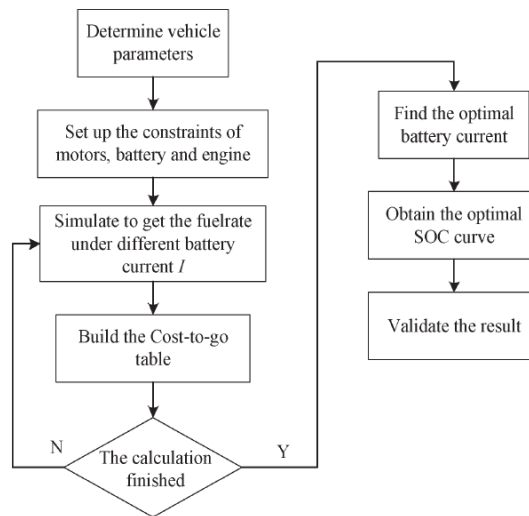


Figure 2.12: Procedure to realize DP [Chen et al., 2014b]

networks controllers - N1 and N2. The major difference between N1 and N2 is that N1 needs the trip information: trip duration and trip length. The function of N1 is to output the battery current command on the basic trip information. It needs the knowledge of

the length and trip duration in advance. The N1 controller contains 11 variables in order to train the controller: vehicle speed, driveline power, battery SOC, average speed, idle rate (the ratio of vehicle idle time during a certain time range), maximum and minimum acceleration, also trip length, trip duration, current drive length, and current drive time.

Compared to N1, N2 does not consider the trip information and only has seven inputs: vehicle speed, driveline power, battery SOC, average speed, idle rate, maximum acceleration, and minimum acceleration. The switch between two controllers is shown on the Figure 2.13. The interesting idea is that the NN modules were learned by three road

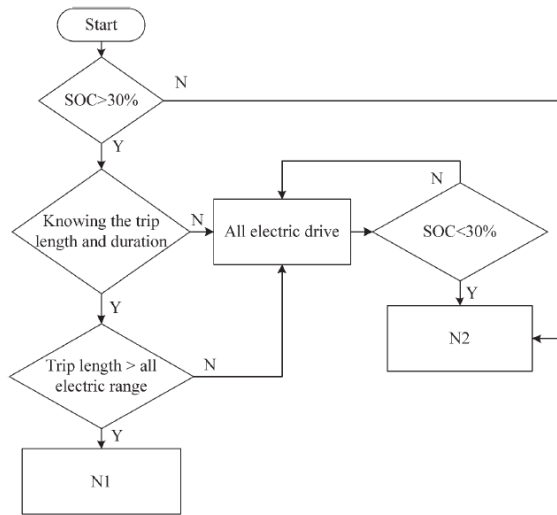


Figure 2.13: N1 and N2 switch algorithm [Chen et al., 2014b]

profiles and six speed profiles. It ensures that the controller during the trip approaches the optimum of its performance.

[Chen et al., 2014a] developed a real-time fuzzy logic controller for an extended-range electric vehicle. Extended-range electric vehicle is a vehicle that functions as a full-performance battery electric vehicle when energy is available from an onboard RESS (rechargeable energy storage system) and having an auxiliary energy supply that is only engaged when the RESS energy is not available [Tate et al., 2008]. Particularly, the range extender consists of an engine and a generator (genset), which provides an extra electric power for charging the battery. The proposed strategy employs a driving pattern recognition technique of switching among the control rule sets extracted from DP results of each representative driving pattern.

A single state variable was defined:

$$\begin{aligned}
 x(k+1) &= f(x(k), u(k)) \\
 x &= SOC \\
 u &= P_{gs_{elec}}
 \end{aligned}$$

where the state variable  $x$  is battery SOC; and the control input  $u$  is the electric demand for genset. In this paper  $SOC$  is constrained between 20% and 80%.

Two different cost functions were defined - battery energy losses  $L_{inst}^b$  and fuel energy

losses  $L_{inst}^f$ :

$$L_{inst}^b = \int_k^{k+1} R_{tot} i_b^2 dt \quad (2.55)$$

$$L_{inst}^f = \int_k^{k+1} (\dot{m}_f Q_{HV} - 2\pi T_{eng} N_{eng}) dt \quad (2.56)$$

where  $i_b$  is the battery current;  $\dot{m}_f$  is the fuel mass flow rate of engine;  $Q_{HV}$  is the heating value of fuel; and  $T_{eng}$  and  $N_{eng}$  are the engine torque and speed, respectively.

The system is constrained by the following relations:

$$\begin{cases} SOC_{min} \leq SOC(k) \leq SOC_{max} \\ P_{b,chg}(SOC(k)) \leq P_b(k) \leq P_{b,disch}(SOC(k)) \\ T_{m,min}(\omega_m(k), SOC(k)) \leq T_m(k) \leq T_{m,max}(\omega_m(k), SOC(k)) \\ T_{gs,min}(\omega_{gs}(k)) \leq T_{gs}(k) \leq T_{gs,max}(\omega_{gs}(k)) \\ \omega_{gs,min} \leq \omega_{gs}(k) \leq \omega_{gs,max} \end{cases} \quad (2.57)$$

where  $P_b$  is the battery power which is positive for battery discharging;  $P_{b,disch}$  and  $P_{b,chg}$  are the power limits for battery discharging and charging, respectively;  $T_m$  is the motor torque;  $T_{gs}$  and  $\omega_{gs}$  are the torque and rotational speed of genset respectively which should be limited to satisfy the operating constraints of engine and generator.

Based on Bellman's principle of optimality, the two point boundary DP processes are solved backwards from the final state to the initial state by decomposing it into a sequence of simpler minimization problems that are illustrated on the Figure 2.14 and expressed in equations 2.58-2.60.

At step  $N$  (final time step)

$$J_f^*(N) = g(x(N)) \quad (2.58)$$

At step  $k$ , for  $1 \leq k \leq N - 1$

$$J_n^*(k) = \min_{u(k)} [L_{inst,n}(k) + J_n^*(k+1)] \text{ for } n = 1 : m \quad (2.59)$$

At step 0 (initial time step)

$$J_i^*(0) = h(x(0)) + \min_{u(0)} [L_{inst,n}(0) + J_n^*(1)] \text{ for } n = 1 : m \quad (2.60)$$

where the subscripts  $i$  and  $j$  denote for the initial and final state, respectively;  $J^*$  denotes for the cost-to-go for each feasible state variable in each time step;  $m$  is the number of the feasible  $SOC$  grids;  $g$  is the final state cost which is zero for the final state  $x(N) = 0.2$  and becomes larger for the initial state deviated from 0.2;  $h$  is the initial state cost which is zero for the initial state  $x(0) = 0.8$  and becomes larger for the initial state deviated from 0.8.

Saerens in [Saerens et al., 2013] proposes several cost functions to asses the consumption of the fuel in the cruise-control mode (eco-cruise control) for the conventional one engine vehicle. Essentially, the goal is minimize the fuel consumption  $L$  [kg/m]. Given a travel distance  $s$  [m] this results in:

$$\min_{v(\cdot), s(\cdot), P(\cdot)} \int_0^T L ds, \quad L = \frac{\dot{m}_f}{v} \quad (2.61)$$

with  $v$  velocity of the vehicle,  $P$  the power of the engine,  $\dot{m}_f$  the fuel rate.

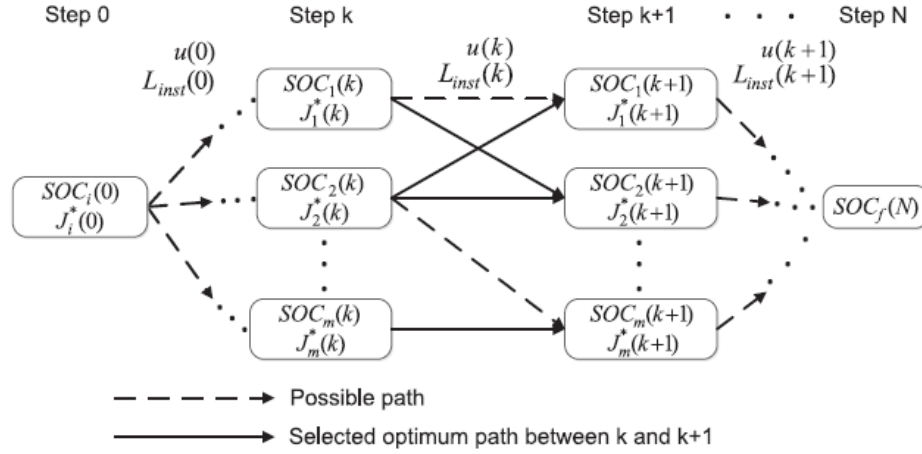


Figure 2.14: DP processes [Chen et al., 2014a]

However, such cost function may result in the velocity that significantly differs from the reference velocity. This is not desirable in terms of the cruise control. One of the solutions to penalize a deviation from the reference velocity:

$$L = \frac{\dot{m}_f + \phi(v_{ref} - v)^2}{v} \quad (2.62)$$

This cost function may be interesting if we design a cruise control for the Businova, in order to reduce the driver's behavior influence on the fuel consumption.

[Hellström et al., 2009] propose a cost function for the heavy truck that must deliver the load in minimum of time, consuming less possible fuel. So bearing in mind these constraints, they also added a constraint to the maximum acceleration from the security consideration. So finally, the cost function proposed is:

$$\min_{u \in U} J(u) := \int_0^T (\dot{m}_f(u) + \beta t + \gamma a) dt \quad (2.63)$$

The introduction of the acceleration to the cost function may be justified by the comfort of passengers, which is very important for the case of Businova.

[Fang et al., 2011] proposed a methodology based on the non-dominated sorting genetic algorithm II (NSGA II) to achieve parameter optimization for powertrain components and control system simultaneously and successfully find the Pareto-optimal solutions set. The optimization problem aims at improving fuel economy and reducing the emissions ( $CO$ ,  $HC$ ,  $NO_x$ ) without sacrificing vehicle performance. The author says that the relation between  $[FC, HC, CO, NO_x]$  and  $[\text{engine speed, torque}]$  cannot be described by any specific analytical function ( $FC$  stands for fuel consumption). The relation is obtained by experiments and graphs (cf. Figure 2.15).

[Musardo et al., 2005] propose an Adaptive ECMS (Equivalent Consumption Minimization Strategy) which provides near optimal solution, compared to DP solution. ECMS approach consists of evaluating the instantaneous cost function as a sum of the fuel consumption and an equivalent fuel consumption related to the  $SOC$  variation. The cost function is defined as follows:

$$J = \dot{m}_{ice}(P_{ice}(t)) + \xi(P_{em}(t)) \quad (2.64)$$

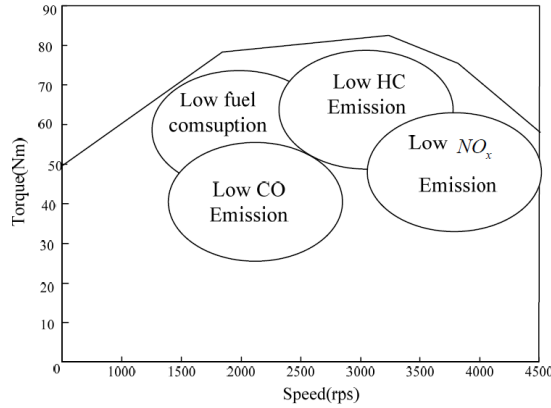


Figure 2.15: ICE operating points [Fang et al., 2011]

where the function  $\xi(P_{em}(t))$  represents the fuel equivalent of the electric energy. The equivalence between electrical energy and the fuel energy is basically evaluated by considering average energy paths leading from the fuel to the storage of electrical energy. The assumption behind this approach is that every variation in the  $SO C$  will be compensated in the future by the engine running at the current operating point. The equivalent fuel flow owing to the use of EM is:

$$\gamma = \frac{1 + \sin(P_{em}(t))}{2} \quad (2.65)$$

$$\xi(P_{em}(t)) = \gamma \cdot s_{dis} \frac{1}{\eta_{batt}(P_{em})\eta_{em}(P_{em})} \frac{P_{em}(t)}{H_{LHV}} + (1 - \gamma) \cdot s_{chg} \cdot \eta_{batt}(P_{em})\eta_{em}(P_{em}) \frac{P_{em}(t)}{H_{LHV}} \quad (2.66)$$

where  $s_{dis}$  and  $s_{chg}$  represent the equivalence factors when the electrical energy is discharged, respectively recharged, and considered as control parameters of the ECMS approach. The drawback of this approach is that the optimal choice of  $(s_{dis}, s_{chg})$  is different for each driving cycle. So the authors presented an on-the-fly algorithm for the estimation of the equivalence factors according to the driving conditions. The main idea is to periodically refresh the control parameters according to the current road load, so that the  $SO C$  is maintained within the boundaries and the fuel consumption is minimized. The algorithm identifies the mission that the vehicle is following and determines the optimal equivalence factors for the current mission. The mission is built combining the past and predicted data. In the presence of the altitude variation, the prediction of the velocity prediction is not enough, and external information from GPS is used to predict the slopes. At each instant when the equivalence factors must be updated, the algorithm first builds the current mission combining past and predicted vehicle speed and GPS data, then determines the control parameters that minimize the fuel consumption, while respecting charge sustainability constraint. Their studies showed that the optimal choice of  $(s_{dis}, s_{chg})$ , such that  $s_{dis} = s_{chg}$  minimizes the calculation time, which makes it possible for a real time application and barely influences optimality.

As we could see from the references mentioned above, one of the powerful techniques that provides the global optimal solution is a Dynamic Programming. Depending on the

aim of the optimization, different cost functions, as well as different state variables can be chosen. Due to its high computational cost the DP is difficult to apply online. However, the solutions obtained by the DP can be an indicator for an online intelligent regulator based on the fuzzy logic rules, neural network, genetic algorithm etc. In the previous papers, the DP was used in order to find the optimal control inputs in order to provide optimal performance (minimize the fuel consumption or battery charging/discharging).

## 2.4/ CONCLUSION

This chapter described the modeling techniques of a hybrid vehicle, as well as its powertrain components for a complex multi-source powertrain architecture of Businova.

When it comes to energy optimization in hybrid vehicles, most researches rely solely either on powersplit optimization, or speed profile optimization. Combination of both these two problematics may lead to a higher energy/fuel economy. The question is what is the price in terms of calculation time, feasibility, level of assisting in driving, optimality? This idea is explored in the following chapters.



# GLOBAL CONTROL ARCHITECTURE AND MAIN HYPOTHESIS

---

## **Abstract**

The main objective of this chapter is to introduce the proposed overall control architecture. The control scheme is detailed and explained to lead to the logics of the interaction of different blocks composing this architecture. This chapter also describes the main traction components of the Businova, as well as the main assumption made for developing the proposed energy management strategies later.

---

## 3.1/ PROBLEM STATEMENT

The Businova is an urban/suburban transportation system. Consequently, it is subject to frequent starts and stops in its environment. Bearing in mind the heavy weight of the system, these phases are considerably energy consuming. Beside an efficient powersplit control, a smooth driving velocity transition also ensures a fuel economy, as well as passengers' comfort. However, following an optimal speed profile in a cluttered environment is not always possible due to the interaction of the bus with other vehicles and infrastructure (e.g., traffic jam, traffic lights, pedestrian passage, etc.). Hence, the hybrid system can be supplied with one more layer of "intelligence" by adding a feature related to an ADAS (cf. definition 1.3) to diminish a human intervention and improve active safety, particularly in complex situations, and/or to enhance the driver's sense of comfort. To this end, ACC has reached a good quality in driver assistance. A large part of the driver's tasks can be assigned to an automatic system and the driver relieved to a substantial degree. Based on CC, ACC adjusts the vehicle speed to the surrounding traffic (cf. section 1.3.1). It accelerates and decelerates automatically when a preceding vehicle is within an inter-vehicular less than a certain value and is traveling at the speed which is less than the one desired by the driver. As ACC is limited for relatively high velocities, this technology can be ameliorated by including a "Stop&Go" functionality (cf. section 1.3.2). Stop&Go driving can be said to be a typical maneuver in city streets, where, for instance, speed is reduced to stop the car at a red traffic light [Murphey, 2008b]. The automatic control of the velocity of the vehicle is subject of section 6. Indeed, the main focus of the PhD research is development of an optimal EMS for a hybrid vehicle and the automatic control of this possible degree of freedom to enhance the energy efficiency of the Businova will be used once we exploit the most efficient vehicle power-split according to imposed velocity (by

the driver or according to standard velocity profile). An optimal EMS must ensure that, in spite of the environmental conditions (road slope, wind speed, etc.) and the current bus' weight (which depends on the number of passengers), the bus has to operate in an efficient manner, complied with the energy minimization and comfort criteria. These criteria are subject to different physical constraints and efficiency criteria [Ozatay et al., 2014b].

### 3.2/ GLOBAL CONTROL ARCHITECTURE SCHEME

Considering that the vehicle operates in an urban/suburban zone and, inevitably, it interacts with other vehicles, the following global control architecture scheme is given in Figure 3.1, in order to envelop the aforementioned objectives. The scheme consists of the following blocks:

- ① **Driver.** Businova (cf. section 3.3) is controlled by a driver. The driver chooses a driving mode (cf. item ③).
- ② **Environment and Sensor Information.** This block contains information about the current environment conditions and bus state measured by the on-board sensors, for instance, road slope, bus weight, distance to a preceding car, Battery State of the Charge (*SOC*), etc. A relevant information is exploited for better estimation of the state of the vehicle and to react effectively by applying developed control algorithms.
- ③ **Driving Mode.** The driver can activate the Adaptive Cruise Control with Stop & Go mode (eACCwSG, cf. section 6). When eACCwSG mode is on, the algorithm ensures maintaining of a safety distance between the bus and the preceding vehicle by adjusting an appropriate speed  $v_{ref}$ . The safety distance, determined according to the current bus speed  $v_{bus}$  and current inter-vehicular distance, constrained to acceleration/deceleration capabilities of the bus.
- ④ **Energy Management Strategy** block contains an algorithm aimed to deliver an efficient (optimal or sub-optimal) powertrain powersplit  $P_{pt,opt}$  and speed profile  $v_{opt}$ , according to defined objectives and imposed constraints. In this work, several approaches based on deterministic (cf. Chapter 4) and stochastic (cf. Chapter 5) methods have been investigated for Energy Management Strategy.
- ⑤ **Preliminarily Available Information** contains any useful data, based on statistical data analysis (for instance, average energy consumption/speed/acceleration, etc.) and/or any imposed constraints to steer the decision maker (for instance, battery *SOC* discharge curve (cf. section 3.4)).

### 3.3/ BUSINOVA COMPONENTS

The aim of this section is to illustrate the architecture of the Businova<sup>1</sup> developed by SAFRA company (cf. Figure 3.2).

---

<sup>1</sup><http://www.businova.com>

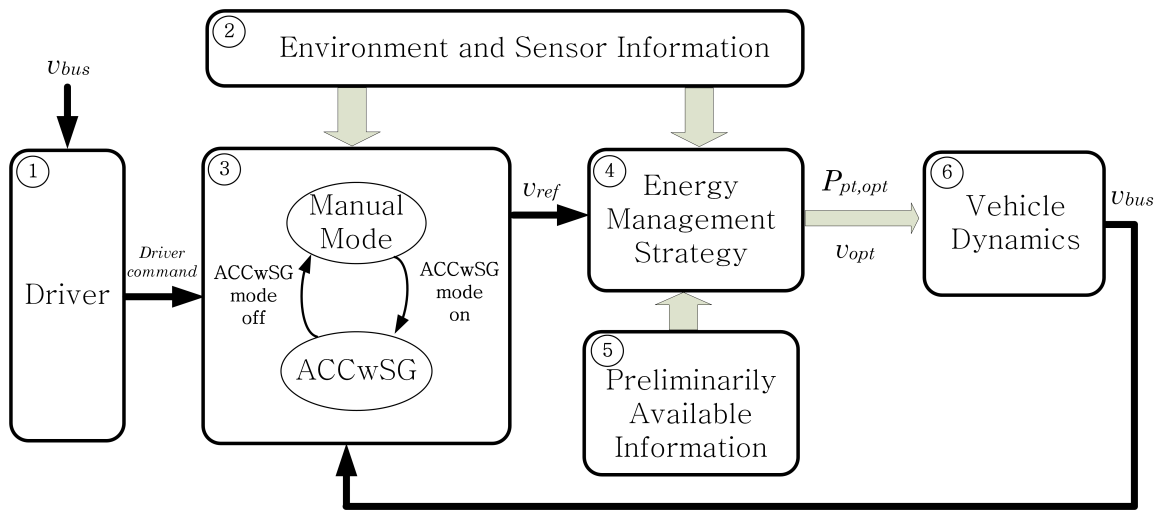


Figure 3.1: Proposed overall control architecture

This bus is composed of an electric motor (EM), a hydraulic motor (HM), an internal combustion engine (Engine) as the propulsion powertrain system of the vehicle. The Businova powertrain architecture is presented in the Figure 3.3. Businova powertrain has a serial-parallel plug-in configuration.

The colors forming the contour of the blocks correspond to different type of connections existing in the powertrain. The description of the powertrain and energy storage elements is given in sections 3.3.1 and 3.3.2, respectively.

The parametric identification of the Businova dynamical model (see equation 2.24) was carried out as follows. To begin, the geometric parameters of the Businova measured accurately directly on the Businova. Several other parameters and characteristics of the dynamical model have been evaluated /obtained. The moment of inertia  $J_m$  ( $kgm^2$ ) of the engines consists of 3 parts:

$$J_m = 0.0082 + 0.21 + 0.46 = 0.6782 \quad (3.1)$$

With moments of inertia that correspond respectively to the moment of inertia of the hydraulic motor, electric motor and engine. Several experimental data has been acquired by SAFRA. The analysis of the obtained data permitted to identify the Businova dynamical parameters. The second column of the table 3.1 shows the parameters of the studied vehicle and the surrounded environment.

### 3.3.1/ POWERTRAIN ELEMENTS

**Electric motor** The Businova is equipped with Permanent Magnet Synchronous Machine (PMSM). The advantage of this type of motors is the high power density, efficiency, high rate torque/inertia, and a high reliability.

The main electric motor characteristics are presented in the table 3.2.

**Hydraulic motor and pump** The hydraulic motor is a motor that converts hydraulic pressure and fluid flow into hydraulic torque, while a hydraulic pump has the opposite



Figure 3.2: Businova

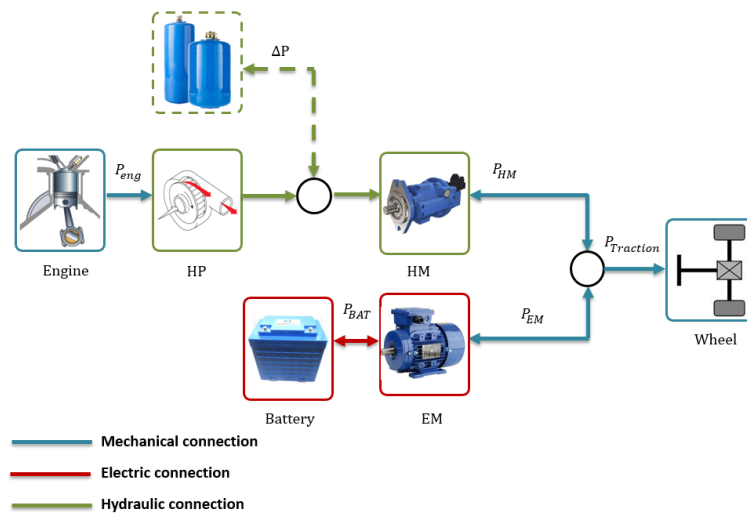


Figure 3.3: Businova powertrain architecture

Table 3.1: Actual Businova dynamic model parameters

Parameter	Actual value
Empty Bus weight, $m$	13000 kg
Rolling resistance coefficient, $\mu$	0.0092
Gravity acceleration, $g$	$9.81 \text{ m/s}^2$
Frontal area, $A$	$6.7 \text{ m}^2$
Aerodynamic coefficient, $C_d$	0.61
Air density, $\rho$	$1.25 \text{ kg/m}^3$
Motors moment of inertia, $J_m$	$0.91 \text{ kgm}^2$
Wheel radius, $r$	$0.484 \text{ m}$
Driving shaft ratio, $i_g$	[1/0.0613 1/0.0981]
Final drive ratio, $i_0$	1
Transmission efficiency, $\eta$	0. 0.931

function, so it transforms mechanical power into hydraulic power. The hydraulic motor is driven with the displacement that regulates the flow at the engine inlet. The torque provided by the hydraulic motor depends on two important factors:

<b>PMSM technical characteristics</b>	
<i>Parameter</i>	<i>Value</i>
Nominal Speed, rpm	3240
Nominal Torque, Nm	305
Nominal Power, kW	103
Nominal Current, A	137
Maximum Torque, Nm	660
Nominal Frequency, Hz	324
Volts/speed ratio, V/rpm	0.15
Maximum Speed, rpm	4000

Table 3.2: Permanent Magnet Synchronous Machine technical characteristics

- the motor displacement  $D$ ,
- pressure  $\Delta P$  (pressure difference at the input and the output of the HM).

The displacement  $D$  of a hydraulic motor corresponds to the volume or the quantity of fluid that must be supplied to a motor so that its coupling shaft performs a complete rotation.

In the case of Businova and as underlined in the Figure 3.3, its hydraulic motor/pump operates in the two following modes:

- **Mode of supply through the hydraulic accumulators.** In this mode HM is directly coupled to hydraulic accumulators of high and low pressure. This mode is basically used for starting the bus.
- **Mode of functioning using engine.** The engine power  $P_{eng}$  is transformed into hydraulic pressure by means of the hydraulic pump (HP), which has a fixed displacement, which supplies the HM, resulting into a higher output power (compared to engine). This configuration allows to downsize the engine.

**Internal Combustion Engine** The Internal Combustion Engines are the most used type of propulsion elements in personal vehicles and this due to its high power/weight ratio, reasonable fuel consumption, easy starting, and reliability of service for over a century [J.Y.Wong, 2008]. The engine for vehicles can be either gas, or fuel (petrol or diesel). The Businova is equipped with a diesel engine. Depending on the needs we can build engine models of different accuracies/fidelities. For example, [Assanis et al., 2000] have developed the diesel engine model with high fidelity for trucks. The model includes cylinder, compressor and turbine modules, area filters, etc. For our needs, we will build a model that is not very complex that will serve us primarily for the calculation of fuel consumption according to power and torque desired.

Here is the Fuel Consumption model that has been applied for estimating the amount of consumed fuel. The fuel flow in the engine is given by [Zeng, 2009]:

$$\dot{m}_f = \frac{P_{ICE} + P_{ICE_{fric}}}{\nu_{ICE} Q_{LHV}} \quad (3.2)$$

where:

$P_{ICE}$  the output power of the engine,

$P_{ICE_{fric}}$  the power of the friction produced by the movement of the components in the engine,

$\nu$  thermal efficiency of the motor,

$\nu_{CE}$  combustion efficiency,

$Q_{LHV}$  lower calorific value of diesel.

Lower Calorific Value of diesel (LHV) is a property of fuels. This is the amount of heat generated by the complete combustion of a fuel unit, the water vapor being assumed to be uncondensed and the heat unrecovered.

$$P_{ICE_{fric}} = \frac{f(\omega_{MT})D_e\omega_{MT}}{2} \quad (3.3)$$

where

$D_e(m^3)$  displacement (per revolution) of the engine,

$\omega_{MT}$  the angular velocity of the engine in rad/s.

The empirical quantity  $f(\omega_{MT})$  represents the friction of the motor, the losses in the engine and the pumping torque of the engine. For the diesel engine, the quantity  $f(\omega_{MT})$  is given by:

$$f(\omega_{MT}) = C_1 + 48\left(\frac{rpm}{1000}\right) + 0.4\bar{s}_p^2 \quad (3.4)$$

where

$C_1$  constant expressed in kPa,

$\bar{s}_p$  the average speed of the piston.

$$\bar{s}_p = 2L\omega_m \quad (3.5)$$

where

$L$  the piston stroke (m).

Thermal efficiency:

$$\nu = 0.87\nu_{ideal} \quad (3.6)$$

To get the value of  $\nu_{ideal}$ , we make use of the Otto cycle. The Otto cycle is a thermodynamic cycle that describes the operation of the engine (cf. Figure 3.4). This cycle consists of four phases [Mollenhauer et al., 2010]:

1. a-b adiabatic compression of the air,
2. b-c fuel injection and combustion under constant pressure and volumetric expansion,
3. c-d adiabatic expansion (the power stroke),
4. d-a isovolumetric exhaust (with constant volume).

By performing this cycle we can find the values of the parameters to compute  $\nu_{ideal}$ .

Compression ratio  $r$ :

$$r = \frac{V_1}{V_2} \quad (3.7)$$

Cut-off ratio  $r_c$ :

$$r_c = \frac{V_3}{V_2} \quad (3.8)$$

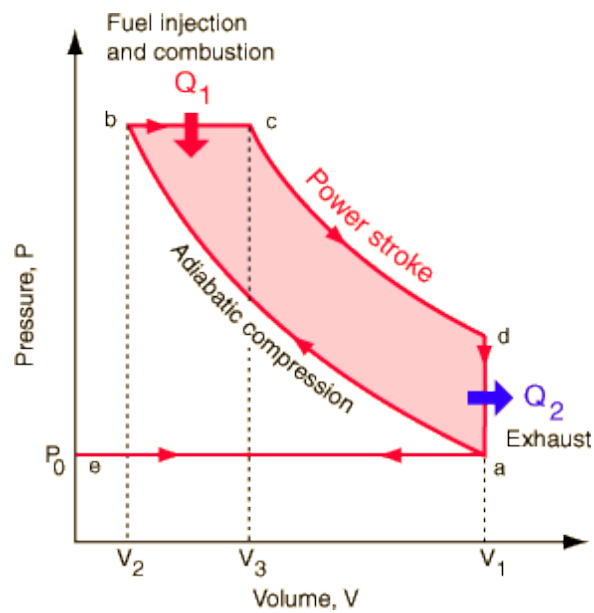


Figure 3.4: Otto cycle [Mollenhauer et al., 2010]

$k$  specific heat rate:

$$k = \frac{C_P}{C_V} \quad (3.9)$$

The ideal thermal efficiency:

$$\eta_{ideal} = 1 - \frac{1}{r^{k-1}} \left( \frac{r_c^k - 1}{k(r_c - 1)} \right) \quad (3.10)$$

The main engine characteristics presented in table 3.3 have been used in the fuel consumption model.

Table 3.3: ICE parameters

Parameters	Value
Displacement $D_e$ , $mm^3$	82,2
Lower calorific value $Q_{LHV}$ , $kJ/kg$	42946
Combustion efficiency $\nu$	0.85
Piston stroke $L$ , $m$	0.107
Compression ratio, $r$	17,8 [Klein, 2004]
Cut off ratio, $r_c$	2 [Klein, 2004]
Specific heat ratio, $k$	1.28
Diesel density $\rho_f$ , $g/cm^3$	0.8355

### 3.3.2/ ENERGY STORAGE ELEMENTS

**Electric battery** Electric batteries are a key component in hybrid Electric Vehicle. Batteries are devices that transform chemical energy into electrical energy. It is a reversible electrical energy storage system.

The electric batteries encompass the following features:

1. **High Energy Density.** Energy density is the amount of energy stored in a given system per unit volume.
2. **Average Power Density.** Power density (or volume power density or volume specific power) is the amount of power (time rate of energy transfer) per unit volume. In energy transformers including batteries, fuel cells, motors, etc., and also power supply units or similar, power density refers to a volume. It is then also called volume power density, which is expressed as  $W/m^3$ .
3. **Long Life Span.** Battery lifespan is closely related to the number of charge /discharge cycles. Therefore, longer battery operating time means longer battery lifespan [Ci et al., 2007].
4. **High Cost.** In 2016 the price of lithium-ion batteries was 273\$/kWh [Curry, 2017]. Though the price is decreasing each year, it remains relatively expensive.

**Hydraulic accumulators** Hydraulic accumulators represent a short-term storage element. Hydraulic accumulators characterized by a higher power density and a lower energy density than electrical batteries.

Due to the high power flow that can be recuperated during deceleration, the hydraulic hybrid concept has been of interest for use in heavy vehicles, as urban buses or trucks. The hydraulic accumulators have the capacity to accept both frequencies and high rates of charging/discharging [Guzzella et al., 2007].

As any type of hybrid-hydraulic propulsion systems, the Businova includes a high-pressure (HP) and low-pressure (LP) accumulators (cf. Figure 3.5). The accumulator contains the hydraulic fluid and a gas, such as nitrogen ( $N_2$ ), separated by a membrane. When the hydraulic fluid in HP flows in, the gas is compressed. During the discharge phase, the fluid flows out through the motor and then into the LP.

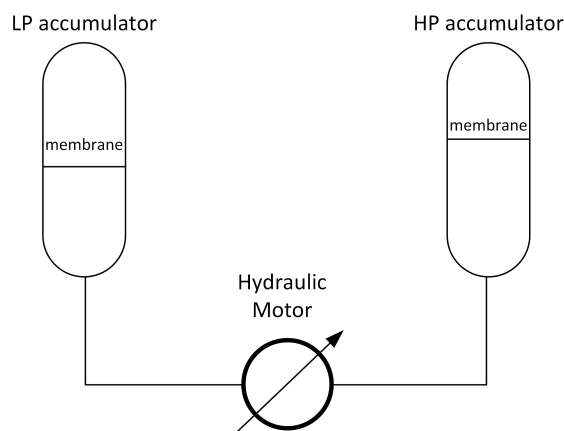


Figure 3.5: Schematic of hydraulic system

The dynamic equation of the accumulator is:

$$pV^n = C \quad (3.11)$$

with  $p$  supplied pressure,  $V$  gas volume (nitrogen),  $n$  adiabatic index,  $C$  a constant that depends on pre-charge pressure. The pre-charge pressure is a pressure of the nitrogen in the accumulator without hydraulic fluid.

The maximum volume of the hydraulic accumulators is 32 liters. The pre-charge pressure of the HP  $p_{hp0}$  is 180 bar, and of the LP  $p_{lp0}$  is 15 bar. The maximal pressure in the accumulators is 300 bar and 35 bar for HP and LP, respectively.

### 3.4/ SOC REFERENCE CURVE

The Businova is a plug-in hybrid electric vehicle and we suppose that its standard functioning time is 8 hours a day (and maybe more, during so called “course of a day”). Figure 3.6 illustrates the spatial bounds of a bus running cycle. So the bus travels from its starting location to another route terminus, stopping at Bus Stations (BS) along the route to allow passengers to board on and to get off. This movement is called a *trip*. By the end of a day, the bus reaches its  $SOC_{min}$  value and can be recharged during all the night long to ensure the service the next day.

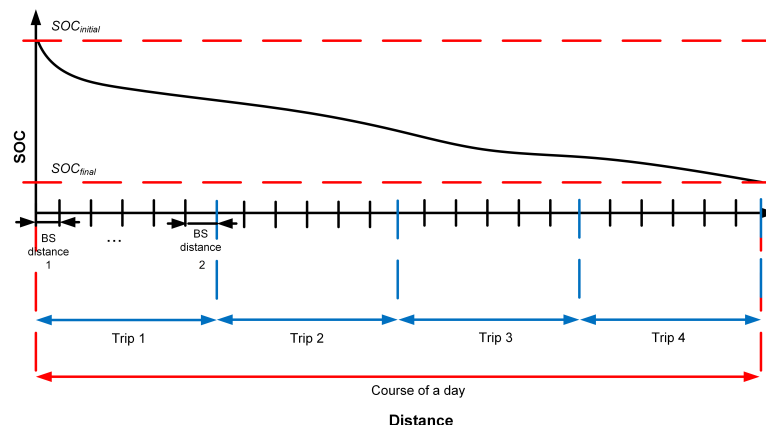


Figure 3.6: Spatial bounds of a bus running cycle

Some research papers have used a similar idea and have proven the relevancy of this assumption. According to [Li et al., 2015], a battery  $SOC_{bat}$  gradual and smooth decrease to a lower threshold leads to better fuel economy, compared with Charge-Depleting and Charge-Sustaining (CDCS) strategy. Authors in [Heppeler et al., 2016], as well as in [Shen et al., 2015] and [Sun et al., 2015b], deal with the problem of prediction of the battery  $SOC_{bat}$ . These papers use an offline global optimal control to generate the desired  $SOC_{bat}$  trajectory, later these values are used as an input in Model Predictive Control (MPC). It is proved that prediction of the future trajectories, based upon either past or predicted vehicle velocity and road grade trajectories, could help in obtaining a solution close to the optimal one [Van Keulen et al., 2010b]. In [Tulpule et al., 2009] assume the battery  $SOC_{bat}$  is linearly decreasing with the distance traveled.

In our work, the main idea is to consider that a better usage of the electric energy is such that it is available until the end of the day (during 8 hour operational cycle), and this is considered as the most suitable functioning of the bus. The working hypothesis behind

this assumption is to use the maximum amount of energy that can be consumed from the battery in one day driving so that the battery energy is spread as uniformly as possible in one working day. This implies the smooth battery discharging rate (C-rate), avoidance of the high or low  $SOC_{bat}$  and excessive depth of charge, which lead to a high rate of battery capacity loss [Tang et al., 2015] [Choi et al., 2002] [Broussely et al., 2005]. As Li-ion batteries represent a big part of a vehicle cost, the clear interest is to prolongate the battery life.

To obtain the targeted profile, several techniques are used in the literature such as Neural Networks [Tian et al., 2017], MPC [Heppeler et al., 2016], Linear Control [Tulpule et al., 2009].

In the presented PhD work, we have proposed to use an Artificial Neural Network (ANN) module that designed to learn the mechanisms of suitable  $SOC_{bat}$  curves according to different trip information. the average speed and length of route segments when the trip starts is used by the ANN module to generate a reasonable and relatively precise  $SOC_{bat}$  reference curve. However, some studies demonstrate that the frequent acceleration phases strongly impact the energy consumption in the vehicle [Larsson et al., 2009]. So to complete the ANN module, an average absolute acceleration value has been added as an input to the ANN module, in order to take into account the dynamics of the speed variation on a given route segment.

Thus, the  $SOC_{bat}$  curve learning module based on ANN which has as inputs:

- $SOC_{bat,initial}$  initial battery  $SOC$ ,
- $v_{mean}$  average speed at each distance segment  $D_n$ ,
- $a_{mean}$  average absolute acceleration value at each distance segment  $D_n$ ,
- $d_{current}$  traveled distance,
- $d_{remain}$  remained distance.

This relation is illustrated in Figure 3.7. The road is divided into segments  $D_n$ . We can see that the more important is the average speed/acceleration (on a given route segment), the more energy is consumed in the corresponding phase and battery is charged and discharged faster.

### 3.5/ REGENERATIVE BRAKING LOGIC FOR BUSINOVA

When braking in a conventional vehicle, the friction converts much of the kinetic energy into heat that is released into the air. Electrified vehicles are designed to capture this kinetic energy during deceleration and store it in the battery pack to be used for propulsion during acceleration.

One of the ways for a hybrid vehicle to maximize its autonomy is the energy recovery during the deceleration phases of the vehicle. Energy recovery can be performed when the brake pedal is not in use and the driver lifts his foot off the accelerator (deceleration without braking). Another way to recover energy is the regenerative braking that occurs when the brake pedal is used.

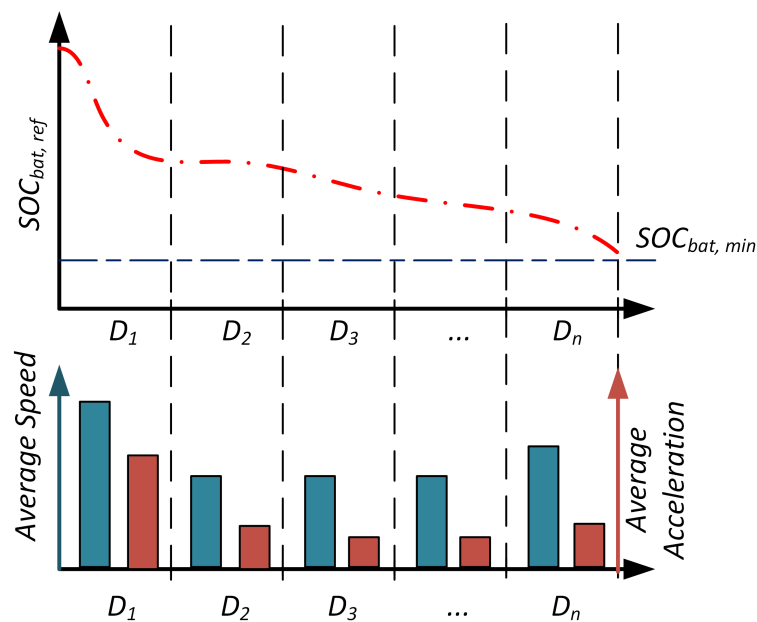


Figure 3.7: Relation among average speed/acceleration and  $SOC_{bat}$  reference.

Regenerative braking allows the hybrid vehicle to recover most of the energy involved in braking owing to the use of the components of the powertrain (electric/hydraulic motor in generator/pump mode) and reversible energy storage system. Nevertheless, the braking system becomes more complex, because it consists of a regenerative braking and a dissipative braking (friction brake).

Figure 3.8 illustrates that an electric machine operates in four quadrants. They are Forward Braking, Forward motoring, Reverse motoring and Reverse braking. In motoring mode, the machine works as a motor and converts the electrical energy into mechanical energy, supporting its motion. In braking mode, the machine works as a generator, and converts mechanical energy into electrical energy and as a result, it opposes the motion. The product of angular speed and torque is equal to the power developed by a motor. Positive power corresponds to motoring mode, negative power to braking (regenerative mode). For multi-quadrant operation of drives the following conventions about the signs of torque and speed are used. When the machine is rotated in the forward direction the speed of the motor is considered positive.

The role of braking energy recovery strategies is to determine the distribution law of braking torque required to the wheels. The distribution law transforms the braking power into the regenerative braking torque demanded at the level of the traction chain and in dissipative braking torque distributed on the mechanical braking system, front and rear axles of the vehicle. Regenerative braking power can also be distributed across both axles of the vehicle to maximize the amount of energy recovered during braking. Indeed, the amount of braking that can be applied to each axle is calculated to handle the law of optimum distribution of braking [Ehsani et al., 2005] which depends on the position of the center of gravity of the vehicle and the load transfer during deceleration.

The regenerative braking management problem is addressed in [Yu et al., 2010]. The requested regenerative braking torque is first estimated based on the vehicle wheel speed

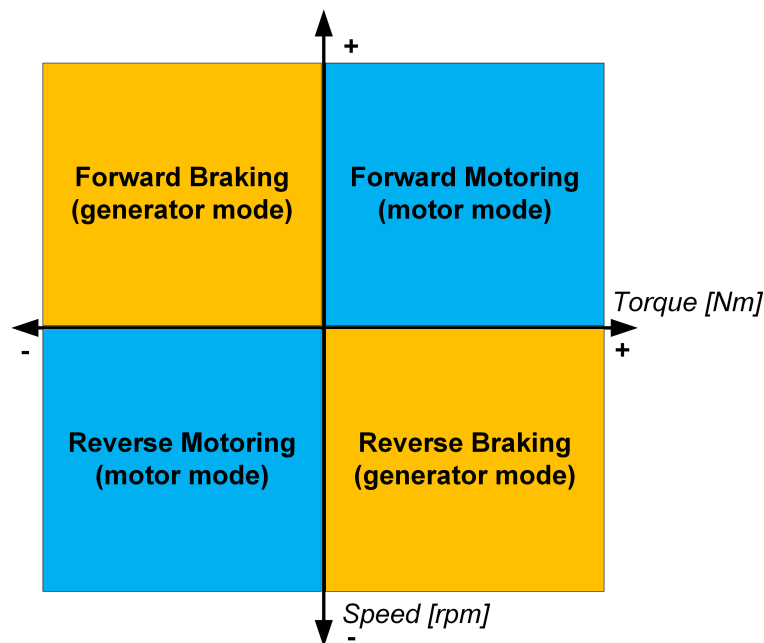


Figure 3.8: Electric machine quadrant in torque-speed

data. The braking torque control strategy is then synthesized in order to generate the control references of the vehicle actuators (the torque references of the electric machine and the dissipative braking system) as a function of the position of the brake pedal, the state of charge of the battery and the estimated braking torque.

Another regenerative braking strategy based on fuzzy logic is proposed in [Xu et al., 2011]. In this strategy, the braking torque is distributed between the front axle and the rear axle as a function of the desired deceleration and the recommended braking distance in order to comply with an optimum law of braking distribution. The fuzzy controller implemented in this work uses the state of charge information and the battery temperature to calculate the maximum regenerative braking power. The braking power required on the axle equipped with the regenerative braking system is provided in priority. If the latter can not be fully absorbed, the dissipative braking system adds the necessary braking power to satisfy the driver's demand. Experimental results show that this strategy considerably increases the efficiency of energy recovery.

Optimizing the energy recovery in Businova deceleration phases is also a very important parameter to consider in the energy management strategy to minimize bus consumption and improve its autonomy.

The current braking system at the Businova includes a regenerative braking system (hydrostatic and electric) and a mechanical braking system. The regenerative braking torque is applied to the rear axle only, while the mechanical braking torque can be distributed to the front and rear axles. It is noted that the regenerative braking energy is a function of the speed of the bus. In low speeds, it will be recovered by the hydraulic pump because of the low electromotive force (EMF) produced in the electric motor in this speed range does not allow effective electrical regeneration of the bus.

A good estimation of the regenerative braking torque must be made in order to determine

an optimal sharing of the braking energy between the traction chain and the mechanical braking system. The principle of the proposed energy recovery strategy is as follows:

1. **if the brake pedal is not used.** The energy will be recovered in this mode only using the electric motors (in generator mode) during coasting.
2. **if the brake pedal is used.** In this case, two modes are distinguished:
  - For speeds above an upper threshold value, it is essentially regenerative braking that will be applied,
  - For speeds between the upper and lower threshold values, regenerative braking will be applied first. However, when the requested braking torque is greater than the maximum regenerative braking torque, the bus will also be stopped by the mechanical braking system (cf. Figure 3.9). The regenerative braking ratio decreases proportionally to the speed decrease.
  - For very low speed under lower threshold, the mechanical brake is used to mark the stop.

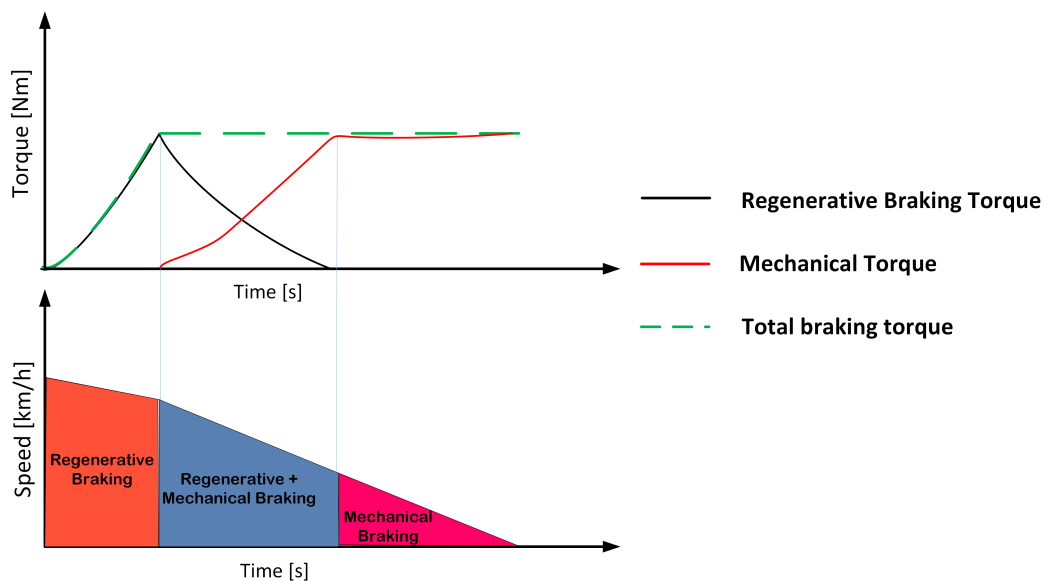


Figure 3.9: Example of regenerative braking profile according to Torque and vehicle Speed

In this work, the upper threshold value for the speed is set to 30 km/h, and the lower threshold value is set to 10 km/h. As regenerative braking is not the focus of my PhD thesis, this regenerative braking logic maintained in all the developed algorithms for energy management strategies (cf. Chapters 4 to 6).

### 3.6/ CONCLUSION

This chapter has showed an overview of the proposed control architecture. The idea behind this control scheme is to try to optimize both a powersplit and to smooth a speed

profile in order to minimize the energy consumption of the vehicle. To address an optimization problem, some assumptions were put in use. This allows to take into consideration the constraints and restriction due to the specifications of the mission performed by the bus in an urban/suburban environment.

The Businova components have been described in this chapter in order to give the idea of the dimensions of the motors and the storage systems. These informations have been used in order to constrain the optimization problems which will be shown in the following chapters.

# DETERMINISTIC ENERGY MANAGEMENT STRATEGY

## **Abstract**

---

This Chapter is dedicated to the description of the proposed deterministic energy management strategy. Firstly, an optimal offline optimization, based on Dynamic Programming (DP), is proposed in this work, permitting to have simultaneous speed profile optimization and optimal powersplit strategy. Afterwards, the basis of the offline optimal strategy has been adapted in order to deal online with the current road profile and driver velocity demand. The proposed online sub-optimal strategy uses mainly a Multi-Dimensional Database (MDD, which gives as output the speed profile and powersplit set-points) and an appropriate interpolation technique in order to cope with the current bus situations.

---

## 4.1/ INTRODUCTION

As it was described in Chapter 2 one of the mostly used and efficient methods for global energy optimization for HEV is Dynamic Programming (DP) [Bertsekas, 1995]. In this work, the DP has been chosen as a basis for developing a deterministic EMS due to the following characteristics:

- DP solves a problem recursively along with storing the calculated information for further usage,
- At each stage in DP the decision rule is determined by evaluating an objective function called recursive equation.

Definition 6 summarizes the main points of the DP.

### **Definition 6: Dynamic Programming**

Dynamic Programming (DP) is a method for solving a complex problem by breaking it down into a collection of simpler subproblems, solving each of those subproblems just once, and storing their solutions. The next time the same subproblem occurs, instead of recomputing its solution, one simply looks up the previously computed solution.

DP breaks down a big optimization problem into subproblems. Each subproblem is solved

once and the solution is stored. Next time the subproblem occurs, instead of the recalculating, the solution is taken from the storage. This procedure is called memoization.

## 4.2/ OFFLINE DYNAMIC PROGRAMMING APPROACH

### 4.2.1/ OPTIMAL CONTROL PROBLEM FORMULATION

The objective of the defined optimal control problem is to find an optimal profile velocity and energy split between the actuators for a given trajectory  $D$  (cf. Figure 4.1), taking into account the bus should meet the timetable requirements, as well as speed limits in a given driving area. The optimization is performed in the spatial domain by means of the following transformation (conversion from time domain equations into spatial domain) [Ozatay et al., 2014a]:

$$a = \frac{dv}{dt} = \frac{dv}{dD} \cdot \frac{dD}{dt} = \frac{dv}{dD} \cdot v \quad (4.1)$$

In that case the dynamics of the Businova given in (2.24) could be re-written by the following equation:

$$\frac{dv}{dD} = \frac{1}{M_{eq}v} \left( \frac{i_g \eta_t T_{pt}}{r} - \mu_{rr} F_N \text{sign}(v) - \frac{1}{2} \rho A C_d (v + v_{wind})^2 - Mg \sin(\theta) - \frac{T_{brake}}{r} \right) \quad (4.2)$$

In general, the parallel-series architecture of the BUS, described in the Chapter 2, can operate according to the following modes:

1. The propulsion is fully supplied by the electric motor (mode I),
2. The propulsion is supplied by the hydraulic motor via accumulators (mode II),
3. The bus is actuated by the hydraulic motor via the diesel engine (mode III),
4. The mode IV implies the hybrid operation of the electric motor and the hydraulic motor via accumulator,
5. The mode V implies the hybrid operation of the electric motor and the hydraulic motor via diesel engine,
6. The recharge of the electric battery or the accumulators via engine (mode VI),
7. The regenerative braking (mode VII) means that a part of the kinetic energy during braking phase is recuperated to recharge an electric battery or/and hydraulic accumulators 3.

In this study the hydraulic accumulators are not taken into account, and we will consider only modes I, III, V and VII. The mode VII considers, consequently, only electric regenerative braking.

According to the considered functioning modes, we derive the cost function  $J_D$  to be minimized. The objective of the optimization is to determine an optimal speed profile and relevant powersplit. The most energy-consuming phases for heavy vehicles are the phases of acceleration. Therefore, the given cost function  $J_D$  aims to smooth acceleration

phases, and reduce a global consumed energy which consists of a fuel rate mass  $\dot{m}_{fuel}$  and the electric power  $P_{EM}$  consumed during the trip  $D$ :

$$J_D = \alpha \int_0^{D_f} \frac{\dot{m}_{fuel}(T_{eng}(D), \omega_{eng}(D), T_{HM}(D), \omega_{HM}(D), D_{HM})}{v(D)} dD + (1 - \alpha) \int_0^{D_f} \frac{P_{EM}(D)}{v(D)} dD + \beta \int_0^{D_f} \frac{|a|}{v(D)} dD \quad (4.3)$$

with

- fuel mass consumed  $\dot{m}_{fuel}$  is a function of diesel engine torque  $T_{eng}$  and speed  $\omega_{eng}$ .
- $P_{EM}(D)$  is an electric motor power:

$$P_{EM}(D) = T_{EM}(D)\omega_{EM}(D) \quad (4.4)$$

where:  $T_{EM}$  is the electric motor torque and  $\omega_{EM}$  is the electric motor speed.

- a third component of the equation, contains  $a$  acceleration,
- $D_f$  is the total traveled distance.
- $v$  a bus speed. For a  $\Delta D$  we consider an average value of the speed for this fragment.
- $\alpha$  is weight coefficient such as  $\alpha \in [0 \ 1]$ ,  $\beta$  is a scale factor.

The minimization of the cost function (4.3) is subject to the dynamic constraint (4.2), as well as to the constraints imposed on the control input and state during optimization (cf. sections 4.2.2 and 4.2.3).

#### 4.2.2/ CONTROL CONSTRAINT SET

The control input  $T_{EM}$  and  $T_{HM}$  are bounded by its maximum and minimum values.

The upper and lower limits of the EM are defined as follows:

$$\mathbb{U}_{D,1} := \{-660Nm \leq T_{EM}(D) \leq 660Nm\} \quad (4.5)$$

The upper and lower limits of the HM are defined as follows:

$$\mathbb{U}_{D,2} := \{0Nm \leq T_{HM}(D) \leq 410Nm\} \quad (4.6)$$

Due to the connection in series of the hydraulic motor and the engine, the hydraulic motor is exerted by the engine whose torque's upper value is limited:

$$\mathbb{U}_{D,3} := \{0Nm \leq T_{eng}(D) \leq 343Nm\} \quad (4.7)$$

The HM output torque is also controlled by the HM displacement  $D_{HM}$  which also varies between its maximum and minimum value:

$$\mathbb{U}_{D,4} := \{22cm^3 \leq D_{HM} \leq 110cm^3\} \quad (4.8)$$

Then, the constraint set becomes  $\mathbb{U}_D = \mathbb{U}_{D,1} \cup (\mathbb{U}_{D,2} \cap \mathbb{U}_{D,3} \cap \mathbb{U}_{D,4})$ .

### 4.2.3/ STATE CONSTRAINT SET

Beside the constraints to the control inputs, there are the constraints to the state variables. Namely, in order to guarantee the vehicle performance in the legal speed range imposed by the traffic law, we set a constraint to the maximum bus speed:

$$\mathbb{X}_{D,1} := \{0 \leq v(t) \leq v_{max}(t)\} \quad (4.9)$$

For example, in the urban zone, the speed  $v_{max}$  could be limited to 40-50 km/h, whereas in the suburban zone the speed  $v_{max}$  can be limited to 70-80 km/h.

Another aspect to satisfy is the passengers comfort, we set constraints to minimum and maximum acceleration/deceleration:

$$\mathbb{X}_{D,2} := \{a_{min}(t) \leq a(t) \leq a_{max}(t)\} \quad (4.10)$$

where  $a_{min}$  has negative value, implying the maximum deceleration. The studies show that the bus mean maximum acceleration and deceleration in real world traffic situations reaches, consequently,  $1.47 \text{ m/s}^2$  and  $-1.86 \text{ m/s}^2$  [Kirchner et al., 2014]. From the point of view of the passengers comfort, [He et al., 2013] affirms that passengers start feeling uncomfortable when acceleration  $a_{max} \geq 1.5 \text{ m/s}^2$ , and the deceleration  $a_{min} \leq -0.75 \text{ m/s}^2$ .

The state constraint state becomes  $\mathbb{X} = \mathbb{X}_{D,1} \cap \mathbb{X}_{D,2}$ .

### 4.2.4/ BOUNDARY CONDITIONS

To set the boundary conditions, we take into consideration a normal operation for an urban bus, traveling from one stop to another with the speed  $v$  (cf. Figure 4.1).

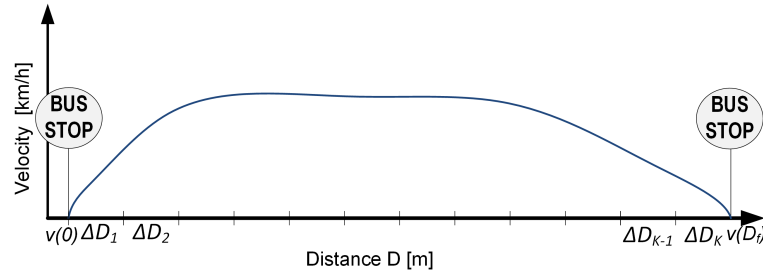


Figure 4.1: Standard bus trip from one bus stop to another.

Thus we consider that the initial  $v(0)$  and final  $v(D)$  is equal to zero:

$$v(0) = v(D) = 0 \quad (4.11)$$

where  $D$  is the total traveled distance.

The final time  $t_f$  to arrive to the next bus stop is imposed by the schedule that must be respected. Concerning the final time, being a little late or ahead of the schedule is permissible due to the traffic jams, traffic lights, pedestrian crossing, etc.:

$$\begin{cases} t_0 = 0 \\ t_f = t_s \pm 5\% \end{cases} \quad (4.12)$$

where  $t_s$  is the time fixed in schedule to reach the considered station.

## 4.2.5/ DP ALGORITHM

The optimization method used to solve the given optimal control problem is based on the dynamic programming [Bertsekas, 1995], which provides the global optimal solution over a given trip. The algorithm proceeds from 0 to K steps:

$$J_k(v_k) = \min_{u_k \in \mathbb{U}_D} \{g_k(v_k, u_k, \Delta D_k) + J_{k-1}(f(v_k, u_k))\} \quad (4.13)$$

where

- $J_k(v_k)$  is the cost-to-go function from step 0 to step  $K$  starting from  $v_0$  with initial cost  $J_0(v_0) = g_0(v_0) = 0$ ,
- $g_k(v_k, u_k, \Delta D_k)$  is the cost-to-go function from node  $i$  to node  $j$  (cf. Figure 4.6). This cost-to-go function is calculated according to the normalized equation 4.3 (see equation 4.15),
- $J_{k-1}(f(v_k, u_k))$  is the total cost starting from the root to the node  $i$ ,
- $u_k \in \mathbb{U}_D$  is the control input determining the velocity at the next step.

The given optimization is aimed to solve two main problems:

1. Find the optimal speed profile from  $x_0$  to  $x_f$  in  $t_f$  minimizing the electric energy and fuel consumption,
2. Find the optimal powersplit strategy for the current speed profile in order to provide an optimal functioning mode while respecting the BUS structural constraints and the constraints issued from traffic conditions.

Thus, this algorithm is called **Dynamic Programming based Simultaneous Speed and Energy Optimization (DP-SSEO)**.

In order to have adequate results, each part of the cost function (cf. equation 4.3) is harmonized. The fuel consumption rate (cf. equation 4.3) is transformed into equivalent consumed engine power  $P_{engine}$  expressed in Watt:

$$P_{engine} = \dot{m}_{fuel} * Q_{LHV} \quad (4.14)$$

where  $Q_{LHV}$  is lower heating value. For diesel  $Q_{LHV} = 43MJ/kg$ .

The normalized cost function is given as follows:

$$J_D = \alpha \int_0^{D_f} \frac{P_{engine}}{v(D)} \cdot dD + (1 - \alpha) \int_0^{D_f} \frac{P_{EM}}{v(D)} \cdot dD + \beta \int_0^{D_f} \frac{|a|}{v(D)} dD \quad (4.15)$$

where

- $P_{EM}$  electric motor power.
- $\alpha$  is a constant weight coefficient such as  $\alpha \in [0 \ 1]$  and  $\beta$  is a scale factor.

This section details the solution of the nonlinear optimization control problem formulated in the spatial domain by using DP algorithm. A set of points defines the route. Namely, the route consists of the points  $P = [p_0, p_1, p_2, \dots, p_K]$ . Every point  $p_k \in P$  for  $k = 0, 1, 2, \dots, K$  has its own characteristics:  $p_k = [x_k, y_k, \theta_k]$ , where  $x_k$  longitudinal position,  $y_k$  lateral position,  $\theta_k$  road slope angle. The given route of the length  $D$  is divided into  $K$  segments of the length  $\Delta D$ . Depending on the acceleration/deceleration limits and on the  $\Delta D$  segment length (cf. Figure 4.1), the velocity  $v(D_k)$  can increase or decrease with a fixed step  $\Delta v$ . The maximum number of  $\Delta v$  is equal to  $2N_v + 1$ :

$$\mathbb{V} = \{-N_v\Delta v, -(N_v - 1)\Delta v, \dots, 0\Delta v, \Delta v, 2\Delta v, \dots, N_v\Delta v\} \quad (4.16)$$

where  $N_v \geq 2n + 1$  with  $n \in \mathbb{N}$ .

In order to be clear, let us define the terms and variables used in the given optimization algorithm:

- Tree ( $T$ ) is a directed rooted acyclic graph [Bondy et al., 1976] (cf. Figure 4.2). The tree  $T$  is characterized by  $T = (V, E)$ , where  $V$  and  $E$  are the set of all vertices (nodes) and all the edges (connection between vertex  $i$  and vertex  $j$ ) of the given  $T$ , respectively.

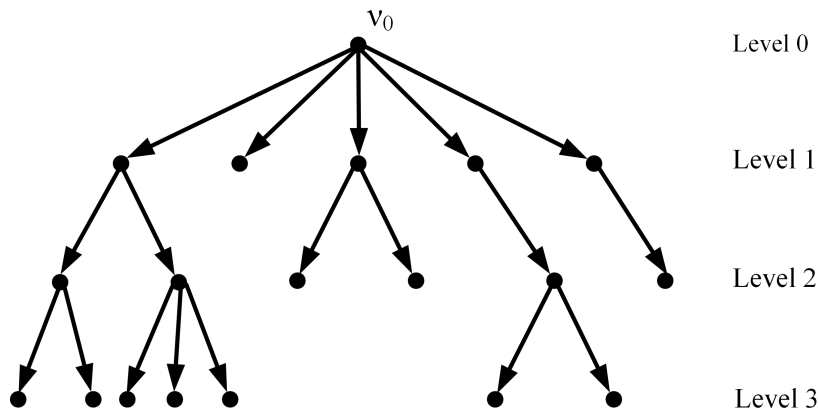


Figure 4.2: Rooted tree illustration

- Each vertex  $v_j \in V$  is characterized by state  $v_j \equiv [P_k, v_j, t_j, Parent(v_j)]$ , where  $v_j$  and  $t_j$  are the speed and the traveled time when the bus reaches this vertex. The tree root  $v_0$  does not have the parent. The vertex  $v_0$  corresponds to the **Level 0** of  $T$  and characterized by a set of vertices represented by  $S_0 = \{v_0\}$ .  $S_k$  corresponds to **Level k** of  $T$  and it will contain all the children vertices generated from the vertices of  $S_{k-1}$  set.
- Each edge  $e_i^j$  is characterized by: a state  $e_i^j = [J_i^j, T_{EM}, T_{HM}]$ , where  $T_{EM}$  and  $T_{HM}$  are, respectively, electric motor and the hydraulic motor torques distributed for the traction of the bus, according to which the cost  $J_i^j$  has been calculated. This power-split is calculated according to the vector  $\Lambda$  which is defined below.
- To perform the simultaneous powersplit optimization, the specific vector  $\Lambda = \{0, 0.1, 0.2, \dots, 1\}$  is assigned with  $Card(\Lambda) = m$  cardinal number of the set  $\Lambda$ . Possi-

ble torque combinations to satisfy current total torque demand  $T_{setpoint}$  of the transmission are found and corresponding vectors are built as follows:

$$\begin{cases} T_{EM} = \Lambda T_{setpoint}, & \text{where } T_{EM} \text{ electric motor torque} \\ T_{HM} = (1 - \Lambda)T_{setpoint}, & \text{where } T_{HM} \text{ hydraulic motor torque} \end{cases} \quad (4.17)$$

It is to be noted that the length of  $T_{EM}$  and  $T_{HM}$  is equal to  $m$ .

- A boolean value  $\psi_{boolean}$  has been introduced and it permits us to reduce the number of children (see below) from the vertices that do not lead *a priori* to a feasible solution. The boolean value  $\psi_{boolean}$  (cf. Algorithm 1 on page 70) is equal to 0 if the following conditions are not satisfied:
  1. During the construction of the tree  $T$ , the nodes that do not satisfy the control and state constraints and boundary conditions (cf. sections 4.2.2, 4.2.3, and 4.2.4) to go from vertex  $v_i$  to  $v_j$  are eliminated in order to stop the development of the tree, therefore we reduce the number of children of the  $v_i$ .
  2. Concerning the speed profile characteristics, it is considered that this profile has only one acceleration and one deceleration phase from one bus stop to another (under assumption, that nothing perturbs the bus). It is supposed that it is not worth lose the kinetic energy (during the deceleration) in order to re-accelerate (and create a power demand peak) to attain the speed to catch up the distance and satisfy the schedule. If this condition is not satisfied, the corresponding nodes are eliminated from the tree  $T$  as well.
- The electric motor and the engine (which exerts the hydraulic motor) have different dynamic characteristics. Electric motors are capable of delivering a high starting torque (cf. Figure 4.3). Unlike the electric motors, the internal combustion engines cannot provide torque at zero speed and it produces maximum power at a certain speed (cf. Figure 4.4). The efficiency of the engine is very much dependent on the operating point in the engine's performance map (cf. Figure 4.5). Thus, to go from one state to another not all the  $\Delta$  torque are feasible. To take this constraint into account, the maximum values  $\Delta T_{EM_{max}}$  and  $\Delta T_{HM_{max}}$  are used. Thus,  $\psi_{boolean} = 0$  if:

$$\begin{cases} \Delta T_{EM} > \Delta T_{EM_{max}} \\ \Delta T_{HM} > \Delta T_{HM_{max}} \end{cases} \quad (4.18)$$

- The maximum number of children from each vertex  $v_i$  is fixed to the value  $(2N_v + 1)m$ , which corresponds to the product of the maximum number of  $\Delta v$  and the number of possible actuation combinations to propel the bus. The number of vertices  $\gamma$  if each vertex generates  $(2N_v + 1)m$  children is given by the formula [Bondy et al., 1976]:

$$1 + (2N_v + 1)m + ((2N_v + 1)m)^2 + \dots + ((2N_v + 1)m)^K = \frac{((2N_v + 1)m)^{K+1} - 1}{(2N_v + 1)m - 1} \quad (4.19)$$

where  $K$  number of segments of the road,  $m$  is the length of the vector  $\Lambda$ ,  $2N_v + 1$  number of  $\Delta v$ .

To construct a decision tree for the DP algorithm the following assumptions have been taken:

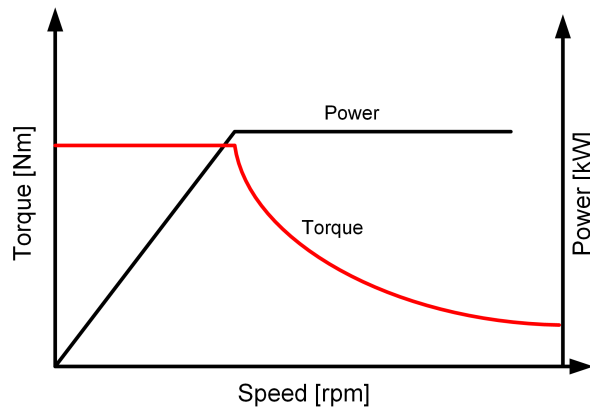


Figure 4.3: Standard PMSM characteristics

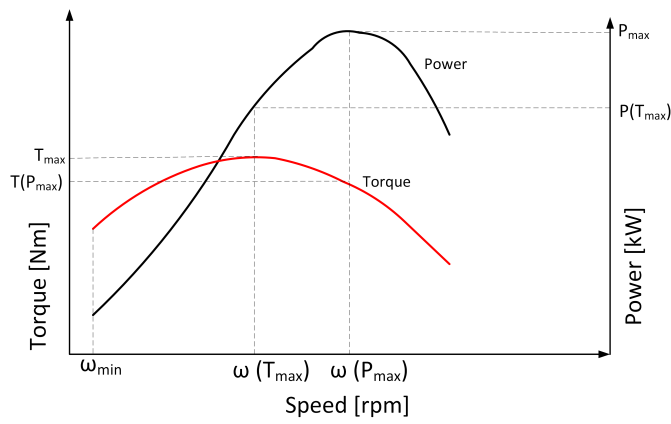


Figure 4.4: Standard engine characteristics

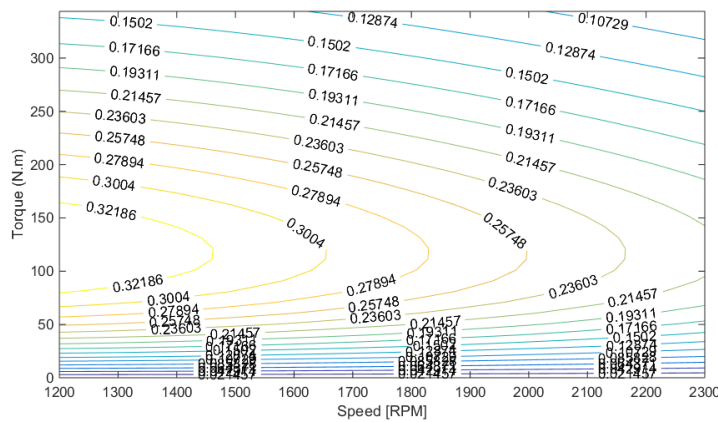


Figure 4.5: Standard engine efficiency map

1. The road profile is known, consequently,  $x_k$  and  $y_k$  for  $k = 1, 2, \dots, K$  are known,
2. The value of  $\theta_k$  is constant for a given  $\Delta D_k$ .

The construction of the tree  $T$  for speed profile optimization and the proposed energy management strategy is given in the algorithm 1-3. This algorithm is a basis of the the proposed EMS proposed in PhD thesis.

An example of the obtained tree is given in the Figure 4.6, where  $\gamma$  represents the total number of nodes (or states).

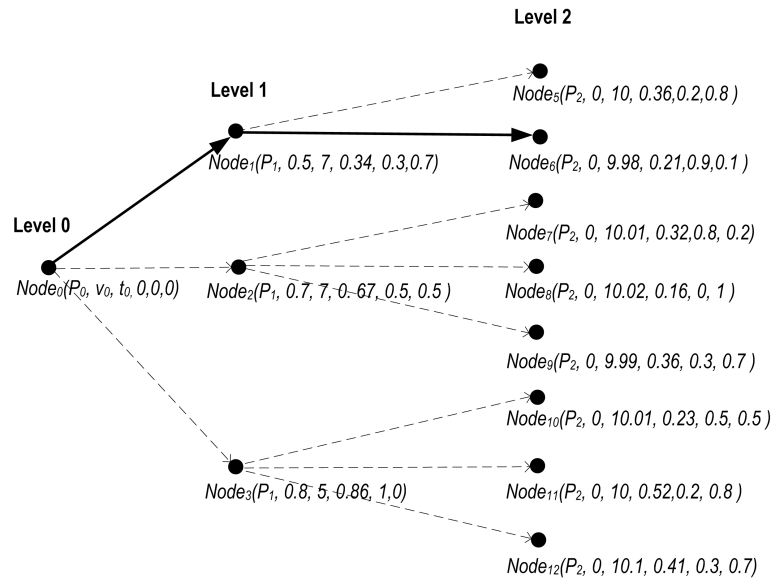


Figure 4.6: Tree example: position, speed, time, cost, EM torque, HM torque.

#### 4.2.6/ SIMULATION RESULTS AND ANALYSIS

This section describes the simulation results of the proposed simultaneous speed and powersplit optimization. For that end, the following scenario has been proposed.

The bus runs on a road with variable slope (cf. Figure 4.7) with distance of 250 m. The road is divided into 5 segments of 50 m. Initial and final speeds  $v_0 = v_f = 0$ . The time constraint is 36 s. Maximal velocity is limited to  $v_{max} = 50$  km/h.

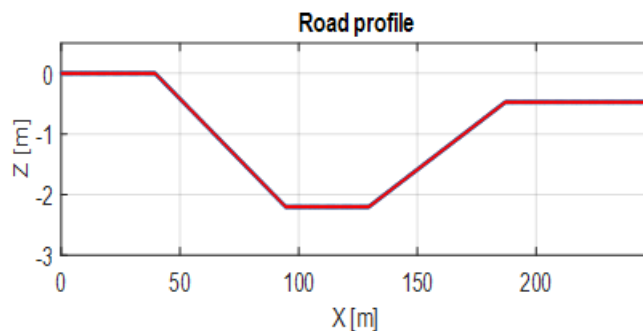


Figure 4.7: Road profile

**Data:** Road profile data:  $P = \{X, Y, \Theta\}$

$\Delta D, K$ , initial state; /\* distance discretization step; number of  $\Delta D$ ; initial state contains: initial speed, time, cost, EM torque, HM torque \*/

$\mathbb{V}, \Lambda$ ; /\* set of maximum permissible values of speed increment  $\Delta v$ ; powersplit vector \*/

**Result:** Dynamic Programming based Simultaneous Speed and Energy Optimization (DP-SSEO)

**begin**

$S_0 = \{v_0\}$ ; /\* The set of the vertices at the **Level 0** of the tree  $T$  \*/

**for**  $k = 1 \dots K$  **do**

**for**  $\Delta v \in \mathbb{V}$  **do**

**if**  $(0 \leq v_{current} \leq v_{max}) \ \& \ (t_{current} \leq t_f + 5\%)$  **then**

$\psi_{boolean} = 1$

**end**

**else**

$\psi_{boolean} = 0$

**end**

**if**  $\psi_{boolean} == 1$  **then**

      Calculate the total required torque  $T_{setpoint}$  to move the bus;

**if**  $T_{setpoint} > 0$  **then**

$T_{EM} = \Lambda T_{setpoint}$ ;  $T_{HM} = (1 - \Lambda)T_{setpoint}$ ; /\* distribute the total torque between the motors with possible  $m$  combinations, where  $m$  is the cardinal of the  $\Lambda$  \*/

**Procedure 1 (cf. Algorithm 2)**

        Calculate the  $m^*$  costs  $J$ ;  $S_i \leftarrow v_{m^*}$ ; /\* Add  $m^*$  vertices to the tree  $T$  \*/

$e_i^{m^*} \leftarrow \{J(\Delta v, \Delta D_k, \Lambda), T_{EM}, T_{HM}\}$ ; /\* Attribute calculated costs and corresponding EM and HM torques to  $m^*$  number of edges \*/

**end**

**else**

**Procedure 2 (cf. Algorithm 3)**

        //  $T_{total} \leq 0$  Regeneration mode //

        Calculate the cost  $J$ ;  $S_i \leftarrow v_j$ ; /\* Add the vertex  $j$  to the tree  $T$  \*/

$e_i^j \leftarrow \{J(\Delta v, \Delta D_k), T_{EM}, 0\}$ ; /\* Attribute calculated cost and corresponding EM torque to the edge  $e_i^j$  \*/

**end**

**end**

**end**

**end**

// Apply the Dynamic Programming algorithm to on the obtained final tree  $T$ //

DP-SSEO = Dynamic Programming based Simultaneous Speed and Energy Optimization( $T$ )

**end**

**Algorithm 1:** Dynamic Programming based Simultaneous Speed and Energy Optimization ( DP-SSEO )

```

while Not all the  $m$  torque combination are checked ;      /* verify if all the  $m$ 
  combinations are feasible */
do
  for  $n$  from 1 to  $m$  do
    if ( $|T_{EM}(n) - T_{EM_{previous}}| > \Delta T_{EM_{max}}$ ) OR ( $|T_{HM}(n) - T_{HM_{previous}}| > \Delta T_{HM_{max}}$ ); /* check
      that the torque rate does not exceeds the max limit */
    then
      | Remove  $\Lambda(n)$ 
    end
  end
  Update the  $\Lambda$  with new size  $m$ 
end

```

**Algorithm 2:** Procedure 1 - Check the feasibility of the combinations

```

Data:  $T_{total}$ ,  $v$ ,  $v_{max,regen}$ ,  $v_{min,regen}$ 
if  $T_{total} \geq -600Nm$  then
  |  $T_{EM} = T_{total}$  ;
end
else
  |  $T_{EM} = -600$  ; //The rest will be provided by mechanical brake//
end
if  $v \geq v_{max,regen}$  then
  |  $w = 0.3$ ; //Regeneration coefficient //
end
else if  $v_{min,regen} \leq v \leq v_{max,regen}$  then
  |  $w = 0.3 \frac{v}{v_{max,regen}}$  ;
end
else
  |  $w = 0$ 
end
 $T_{regen} = w \cdot T_{EM}$ 

```

**Algorithm 3:** Procedure 2 - The regenerative torque calculation

The algorithm is run offline and generated 8856 possible speed profiles with different powersplit combinations that satisfy the constraints. To illustrate the efficiency of the proposed algorithm, optimal solution in terms of energy consumption is compared to a feasible solution with a cost function in the average of the obtained solutions.

Figure 4.8 presents an optimal solution for formulated problem. Upper sub-figure shows the speed profile, and the second sub-figure the powersplit (100% corresponds to pure electric mode). We can see that in the beginning the bus achieves a higher speed, which permits to profit from the downhill slope and reduce the consumption. According to the third sub-figure total consumed energy is 1983 kJ. The obtained results show that the fuel consumption is equal to 17.21 l/100 km.

In the contrast to that, Figure 4.9 shows a non-optimal solution, but however belonging to 100 first best results. We can see that the speed profile is different, as well as the powersplit. Such powersplit leads to a higher energy consumption (4605 kJ) and a fuel consumption of 41,84 l/100 km.

Although this algorithms allows to obtain a global optimal solution for speed profile and

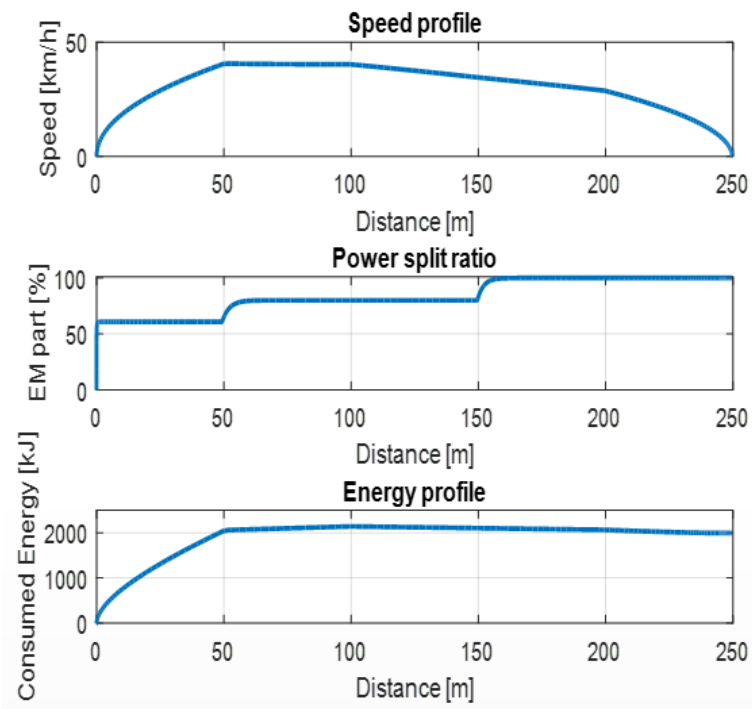


Figure 4.8: Optimal DP SSEO solution

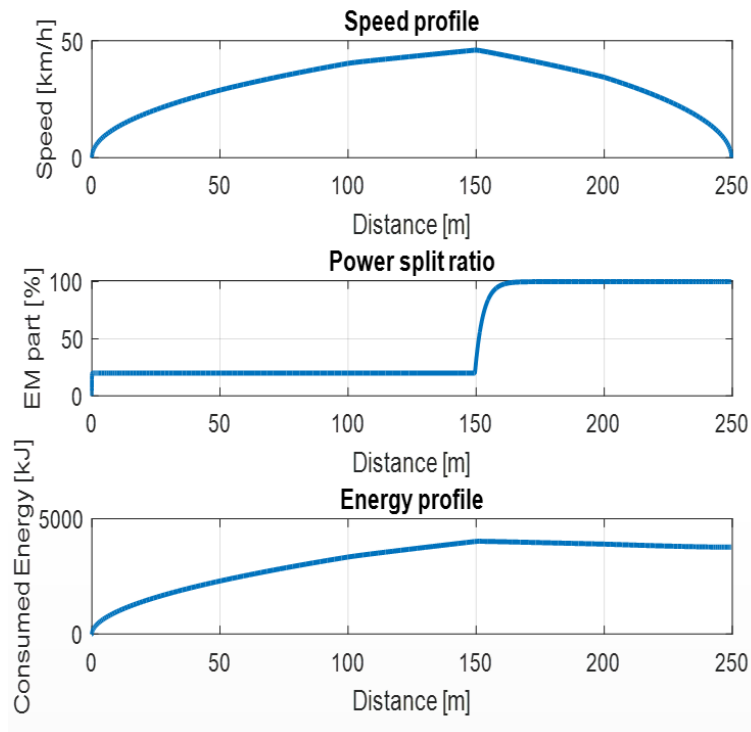


Figure 4.9: Non optimal DP SSEO solution

related powersplit, the generation of the solutions took several hours on Intel Core i-7

processor. So it is not usable in real-time applications. However this can be a basis for generating an optimal database. The idea is developed further in the section 4.3.

### 4.3/ ONLINE ENERGY MANAGEMENT

This section is dedicated to the description of the methodology for being able to use offline DP results in real time application. Before detailing the proposed methodology, a very brief review of the works that proposed techniques to overcome the computational burden of DP is presented below.

Authors in [Huang et al., 2011] propose an intelligent multi-feature statistical approach to automatically discriminate the driving condition of the HEV, called Intelligent Multi-feature Statistical Discrimination (IMSD). Based on the driving data of the HEV, the algorithm uses statistical analysis to extract and select multiple valid features. After the neural networks classifier learned the information on these features, it can intelligently discriminate the driving conditions in real time. The switch between two controllers is used depending on the driving conditions.

The work shown in [Larsson et al., 2015] investigates how the computational demand and the memory requirements of the DP algorithm can be reduced in HEV energy management problems. The key concept is to derive an analytical solution for the continuous control signal in each sub-problem, thereby avoiding the need to quantize the control signal and interpolate in the cost-to-go. However, the idea is not to solve the non-linear Hamilton-Jacobi-Bellman (HJB) partial differential equation, which would be non-trivial even with a simple powertrain model. The proposed method is to approximate the gridded cost-to-go, locally, with a low order polynomial. The local approximation is then only used to compute the continuous control signal at each point in the time and state grid. Two different approximations are considered in the paper: i) a local linear approximation, and ii) a quadratic spline approximation. The latter is also beneficial from a memory point of view as the cost-to-go can be stored as a small number of spline parameters at each time step, rather than a vector defined over the gridded state.

A four-step method to design and analyze an optimal Energy Management Strategy (EMS) for a powersplit HEV was presented in [Zhu et al., 2004]. *Step 1* A hybrid dynamical system theory is used to formulate the HEV control system that incorporates both continuous and discrete dynamics. *Step 2* The Sequential Quadratic Programming (SQP) method is applied to optimize power distribution. The DP method is employed to solve the complex vehicle operating mode transition problem. *Step 3* A rule-based system and a fuzzy rule system are developed based on the statistical numerical solutions derived from Step 2. *Step 4* A Genetic Algorithm is applied to a simultaneous optimization of parameters of membership functions, weights of the rules and rule sets for the fuzzy system and parameters of a rule-based system.

An approach to minimize the calculation time of a DP in order to implement it online is proposed in [Luu, 2011]. Basically, this approach looks like greedy algorithm: at each step  $t_n$  only the state that gives minimal cost is developed further at the instant  $t_{n+1}$ . Obviously, this approach will not give the optimal solution, but it significantly reduces the calculation time (from 11h to 180 ms). A supplementary mean to reduce the calculation time proposed in the thesis was setting an upper and lower bounds of the vehicle dynamics. That depends on the current moving mode (acceleration, deceleration, cruise speed) and on

speed limits imposed by laws.

The next section details the proposed approach and explains how this method can be applied.

#### 4.3.1/ SUB-OPTIMAL PROFILES DATABASE BASED ON DYNAMIC PROGRAMMING

Even if the proposed strategy of the DP-SSEO (cf. section 4.2) gives optimal results as all the possible states are explored and the global minimum is found, nevertheless it is too time consuming.

The proposed idea for overcoming the computational burden of the DP, detailed below, stems from a profound analysis of the DP-SSEO algorithm results. For a fixed length of road segment  $D$ ,  $K$  number of  $\Delta D$  and  $\Lambda$  the DP-SSEO algorithm (cf. Algorithm 1) has been performed under different elementary conditions of road slope and desired velocity progress:

- cruise speed, thus initial and final speeds are equal ( $v_0 = v_f$ ),
- acceleration phase thus  $v_0 < v_f$ ,
- deceleration  $v_0 > v_f$  phases.

The strategy corresponds to different initial and final conditions Algorithm 1 in order to find an optimal powersplit Figure 4.11. The speed varies from 0 to 20 m/s, hence 72 km/h. In order to ensure passenger's comfort, acceleration is limited to  $1.25 \text{ m/s}^2$ .

Figure 4.11 shows the average energy consumption for different road slopes  $\theta$  for aforementioned phases. It can be seen that the energy consumption obviously increases with a bigger  $\theta$ . A bigger bus weight also increases logically the fuel consumption. To maintain a cruise speed (*yellow bars*) on the downhill slope (negative  $\theta$ ), the acceleration produced by the bus' own dynamics is enough (sometimes even excessive and it is necessary to apply a brake).

So on the downhill slope the EM part is 100% for deceleration (*turquoise bars*) and cruise speed phases (cf. Figure 4.10), which means only electric motor is activated. When the vehicle accelerates (*purple bars*), the EM torque goes to its peak (cf. section 4.2.2) with the increase of the uphill slope, and it is complemented by the HM (via ICE), so we can see that EM ratio increases (in Figure 4.10 yellow corresponds to EM ratio and green to HM ratio). From the results of the optimization presented above, the optimal offline solutions can be used online in order to generate the sub-optimal solutions. For that purpose, the optimal profiles have been generated offline for the distance of  $\Delta d$  (chosen prediction horizon), with different  $\Delta v$  for several masses and slopes.

#### 4.3.2/ MULTI-DIMENSIONAL INTERPOLATION METHOD

Based on the offline optimal solutions, **DP based Optimal Profiles Database (OPD-DP)** will be used to generate the speed profiles and the related powersplit in the proposed real-time system.

A multi-dimensional OPD-DP is proposed for online speed profile and its powersplit generation. The scheme of the online control implementation is presented in Figure 4.12.



Figure 4.10: Average powersplit for different slopes

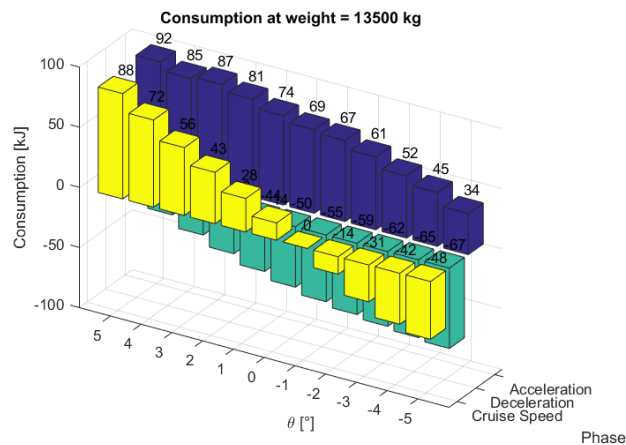


Figure 4.11: Average energy consumption for different slopes

The inputs of the multi-dimensional OPD-DP are the road profile  $(x, y, \theta)$ , the bus weight, the current speed and the driver’s reference (desired) speed, and the current road slope. It is supposed that the slope is known owing to on-board sensors. The multi-dimensional OPD-DP generates the sub-optimal speed profile reference and torque split depending on the current state of the vehicle and the road profile. The bus weight is considered constant for a single trip between two stops, thus the weight is susceptible to change only after each stop which is logical since passengers get on and off the bus. The reference speed  $v_{ref}$  must be followed as precise as possible due to the safety measures, ensuring the collision avoidance. The OPD-DP generates the sub-optimal profile references  $v_{opt}$ , as well as  $T_{EM}$  and  $T_{HM}$  set points. The set point torques are sent to EM and HM local controllers, which generate the control input to the motors ( $I_{EM}$  EM current,  $D_{HM}$  HM displacement).

Knowing that the multi-dimensional OPD-DP has only discrete values of each parameters (slope  $\theta$ , weight  $M$ , etc.), it is very important to have a mean to use this Multi-Dimensional

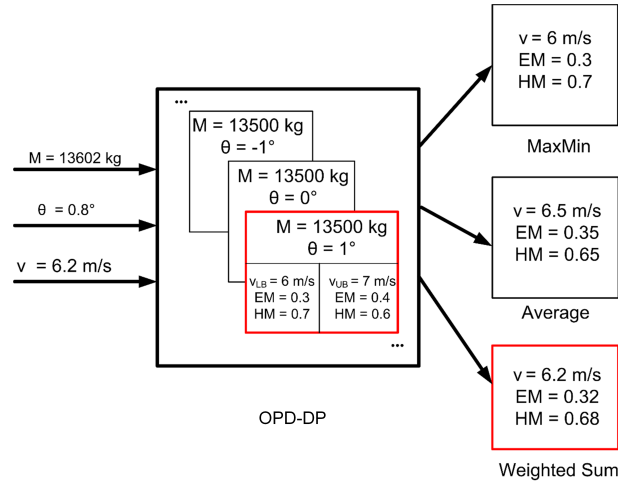


Figure 4.12: DP based Optimal Profiles Database (OPD-DP) illustration

Database (MDD) even for values not belonging to it. For this purpose, several techniques are proposed in order to extend the knowledge existing in the MDD.

1. **MinMax Value:** the values which are closer to the upper or the lower bound values are extracted for the mass, slope, speed profile and energy management split.
2. **Average Value:** the values which are closer to the current mass and slope are extracted. The average value of the speed between the upper and the lower bounds are calculated. The average value of the powersplit is applied as well.
3. **Linear Multi-Dimensional (LMD)** interpolation method [LaValle, 2006]. As a desired velocity value  $v$  lies generally between two values in the OPD-DP, a weighted sum of the lower bound speed  $v_{UB}$  and the upper bound speed  $v_{LB}$  are applied to generate the speed profile:

$$v_{opt} = \zeta_v v_{LB} + (1 - \zeta_v) v_{UB} \quad (4.20)$$

If  $v = v_{LB} = v_{UB}$  then we obtain:

$$v_{opt} = \zeta_v v + (1 - \zeta_v) v = v \quad (4.21)$$

The weight coefficient  $\zeta_v$  is obtained as follows:

$$\zeta_v = 1 - \frac{v - v_{LB}}{v_{UB} - v_{LB}} \quad (4.22)$$

The weight coefficients applied to calculate the corresponding powersplit  $\Lambda_{opt} = [\lambda_{opt1}, \lambda_{opt2}, \dots, \lambda_{optm}]$ , depend on the current speed  $v$ , the bus weight  $M$ , and the road slope  $\theta$ . This results into three dimensional interpolation function which is

given as follows:

$$\begin{aligned}
\Lambda_{opt}(v, M, \theta) = & \zeta_v \zeta_M \zeta_\theta \Lambda(v_{LB}, M_{LB}, \theta_{LB}) + \\
& (1 - \zeta_v) \zeta_M \zeta_\theta \Lambda(v_{UB}, M_{LB}, \theta_{LB}) + \\
& \zeta_v (1 - \zeta_M) \zeta_\theta \Lambda(v_{LB}, M_{UB}, \theta_{LB}) + \\
& \zeta_v \zeta_M (1 - \zeta_\theta) \Lambda(v_{LB}, M_{LB}, \theta_{UB}) + \\
& (1 - \zeta_v) (1 - \zeta_M) \zeta_\theta \Lambda(v_{UB}, M_{UB}, \theta_{LB}) + \\
& (1 - \zeta_v) \zeta_M (1 - \zeta_\theta) \Lambda(v_{UB}, M_{LB}, \theta_{UB}) + \\
& \zeta_v (1 - \zeta_M) (1 - \zeta_\theta) \Lambda(v_{LB}, M_{UB}, \theta_{UB}) + \\
& (1 - \zeta_v) (1 - \zeta_M) (1 - \zeta_\theta) \Lambda(v_{UB}, M_{UB}, \theta_{UB}) \quad (4.23)
\end{aligned}$$

where  $\Lambda_{opt}$  is the powersplit vector, and weight coefficients  $\zeta_M$  and  $\zeta_\theta$  are calculated as follows:

$$\zeta_M = 1 - \frac{M - M_{LB}}{M_{UB} - M_{LB}} \quad (4.24)$$

$$\zeta_\theta = 1 - \frac{\theta - \theta_{LB}}{\theta_{UB} - \theta_{LB}} \quad (4.25)$$

with indexes  $LB$  - lower bound and  $UB$  - upper bound of the corresponding parameter.

To illustrate how this method works in 3D, let us fix speed parameters, and suppose that the powersplit  $\Lambda$  change depends only on the variation of the bus weight and the road slope. Figure 4.13 illustrates the case when for different combinations of weight and slope angle, we have four known values of  $\Lambda$  stored in the OPD-DP. Now let us address the case when weight and slope angle values lie in between the known data. This method permits to calculate the corresponding powersplit.

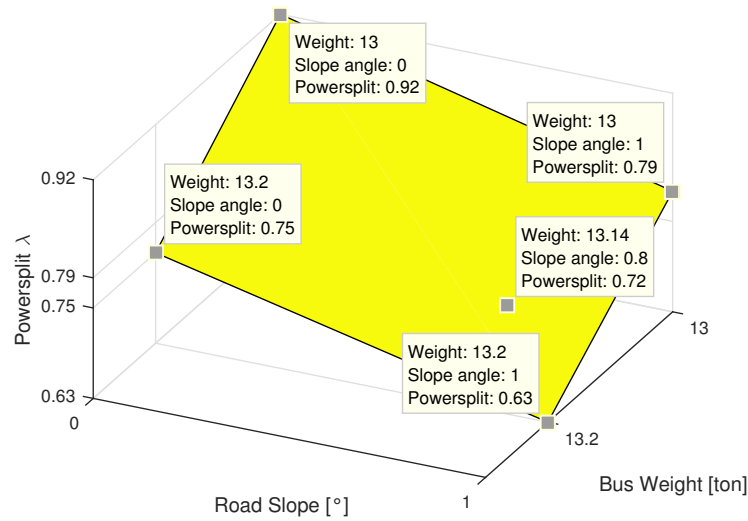


Figure 4.13: Linear Multi-dimensional Interpolation method illustration

### 4.3.3/ SIMULATION RESULTS

It is presented below several results of the use of the OPD-DP based real energy optimization for different proposed interpolation methods. Two scenarios are tested to validate the strategy. For both of them the bus travels a trip consisting of five Bus Station distances.

1. The bus arrives at all the Bus Stations without stopping at the traffic lights and without being stuck in a traffic jam.
2. In this case, at some points it had to stop because of the traffic lights or before the vehicle ahead, which entailed underspecified stops along the trip.

Road profile and the weight of the bus change during the trip (cf. Figure 4.14). However, the weight changes only after each bus stop when people get on or get off the bus. It is considered in this simulation that the road-tire frictional coefficient, which depends on the surface where the bus moves and on the weather conditions, is constant and equal to 1, which corresponds to the dry pavement [Ming, 1997]. Basically, the  $SOC_{initial} = 90\%$ , and

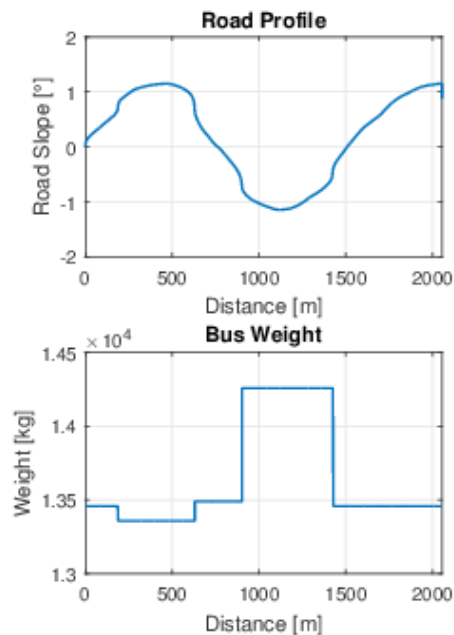


Figure 4.14: Road slope and bus weight

in the end of the trip must be around  $SOC_{min} = 87.77\%$ , according to the  $SOC$  reference (cf. section 3.4). Total trip distance is 2 km (more precisely 2058m in this simulation).

Figure 4.15 represents the results of the first scenario. The Figure 4.15(a) shows the obtained speed profile. Red crosses indicate the driver's demanded speed at each  $\Delta d$ . The average error between the driver's reference and the generated speed is less for LMD interpolation. Globally, the LMD interpolation method outperforms the presented interpolation methods. It provides minimal speed error tracking, consuming less energy (a sum of electric and heat (engine) energy, see Figure 4.15(c)). The SOC is closer to its desired value according the LMD method as well (cf. Figure 4.15(c)).

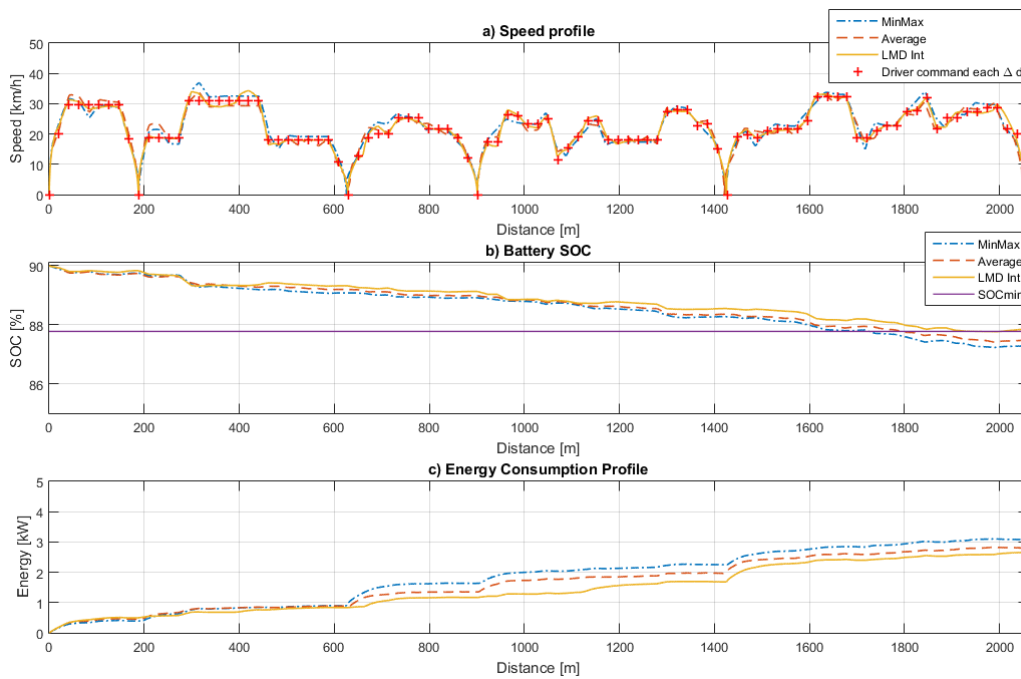


Figure 4.15: First scenario: a) speed profile b) actual  $SOC$  and the desired value in the end of the trip  $SOC_{min}$  c) Energy consumption

Figure 4.16 represents the second scenario. In this case, we can see that at the distance  $\approx 500m$  there is a non-planned stop, as well as at the distance  $\approx 1200m$ , etc. Although the speed profile changed, the online energy optimization strategy is adapted in such a manner that it will always tend to  $SOC_{min}$  at the end of the trip. Despite the real-time profile change, the LMD interpolation method shows better results compared to other interpolation methods.

Table 4.1: OPD-DP online strategy: interpolation methods comparison

$SOC_{min} = 87.77\%$						
	MinMax		Average		LMD	
	$SOC_{final}, \%$	Energy, kW	$SOC_{final}, \%$	Energy, kW	$SOC_{final}, \%$	Energy, kW
Scenario 1	87.28	3.08	87.47	2.81	87.84	2.64
Scenario 2	87.72	4.48	87.63	4.25	87.91	3.13

## 4.4/ CONCLUSION

This Chapter described the proposed deterministic energy management strategy algorithm. The Dynamic Programming based Simultaneous Speed and Energy Optimization(DP-SSEO) algorithm is proposed in this chapter. Based on the offline optimal strategy results, an online approach has been proposed in order to deal with the real-time road profile and driver velocity demand. The proposed online suboptimal strategy uses mainly a Multi-Dimensional Database (MDD, which gives as output the speed profile and powersplit set-points) and an appropriate interpolation technique in order to cope with the current bus situations.

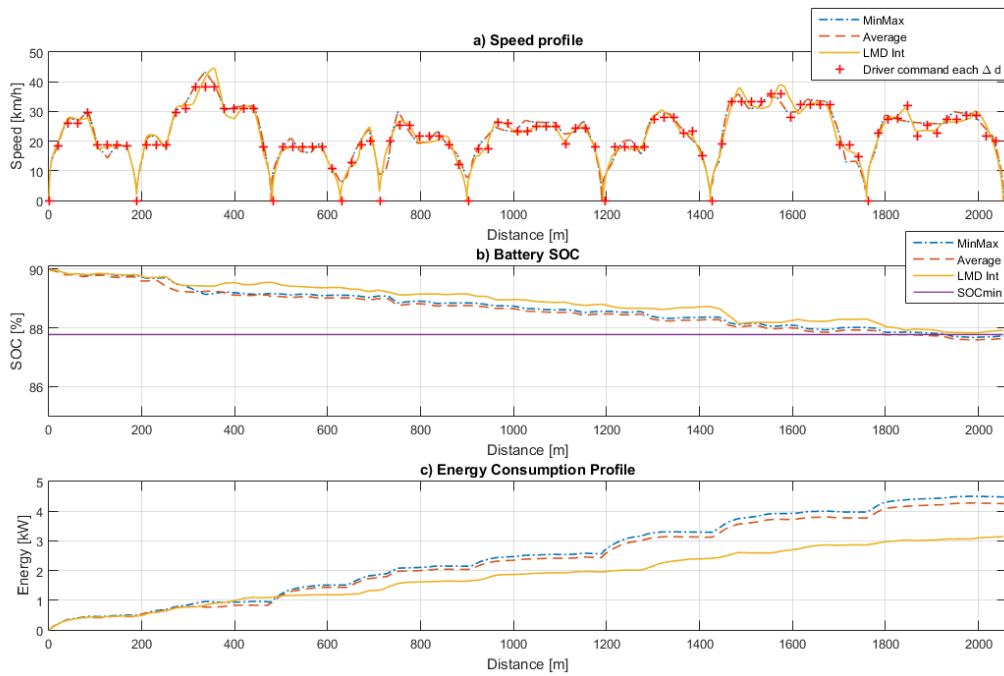


Figure 4.16: Second scenario: a) speed profile b) actual  $SOC$  and the desired value in the end of the trip  $SOC_{min}$  c) Energy consumption

# STOCHASTIC ENERGY MANAGEMENT STRATEGY

## **Abstract**

---

This chapter presents two proposed energy management strategies based on stochastic approaches. A Stochastic Model Predictive Control (SMPC) based strategy has been developed to optimize the powersplit which presents power demand as a Markov Decision Process (MDP). The second approach which is more a focus of this chapter corresponds to a sub-optimal energy management strategy, based on Stochastic Dynamic Programming (SDP), for efficient powersplit of a HEV and speed optimization. Formulated as a multi-objective optimization problem, an  $\epsilon$ -constraint method has been used to find the Pareto front of the energy optimization task. Traffic conditions and driver behavior are assimilated to a stochastic nature, thus, it is proposed in this strategy to address the vehicle power as an MDP. A Stochastic Database is used to store Transition Probability and Reward Matrices, corresponding to suitable vehicle actions w.r.t. specific states. They are used afterwards to calculate sub-optimal powersplit policy for the vehicle via an infinite-horizon SDP approach.

---

## 5.1/ INTRODUCTION

In effective transportation systems, a totally deterministic model is unlikely to include various uncertainties, associated with sensor's measurement errors, power demand with stochastic nature. To overcome this drawback, some researchers make use of Stochastic approaches, for instance Stochastic Dynamic Programming (SDP) [Elbert et al., 2015] [Johannesson et al., 2007]. The basic idea behind SDP is the fact that the driver behavior can be modeled and predicted by a Stationary Markov Chain [Puterman, 2014]. Plotting the data in the speed-power plane reveals that the driver behavior can be predicted to some extent [Elbert et al., 2015]. Authors in [Johannesson et al., 2007] carried out a study to investigate what can be achieved if all the available on-board information is used optimally to assess the potential of predictive control for HEV powertrains. The Deterministic Dynamic Programming (DP) is used for dimensioning of the energy storage elements and the SDP is used to find a causal operating strategy as in [Romaus et al., 2010]. A time-invariant state feedback based control law, derived from SDP, is proposed in [Lin et al., 2004] as a power management strategy.

This chapter is dedicated to the description of the stochastic approaches based algorithms. In order to clearly explain the methodology, this chapter starts with a brief introduction of Markov Decision Processes modeling, definition of used variables and terms.

Afterwards, proposed Stochastic Model Predictive Control and Stochastic Dynamic Programming based approaches are described in the sections below. Two methods have been explored in this chapter.

## 5.2/ STOCHASTIC MPC

The first approach presented in this chapter is based on Stochastic MPC. This control strategy is a part of the global control architecture (cf. Chapter 3). As highlighted in chapter 3 the studied HEV corresponds to a series-parallel configuration of powertrain where the electric motor (EM) is linked to hydraulic motor (HM) in parallel, meanwhile the HM power is supplied via the internal combustion engine (ICE) connected in series.

[Hemi et al., 2015] proposed a real time optimal control strategy based on Pontryagin's Minimum Principle (PMP), combined with a Markov chain approach for a fuel cell/supercapacitor electrical vehicle. A Markov chain model is added as a separate block for a prediction of required power. In recent years various stochastic model based predictive control (SMPC) algorithms have been proposed. An SMPC algorithm was developed by [Ripaccioli et al., 2010] for power management, with the goal of optimizing the power-splits in hybrid electric vehicle (HEV), while fulfilling bounds on the state of charge ( $SOC$ ) of the battery and on the power availability. The power requested from the driver is represented by a Markov model. Instead of optimizing over driving cycle known a priori, the SMPC strategy optimizes over a distribution of future requested power demand, given the current one, at each sample time. [Bichi et al., 2010] developed an approach based on SMPC used for improving the performance of powertrain control algorithms, by optimally controlling the complex system composed of driver and vehicle. The vehicle was modelled as a deterministic dynamical system, and the driver as a stochastic process, whose dynamics is updated online. Stochastic model predictive control is applied to optimize expected performance over a tree of scenarios, while enforcing constraints on states, inputs, and outputs. From a computational viewpoint, by assuming a linear system model they solve the SMPC problem via standard quadratic programming.

The Stochastic MPC developed in this chapter is presented in details in section 5.2. The SMPC algorithm presented in [Bichi et al., 2010], [Ripaccioli et al., 2010], is adopted for this strategy in order to cope with the uncertainty on the requested power  $P_{req}$ . The proposed cost function with time depending references, is the new added element compared to the cited references, where the  $SOC$  is a time-invariant constant value.  $P_{ICE_{ref}}(k)$  keeps the electric motor working with its maximum efficiency to respect the  $SOC_{ref}(k)$ , so as to maintain the battery charge above a certain threshold until the end of the day (cf. Figure 5.1). This method allows a better usage of the electric energy and a better power management of the hybrid vehicle.

### 5.2.1/ STOCHASTIC MPC MODEL

The energy management strategy is conceived in order to minimize the fuel consumption by optimally delivering the requested power.  $P_{req}$  is the total requested power that must be generated by the powertrain, the controller selects the  $P_{EM}$  which must be provided by the electric motor through the electric battery, and the  $P_{ICE}$  which must be provided by the HM through the ICE. The power balance equation for each sampling step  $k$  is given

by equation 5.1:

$$P_{req}(k) = P_{EM}(k) + P_{ICE}(k) - P_{br}(k) \quad (5.1)$$

where  $P_{br}$  is the braking power by conventional friction brakes, in case where the braking kinetic energy can not be recovered or regenerative braking is not sufficient to provide the desired vehicle braking power. As the dynamics of the engine and the electric motor are much faster than the dynamics of the battery charge, the equation that connects the dynamics of the actuators with the one of the battery is:

$$SOC(k+1) = SOC(k) - KT_s P_{EM}(k) \quad (5.2)$$

with  $SOC \in [0, 1]$ ,  $SOC = 1$  corresponds to a fully charged battery,  $T_s$  the sampling period, and  $K > 0$  a positive constant identified for a generic HEV battery, it depends on the battery dynamics. Note that a positive value of  $P_{EM}$  indicates that power is provided by the battery to the motor, in the opposite case, the battery is charged by the motor (generator mode) on the regenerative braking phase.

The SMPC controls the variation of the engine power  $\Delta P$  where

$$\Delta P(k) = P_{ICE}(k) - P_{ICE}(k-1) \quad (5.3)$$

Thus, we obtain the linear model from 5.1-5.3:

$$x(k+1) = Ax(k) + B_1u(k) + B_2w(k) \quad (5.4)$$

$$y(k) = Cx(k) + D_1u(k) + D_2w(k) \quad (5.5)$$

where

- $x(k) = \begin{bmatrix} SOC(k) \\ P_{ICE}(k-1) \end{bmatrix}$  the state vector,
- $u(k) = \begin{bmatrix} \Delta P(k) \\ P_{br}(k) \end{bmatrix}$  the control vector,
- $y(k) = P_{EM}(k)$  the output,
- $w(k) = P_{req}(k)$  is considered as a stochastic disturbance, which corresponds to the actions of the driver on the vehicle, where  $w(k) \in W$ . We suppose that at time  $k$ , the value  $w$  can be measured and we denote it by  $w(k)$ .
- $A = \begin{bmatrix} 1 & KT_s \\ 0 & 1 \end{bmatrix}$ ,  $B_1 = \begin{bmatrix} KT_s & -KT_s \\ 1 & 0 \end{bmatrix}$ ,  $B_2 = \begin{bmatrix} -KT_s \\ 0 \end{bmatrix}$
- $C = \begin{bmatrix} 0 & -1 \end{bmatrix}$ ,  $D_1 = \begin{bmatrix} -1 & 1 \end{bmatrix}$ ,  $D_2 = 1$

In order to design the SMPC controller, it is necessary to generate the stochastic perturbation using a Markov chain model.

The required power  $P_{req}$  is considered as a random process, denoted by  $w$ , and it is modeled as a Markov chain with the states  $W = \{w_1, w_2, \dots, w_s\}$ , where obviously  $w_i \in W$ , for all  $i \in \{1, \dots, s\}$ . The  $Card(W) = s$  is chosen in such a way that it ensures a good compromise between the complexity of the stochastic model and its precision. The Markov Chain is defined by a transition probability matrix  $T$  such that:

$$[T]_{ij} = Pr[w(k+1) = w_j | w(k) = w_i] \quad (5.6)$$

where  $i, j \in \{1, \dots, s\}$ ,  $w(k)$  the state of the Markov chain at time  $k$ ,  $Pr$  is the probability distribution of  $w(k+1)$ . Using the Markov chain model with  $w(k) = w_i$ , the probability distribution of  $w(k+l)$  is calculated as follows:

$$Pr[w(k+l) = w_j | w(k) = w_i] = [(T^l)' \cdot e_i]_j \quad (5.7)$$

where  $e_i$  is the  $i^{th}$  unitary vector, i.e.,  $[e]_i = 1$ ,  $[e]_j = 0$  for all  $j \neq i$ .

To predict  $P_{req}$ , a Markov chain with  $s = 300$  states is used. The transition matrix  $T$  is initialized by  $T = I$  ( $I$  Identity Matrix) and then updated online. We run the controller several times for different driving cycles, ECER15 (also known as UDC - Urban Driving Cycle), EUDC (European Urban Driving Cycle), ArtUrban (Urban Artemis), and NEDC (New European Driving Cycle), to learn the transition probabilities. The learning of the transition matrix is done through the power demanded by the driver  $P_{req}$  which translates the behavior of the driver and his way of driving. By counting the number of transitions of a power  $P_{reqi}$  to  $P_{reqj}$ , the number of occurrences for each transition from a state  $i$  to a state  $j$  is stored in  $[n]_{ij}$ .

The transition matrix  $T$  can be updated after each simulation, or when a large number of data is collected. To update the transition matrix, the following procedure has been used. For all  $j \in \{1, 2, \dots, s\}$

$$[T]_j = \frac{[n]_j + \lambda[T]_j}{\lambda + \sum_{k=1}^s [n]_{jk}} \quad (5.8)$$

where  $\lambda$  the filtering parameter,  $[T]_j$  the  $j^{th}$  row of transition matrix  $T$ ,  $[n]_j$  the  $j^{th}$  row of occurrence matrix  $[n]$ .

The SMPC algorithm presented in [Bichi et al., 2010], [Ripaccioli et al., 2010], is adopted in order to cope with the uncertainty on the requested power  $P_{req}$ . The proposed cost function with time depending references, is the new added element compared to the cited references, where the  $SOC$  is a time-invariant constant value.  $P_{ICE_{ref}}(k)$  keeps the electric motor working with its maximum efficiency to respect the  $SOC_{ref}(k)$ , so as to maintain the battery charge above a certain threshold until the end of the day (cf. Figure 5.1). This method allows a better usage of the electric energy and a better power management of the PHEB. The proposed approach based on SMPC is formulated according to the specific features of the PHEB models. The SMPC selects in this work the optimum engine power variation. It is presented in what follows the proposed SMPC formulation where the objective function (to be minimized) relies on an approximation of the expected value of:

$$J(k) = c_1 \Delta P(k)^2 + c_2 (P_{ICE}(k) - P_{ICE_{ref}}(k))^2 + c_3 (SOC(k) - SOC_{ref}(k))^2 \quad (5.9)$$

where  $\Delta P(k)$  engine power variation (cf. equation 2.19),  $P_{ICE}$  actual ICE power,  $P_{ICE_{ref}}(k)$  is the ICE reference power,  $SOC(k)$  actual  $SOC$ ,  $SOC_{ref}(k)$  is the reference  $SOC$ , and  $c_i | i = 1, \dots, 3$  constant positive values, given the weight for each sub-criterion:  $c_1$  enforces smooth mechanical power variations,  $c_2$  leads the system to relieve the electric motor while using the ICE motor when the requested power exceeds electric motor nominal power,  $c_3$  penalizes deviations from battery reference  $SOC_{ref}$  (cf. Figure 5.1).

It is to be noted that  $P_{ICE_{ref}}$  is defined to relieve the electric motor, in order to keep it in the nominal operating area  $P_n$ . For this reason, we proposed a switching logic (cf. Table 5.1).

The reference  $SOC_{ref}$  is time-variable. The Businova is a plug-in hybrid electric vehicle and its standard functioning time is  $n$  hours a day (so called "course of a day"). Figure 5.1

illustrates an example of a reference  $SOC$  baseline for a course of a day corresponding to 8h. By the end of a day, the bus has to reach its  $SOC_{min}$  value and can be recharged during all the night long to ensure the service the next day. Based on this hypothesis,

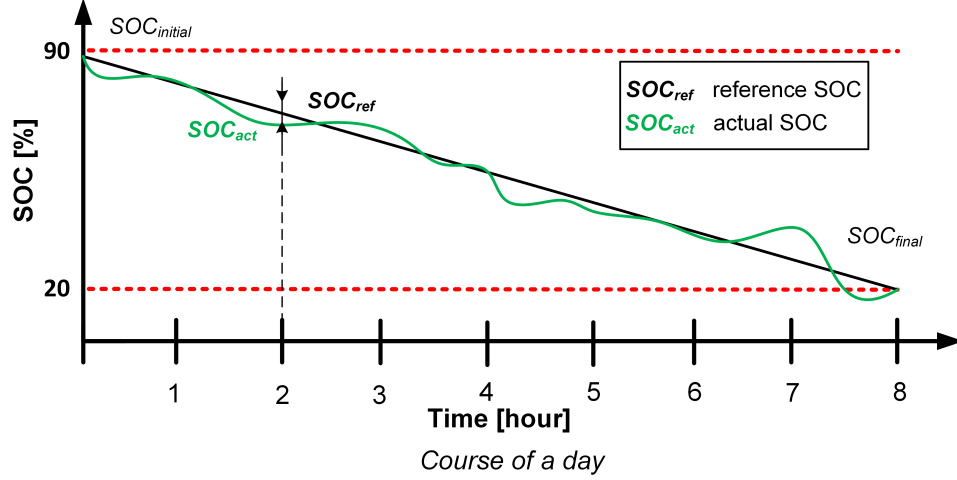


Figure 5.1: Reference  $SOC$  baseline

the  $SOC_{ref}$  is updated each time interval  $\Delta t$  in order to guide the energy management strategy solutions produced by the proposed SMPC.

In order to guarantee a prolonged battery life and to respect electro-mechanical limitations, the state, manipulated inputs and outputs are subject to the constraints:

$$\mathbf{X} = \{x \in \mathbb{R}^2, \begin{bmatrix} SOC_{min} \\ 0 \end{bmatrix} < x < \begin{bmatrix} SOC_{max} \\ P_{ICE_{max}} \end{bmatrix}\}$$

$$\mathbf{U} = \{u \in \mathbb{R}^2, \begin{bmatrix} -\Delta P_{min} \\ 0 \end{bmatrix} < u < \begin{bmatrix} \Delta P_{max} \\ P_{br_{max}} \end{bmatrix}\}$$

$$\mathbf{Y} = \{y \in \mathbb{R}, P_{EM_{min}} < y < P_{EM_{max}}\}$$

### 5.2.2/ SIMULATION RESULTS

Below the simulation results for the proposed global control architecture are presented. The SMPC supporting eACCwSG function has been tested for several standardized urban driving cycles [Barlow et al., 2009] to validate its performance. A driving cycle determines the leader vehicle speed profile. Initial distance between two vehicles is  $d_{min\_safety} = 5$  m (cf. Figure 6.3). The bus driver aims to drive at preset velocity  $v_{cc} = 40$  km/h.

The initial conditions are  $SOC(0) = 0.9$ ,  $P_{req}(0) = 0$ ,  $\Delta P_{max} = \Delta P_{min} = 1kW$  and  $P_n = 10kW$ . The cost function in equation 5.9 is normalized and the weight coefficients are chosen so

Table 5.1: Switching logic for the ICE reference power

Condition	$P_{req} < P_n$	$P_{req} \geq P_n$
ICE reference power, $P_{ICE_{ref}}$	0	$P_{req} - P_n$

that  $\sum_{i=1}^3 c_i = 1$ . For the simulations presented below, the following weight coefficients were chosen:  $c_1 = 0.4$ ,  $c_2 = 0.4$  and  $c_3 = 0.2$ .

In order to validate the proposed control strategy four standard urban driving cycles were chosen: ECER15, EUDC, ArtUrban, and NEDC. The simulation results are summarized in Table 5.2.

1. ECER15 (also known as UDC - Urban Driving Cycle),
2. EUDC (European Urban Driving Cycle),
3. ArtUrban (Urban Artemis),
4. NEDC (New European Driving Cycle).

In order to estimate the efficiency of the proposed SMPC energy management strategy (EMS), it is compared with the results obtained applying a Rule-Based (RB) EMS [Hofman et al., 2007]. The columns **Diff** in Table 5.2 corresponds to the percentage of improvement of the SMPC compared to RB EMS. "+" corresponds to a positive improvement, "-" means that RB EMS demonstrated better performance.

Table 5.2: Comparison of the Rule Based strategy and SMPC strategy

Dr.Cycle	Time	$\Delta SOC$ [%]			Fuel [l]			Energy [kWh]		Diff. [%]
		RB	SMPC	Diff. [%]	RB	SMPC	Diff. [%]	RB	SMPC	
ECER15	389	1.642	1.002	<b>+38.97</b>	0.045	0.064	<b>-42.22</b>	1.208	1.098	<b>+10.01</b>
EUDC	398	2.424	1.779	<b>+26.61</b>	0.010	0.022	<b>-54.50</b>	1.234	1.053	<b>+14.66</b>
ArtUrban	1985	6.376	2.889	<b>+54.68</b>	0.264	0.399	<b>-51.13</b>	5.575	5.131	<b>+7.96</b>
NEDC	2359	7.092	5.987	<b>+15.58</b>	0.116	0.072	<b>+38.00</b>	4.457	3.597	<b>+19.29</b>
Average	-	-	-	<b>+33.96</b>	-	-	<b>-27.46</b>	-	-	<b>+12.98</b>

Globally, the SMPC outperforms RB EMS in average by 12.98% from the consumed energy point of view. The consumed energy  $E_{cons}$  given by the column **Energy [kWh]** in Table 5.2 is calculated as follows:

$$E_{cons} = \int_0^{t_f} P_{EM} dt + \int_0^{t_f} Q_{LHV} \dot{m}_f dt \quad (5.10)$$

where  $P_{EM}$  is the electric motor consumed power,  $\dot{m}_f$  fuel consumption rate, and  $Q_{LHV} = 43 MJ/kg$  lower heat value for diesel.

To illustrate the performance graphics NEDC standard driving cycle (SDC) was chosen. In Figure 5.2-5.5 the simulation results are presented. Fig. 5.2 presents the bus speed profile. The driving cycle lasts 2360 s.

Figure 5.3 presents the Powersplit profile for both EMS. Although the total power demand is the same, the powersplit influences the electric energy and fuel consumption of the bus.

Fig. 5.4 presents the battery  $SOC$  and fuel consumption graphs. One can see that the SMPC distributes power in such a way that the battery  $SOC$  converges to the referenced  $SOC_{ref}$ , as opposed to RB EMS, where the battery final  $SOC$  is lower than the  $SOC_{ref}$ . The rest of the power is supplied by the ICE. Figure 5.4 shows that the SMPC consume less fuel as well for the given cycle. To illustrate a global energetic performance, we make use of equation 5.30. Figure 5.5 proves that from the energy point of view, the SMPC EMS provides less consumption (notably, 4.457 kWh vs 3.597 kWh, thus 19.29% of improvement).

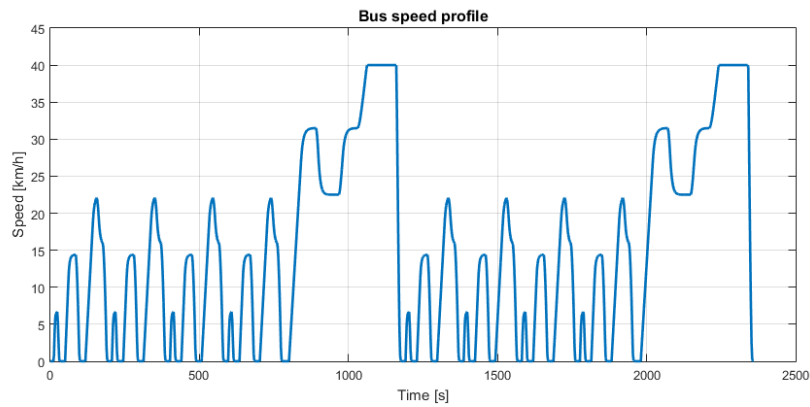


Figure 5.2: Speed Profiles for NEDC SDC

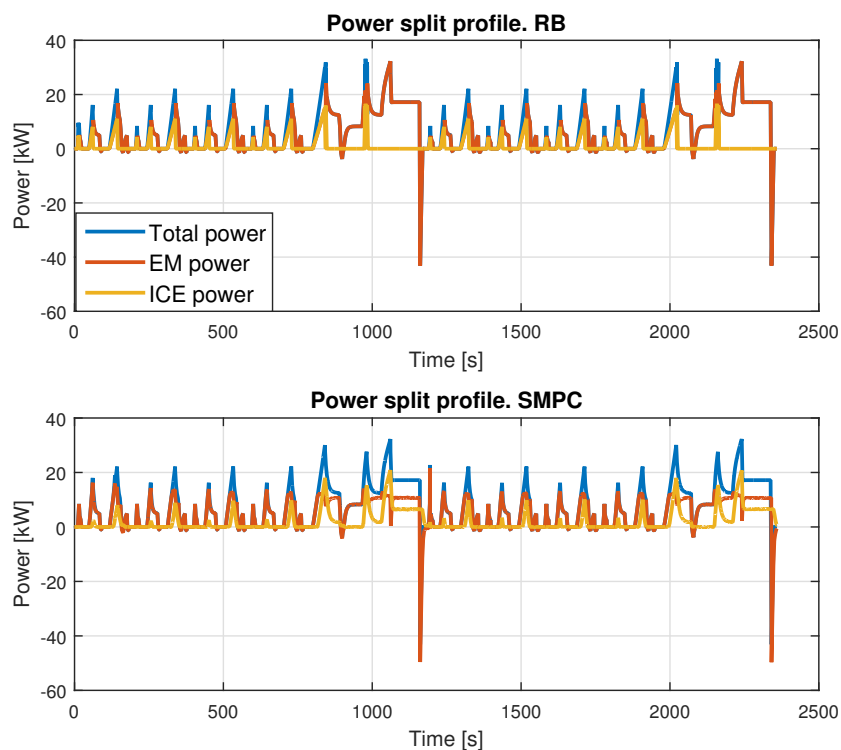


Figure 5.3: Powersplit Profile for NEDC SDC

### 5.3/ STOCHASTIC DYNAMIC PROGRAMMING

The SMPC method described above has an implementation problem due to high calculation time. Also this control law impacts only powersplit and not the speed profile. That is why it has been decided to continue developing the idea of simultaneous speed and powersplit optimization presented in the Chapter 4 in the presence of the uncertainties.

In this section it is proposed an optimization technique based on Stochastic Dynamic Programming (SDP) permitting to have simultaneous speed profile and powersplit optimization. Compared to the strategies, offline and online, developed based on Determin-

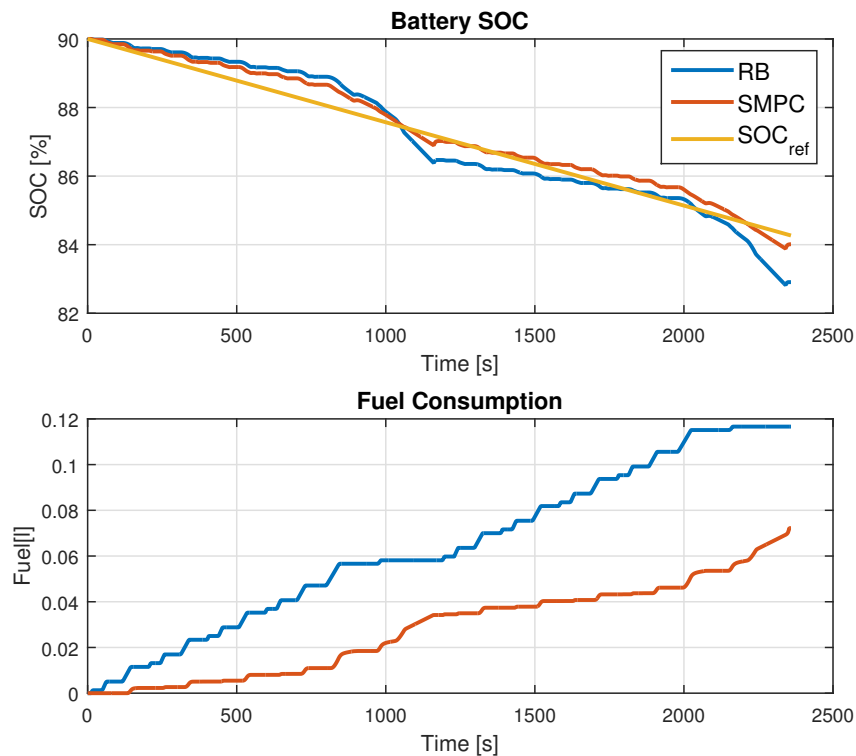


Figure 5.4: SOC and fuel consumption comparison for NEDC SDC

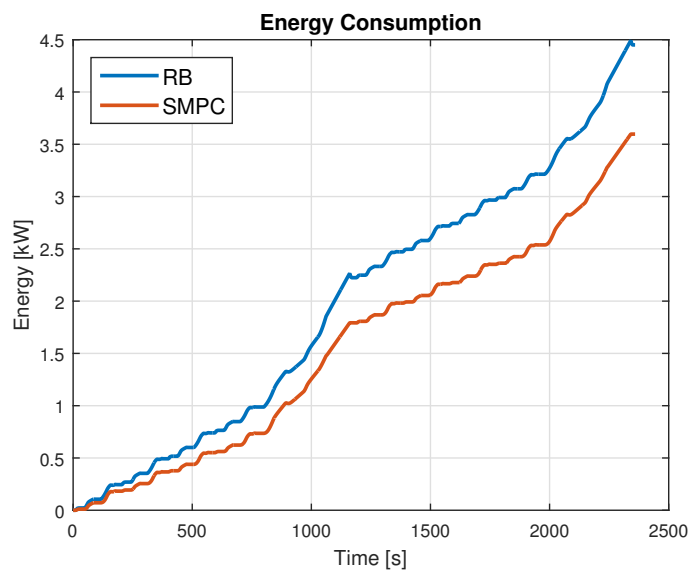


Figure 5.5: Energy Profile for NEDC SDC

istic DP (DDP) in the chapter 4, the stochastic approach calculates a policy (cf. Annex A) prescribing how to act optimally in the face of uncertainty. Unlike the references developing algorithms based on SDP, the present strategy proposes an optimization technique based on SDP permitting to have simultaneous speed profile and powersplit optimization strategy. The driver's behavior can be considered as a stochastic process

[Angkititrakul et al., 2012] [Zeng et al., 2017], therefore the driver model is represented as a Markov Decision Process in this manuscript. For an urban bus the route is normally known in advance, so the optimization is performed taking into account an available information about the trip. One of the most important aspects of the public transportation is the passengers comfort. For that purpose the maximal permitted acceleration and deceleration are taken into account as constraints. Simulation data of several standard urban driving cycles have been used to train Transition Probability Matrices (TPM) using the maximum likelihood estimation technique. The obtained TPM and Reward Matrices have been collected into an Optimal Profile Database based on SDP (OPD-SDP). The OPD-SDP has been then used to calculate sub-optimal speed profiles and related powersplit by Modified Policy Iteration Algorithm using an infinite horizon optimization formulation.

An online sub-optimal speed profile and related powersplit generation is developed to deal online with the current road profile and driver power demand. This is carried out using an Optimal Profile Database based on SDP (OPD-SDP), where different transition probabilities and rewards are collected and utilized depending on reference battery  $SO_{C_{bat}}$  curve (cf. Chapter 3). The reference  $SO_{C_{bat}}$  curve constraint guarantees a smooth battery discharge so that also at the end of the operational cycle (in the end of a course of a day) the  $SO_{C_{bat}}$  do not fall below its permitted minimum level.

### 5.3.1/ STOCHASTIC MODELING OF DRIVER

The driver's throttle and brake pedal commands are interpreted as a power demand to be satisfied by the powertrain. The system is described by the state variable  $x = \{v, P_{dem}, SO_{C_{bat}}\}$ , where  $v$  bus speed,  $P_{dem}$  total power demand, and  $SO_{C_{bat}}$  battery state of charge. The power distribution between two energy storages and the speed profile optimization is controlled by the control signal  $u = \{a, P_{EM}\}$ , where  $a$  is acceleration and  $P_{EM}$  electric motor power. Based on collected and simulated data of driving cycles, the transition probability of the state variable are calculated and modeled as a homogeneous Markov Chain.

The state and control spaces are discretized so that they take a finite number of values. The state variables are discretized as follows:

$$P_{dem} \in \{P_{dem}^1, P_{dem}^2, \dots, P_{dem}^{N_p}\} \quad (5.11)$$

$$v \in \{v^1, v^2, \dots, v^{N_v}\} \quad (5.12)$$

$$SO_{C_{bat}} \in \{SO_{C_{bat}}^1, SO_{C_{bat}}^2, \dots, SO_{C_{bat}}^{N_E}\} \quad (5.13)$$

So the total state space dimension is:

$$\{x^i, i = 1, 2, \dots, N_p N_v N_E\} \quad (5.14)$$

The control variables  $u$  are also discretized:

$$a \in \{a^1, a^2, \dots, a^{N_a}\} \quad (5.15)$$

$$P_{EM} \in \{P_{EM}^1, P_{EM}^2, \dots, P_{EM}^{N_{EM}}\} \quad (5.16)$$

Since the  $P_{dem}$  is assumed to be a Markovian state, the power dynamics is defined as follows:

$$P_{dem,k+1} = w_k \quad (5.17)$$

where the probability distribution of  $w_k$  is assumed to be:

$$Pr\{w = P_{dem}^j \mid P_{dem} = P_{dem}^i, v = v^l\} = p_{il,j} \quad (5.18)$$

$i, j = 1, 2, \dots, N_p, l = 1, 2, \dots, N_v$ , where  $\sum_{j=1}^{N_p} p_{il,j} = 1$ , and  $p_{il,j}$  represents the transition probability of the system in a state  $P_{dem}^j$  at instant  $k + 1$  with regards to the system in state  $P_{dem}^i$  and  $v^l$  at instant  $k$ .

We used standard driving cycles in this study to determine the transition probabilities as follows: various standard driving cycles were selected to represent different urban driving cycles. From the reference speed profile,  $P_{dem}$  has been calculated using the vehicle model. Using nearest-neighbor quantization, the sequence of observations ( $P_{dem}, v$ ) was mapped into a sequence of quantized states ( $P_{dem}^i, v = v^l$ ). The transition probability has been estimated by the maximum likelihood estimator [White, 1982], which counts the observation data as:

$$\hat{p}_{il,j} = \frac{m_{il,j}}{m_{il}} \quad (5.19)$$

where  $m_{il} \neq 0$ , where  $m_{il,j}$  is the number of occurrences of the transition from  $P_{dem}^i$  to  $P_{dem}^j$ , when the speed was at  $v^l$ ,  $m_{il} = \sum_{j=1}^n m_{il,j}$  is the total number of times that  $P_{dem}^i$  has occurred at speed  $v^l$ .

### 5.3.2/ MULTI-OBJECTIVE OPTIMIZATION PROBLEM FORMULATION

As any problem of optimization, it is important to define optimization criteria. In our case, the criteria is defined in order to minimize the energy consumed by the HEV while optimizing both: HEV speed profile and the powersplit during the trip  $D$ . In [Abdrakhmanov et al., 2017a] a minimizing cost function consisted in a compromise between electric motor and engine consumed power. The weighted aggregation method has been used to find a set of sub-optimal trade-off solutions of the cost function. In this work, a driver's power demand is considered as a random MDP (cf. section 5.3.1). Thus, the following cost function  $\zeta$  is proposed and formulated as a Multi-Objective (MO) optimization problem:

$$\zeta = f_1 + f_2 + f_3 \quad (5.20)$$

where  $f_1$  is a criterion responsible for speed optimization,  $f_2$  for battery  $SOC$  discharge curve, and  $f_3$  for powersplit optimization. The given criteria are defined as follows:

$$f_1 = \left( \frac{v_{ref} - v}{dt} - a \right)^2 \quad (5.21)$$

$$f_2 = (SOC(D_n) - SOC_{current})^2 \quad (5.22)$$

$$f_3 = (P_{dem} - P_{EM} - P_{HM})^2 \quad (5.23)$$

where  $v_{ref}$  is a reference driver speed,  $v$  bus current speed,  $dt$  time interval,  $a$  acceleration control input,  $SOC(D_n)$  reference  $SOC_{bat}$  value for a route segment  $D_n$ ,  $SOC_{current}$  current  $SOC_{bat}$  value,  $P_{dem}$ ,  $P_{EM}$  and  $P_{HM}$  demanded power, electric and hydraulic motors supplied power, respectively.

The goal is to find a set of optimal solutions that minimize  $f_1, f_2, f_3$  among all the feasible solutions, i.e., generate a Pareto front (cf. Figure 5.6). To this end,  $\epsilon$ -constraint

method was chosen. It is a MO optimization technique, proposed by [Haimes, 1971], for generating Pareto optimal solutions. It makes use of a single-objective optimizer which handles constraints, to generate one point of the Pareto front at a time. For transforming the MO problem into several single-objective problems with constraints the authors use the following procedure (assuming minimization for all the objective functions):

$$\begin{aligned} & \underset{x}{\text{minimize}} && f_l(x) \\ & \text{subject to} && f_j(x) \leq \epsilon_j, \quad i = 1, \dots, m, j \neq l \\ & && x \in S \end{aligned}$$

where  $l \in \{1, 2, \dots, m\}$  and  $S$  is the feasible region, which can be defined by any equality and/or inequality constraint. The vector of upper bounds,  $\epsilon = (\epsilon_1, \epsilon_2, \dots, \epsilon_m)$ , defines the maximum value that each objective can have. In order to obtain a subset of the Pareto optimal set (or even the entire set, in case if this set is finite), one must vary the vector of upper bounds along the Pareto front for each objective, and make a new optimization process for each new vector.

Based on the defined cost function, the Reward Matrices are calculated and stored in an Optimal Profile Database based on Stochastic Dynamic Programming (OPD-SDP) in order to be used to find optimal policy for infinite horizon problem.

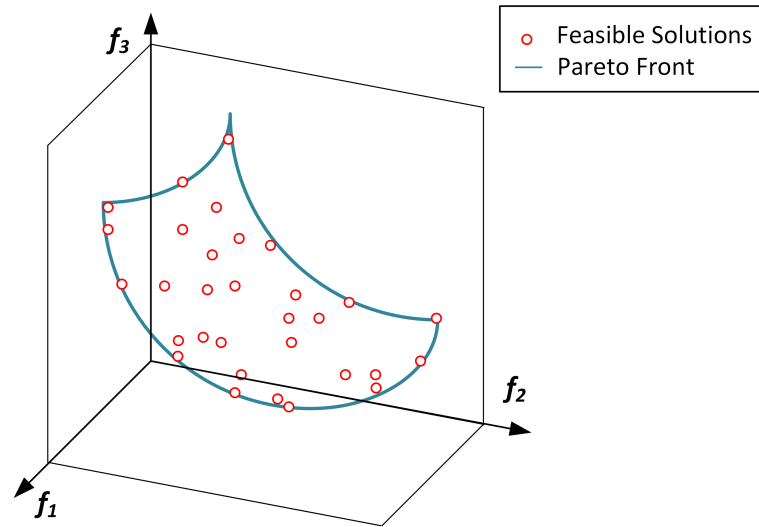


Figure 5.6: Pareto Front of the minimization functions

### 5.3.3/ SUB-OPTIMAL ENERGY MANAGEMENT STRATEGY USING DATABASE BASED ON SDP

After a Markov model has been built, Transition Probability and Reward Matrices are stored in the OPD-SDP, the Stochastic Dynamic Programming is used to find the optimal control, minimizing the expected cost function (5.20), for each vehicle state. The control signal  $u = \{a, P_{EM}\}$ . An infinite horizon problem is formulated on the homogeneous Markov chain. The optimization finds an optimal policy,  $u = \pi(x)$  that minimizes the expected cost

function (5.20) over an infinite horizon [Puterman, 2014].

$$J_{\lambda}^{\pi}(x_0) = \lim_{N \rightarrow \infty} E \left\{ \sum_{k=0}^{N-1} \lambda^k \zeta(x_k, \pi(x_k)) \right\} \quad (5.24)$$

where  $\zeta$  is the cost for one time step,  $\lambda$  is the discount factor,  $x_k$  is the dynamic state vector at the  $k^{\text{th}}$  time point and  $E\{\dots\}$  denotes the expectation with respect to the considered prediction model defined by the time invariant Markov chain. The discount factor  $\lambda < 1$  assures convergence of the infinite sum. The optimal policy  $u = \pi(x)$  is found by using a modified policy iteration algorithm (cf. Figure 5.7). The modified policy iteration consists of the following steps:

1. Initial guess: Set  $i = 1$ . Provide an initial guess for  $\pi_i(x)$  and the discounted infinite horizon future cost  $J_{\lambda}^{\pi_{i-1}}(x)$ .
2. Policy evaluation: Calculate the cost  $J_{\lambda}^{\pi_i}(x)$  of the policy  $\pi_i(x)$  by iterating

$$J_{\lambda}^{\pi_i}(x_k) = \zeta(x_k, u) + E\{\lambda J_{\lambda}^{\pi_i}(x_{k+1})\}$$

backwards  $N$  times starting from  $J_{\lambda}^{\pi_i}(x_N) = J_{\lambda}^{\pi_{i-1}}(x)$  and ending with the truncated cost  $J_{\lambda}^{\pi_i}(x) = J_{\lambda}^{\pi_i}(x_0)$ . If  $|J_{\lambda}^{\pi_{i+1}}(x) - J_{\lambda}^{\pi_i}(x)| \leq \xi$  when iterating backwards terminate the iterations with the answer  $J_{\lambda}^{\pi_i}(x) = J_{\lambda}^{\pi_i}(x_k)$ .

3. Policy improvement: Improve the policy by taking one value iteration step:

$$\pi_{i+1}(x_0) = \arg \min_u \left[ \zeta(x_0, u) + E\{\lambda J_{\lambda}^{\pi_i}(x_1)\} \right]$$

Check for convergence: if  $|J_{\lambda}^{\pi_{i+1}}(x_0) - J_{\lambda}^{\pi_i}(x_0)| \leq \xi$ , then terminate the algorithm with the answer  $\pi(x) = \pi_{i+1}(x)$ . If  $\pi_{i+1}(x)$  has not converged, increase the index:  $i = i+1$ , and go to step 2.

The flowchart of the Modified Policy Iteration Algorithm for SDP is presented in Figure 5.7. The given algorithm efficiency is tested and validated in real-time application. The simulation results are presented in section 5.3.5. The calculation of SDP consumes relatively big amount of memory, so a reasonable resolution of state variables number is very important in terms of computation effort. With trials and errors method, the following discretization sets for state and action variables have been applied:

$$P_{dem} = \{-200 : 20 : 160\} \text{ kW} \quad (5.25)$$

$$v = \{0, 5, 10, 20\} \text{ m/s} \quad (5.26)$$

$$SOC_{bat} = \{0.2 : 0.1 : 0.9\} \quad (5.27)$$

$$a = \{-3, -1, 0, 0.5, 1, 1.25, 1.5\} \text{ m/s}^2 \quad (5.28)$$

$$P_{EM} = \{-10 : 5 : 60\} \text{ kW} \quad (5.29)$$

Based on the defined sets, the Transition Probability and Reward Matrices are calculated.

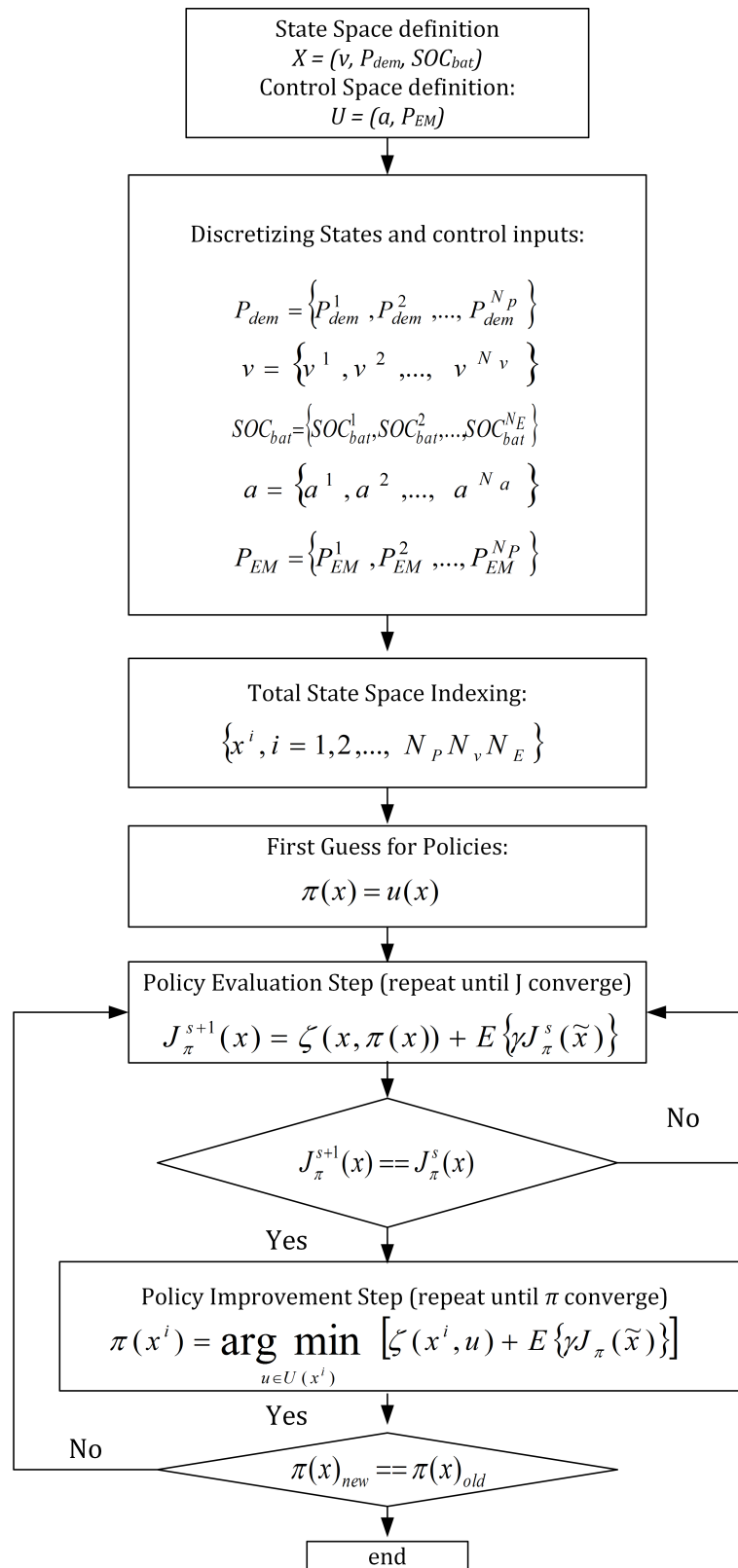


Figure 5.7: Modified Policy Iteration Algorithm Flowchart

### 5.3.4/ TRANSITION PROBABILITY MATRICES GENERATION

As it was aforementioned in section 5.3.2, the Transition Probability Matrices (TPM) are calculated using maximum likelihood estimation (cf. equation 5.19). In order to have a richer database for TPM estimation, data from the following standard driving cycles (SDC) have been collected: ECER15, EUDC, ArtUrban, and NEDC. These SDC represent common driving conditions in an urban environment, emulating different driver's behavior (abrupt and smooth acceleration/deceleration, cruise speed phases, etc).

The variation of bus weight significantly influences the vehicle dynamics (thus its consumed energy), as it can vary up to several tons. The tested data has been enlarged by simulating each of the SDC for three different masses, corresponding to an empty, half-full, and full bus. Therefore, the bus dynamics will be tested for much more states, as for the same speed profile the power demand will be different. It is considered in these hypotheses that a full bus corresponds to 70 passengers with an average weight of 60 kg.

After obtaining the data from several SDC for different masses, it was concluded that not all states are explored and some of them are barely feasible. That is why it makes sense to eliminate those states and, thus, reduce the state dimension.

### 5.3.5/ SIMULATION RESULTS

In order to evaluate the efficiency of the proposed approach, a validation scenario has been performed for several driving cycles. The given stochastic strategy has been tested and compared to a strategy based on DDP based database as given in [Abdrakhmanov et al., 2017a]. The validation scenario consists of a test with an assumption that bus mass varies during the trip. The bus is a transportation mean, it is considered that the mass changes only during stops in order to take or to drop off the passengers.

Table 5.3 summarizes the obtained results for several SDC. "+" corresponds to a positive improvement, "-" means that DDP approach demonstrated a better performance. The consumed energy  $E_{cons}$  given by the column Energy [kWh] in Table 5.3 is calculated as follows:

$$E_{cons} = \int_0^{t_f} P_{EM} dt + \int_0^{t_f} Q_{LHV} \dot{m}_f dt \quad (5.30)$$

where  $P_{EM}$  is the electric motor consumed power,  $\dot{m}_f$  fuel consumption rate, and  $Q_{LHV} = 43MJ/kg$  lower heat value for diesel.

In order to validate the proposed algorithm, in terms of generalization aspect, it has been additionally tested on an ArtRoad SDC, which has not been used before to estimate the

Table 5.3: Comparison of the SDP w.r.t. DDP based strategies.

Dr. Cycle	$\Delta SOC$ [%]			Fuel [l]			Energy [kWh]		Diff. [%]
	DDP	SDP	Diff. [%]	DDP	SDP	Diff. [%]	DDP	SDP	
ArtRoad	8.15	7.91	+2.91	0.48	0.47	+2.0	8.22	7.81	+4.98
EUDC	4.51	4.45	+1.33	0.11	0.12	-9.1	2.71	2.64	+2.58
ArtUrban	2.15	1.87	+13.3	0.60	0.59	+1.67	7.04	6.64	+5.68
NEDC	4.60	4.66	-1.3	0.15	0.17	-13.3	3.65	3.85	-5.47
Average	-	-	+4.06	-	-	-4.68	-	-	+1.94

TPM. To illustrate the performance, the simulation results for ArtRoad and ArtUrban SDC are presented in Figure 5.8 and 5.9, respectively.

Fig. 5.8 shows the simulation results for ArtRoad (Artificial Road) SDC for the case when it is assumed that the bus weight is variable. We can see that the stochastic algorithm shows results close to the deterministic approach. Global energy consumed during the trip while using DDP approach is 4.95% higher comparing to SDP method. It outperforms the DDP approach due to smoother speed profile and energy management algorithm.

Fig. 5.9 shows the simulation results for ArtUrban (Artificial Urban) SDC. This is one of the profiles that has been used to train the TPM. However, in this case the bus weight is variable as well. In this more realistic scenario, the SDP approach still outperforms the DDP method by 5.68%.

Both ArtRoad and ArtUrban SDC are characterized by frequent acceleration and deceleration phases. In this case, the SDP based approach demonstrates better results. For the SDC with mainly constant speed phases (e.g., EUDC and NEDC) the improvement compared to DDP approach is more modest or even negative (cf. Table 5.3). Therefore, the expediency of the use of the SDP approach is more advantageous in case if a vehicle is subject to some uncertainties, e.g., aggressive driving style and/or traffic conditions (traffic lights, traffic jams, pedestrian crossing, etc.), which lead to frequent acceleration and deceleration phases.

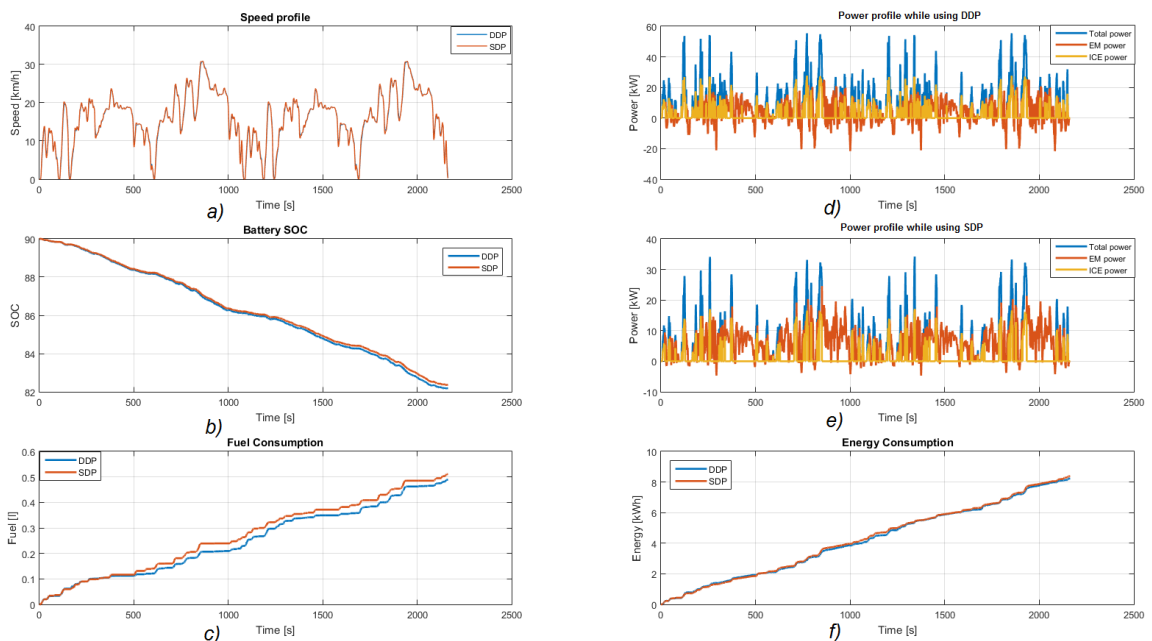


Figure 5.8: ArtRoad SDC. Constant Weight. a) Speed Profile, b) Battery SOC curve, c) Fuel consumption curve, d) Powersplit for DDP approach, e) Powersplit for the proposed SDP approach, f) Total Energy Consumption.

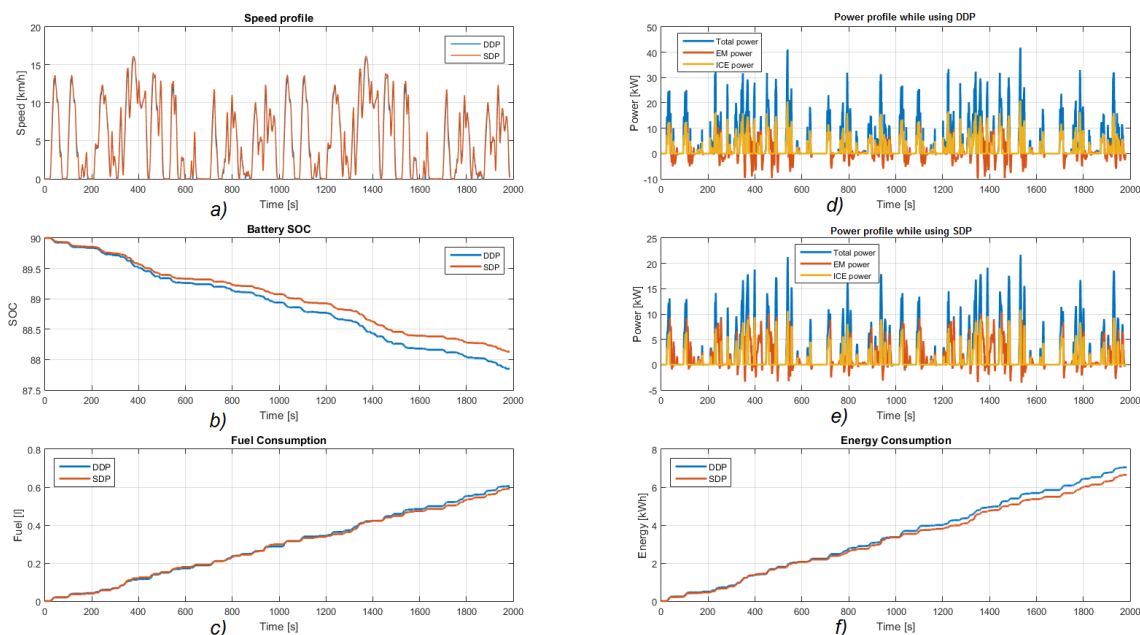


Figure 5.9: ArtUrban SDC. Variable Weight. *a)* Speed Profile, *b)* Battery SOC curve, *c)* Fuel consumption curve, *d)* Powersplit for DDP approach, *e)* Powersplit for the proposed SDP approach, *f)* Total Energy Consumption.

## 5.4/ CONCLUSION

In this chapter, a Stochastic Model Predictive Control (SMPC) based strategy has been developed to optimize the powersplit which presents power demand as a Markov Decision Process (MDP). The required power is considered as a random Markov process, encompassing uncertainties with regards to the road profile, bus weight, etc. The proposed strategy has been tested and validated for several standard driving cycles and has demonstrated its efficiency compared to rule-based methods where an average of improvement about 13% has been observed. The SMPC method has an implementation problem due to high calculation time. Also this control law impacts only powersplit and not the speed profile. That is why it has been decided to continue developing the idea of simultaneous speed and powersplit optimization presented in the Chapter 4 in the presence of the uncertainties.

The Stochastic Dynamic Programming technique has been used in order to develop an Energy Management Strategy that generates simultaneously an optimal speed profile and related powersplit strategy for HEV with the aim of energy optimization in the presence of uncertainties (due to different traffic conditions and/or a driver's behavior). To this end, a driver's power demand has been modeled as a Markov Chain. The formulated energy optimization problem, being intrinsically multi-objective problem, has been transformed into several single-objective ones with constraints using an  $\epsilon$ -constraint method to determine a set of optimal solutions that represent the Pareto Front.

Simulation data of several standard urban driving cycles have been used to train Transition Probability Matrices (TPM) using the maximum likelihood estimation technique. A trained reference  $SOC_{bat}$  curve has been utilized as a constraint to estimate Reward Ma-

trices based on the defined cost function. For a real-time application purpose, the obtained TPM and Reward Matrices have been collected into an Optimal Profile Database based on SDP (OPD-SDP). The OPD-SDP has been then used to calculate sub-optimal speed profiles and related powersplit by Modified Policy Iteration Algorithm using an infinite horizon optimization formulation. The results obtained by the SDP were compared to a Deterministic Dynamic Programming, and it has been shown that near optimal results can be obtained in real-time application.

The main distinctions in features for both approaches are given in Table 5.4

<b>DDP based approach</b>	<b>SDP based approach</b>
The overall controlled process has deterministic properties	The driver's power demand is presented as a random Markov process
Multi-objective optimization problem is solved using weighted aggregation method	Multi-objective optimization problem is solved using $\epsilon$ -constraint method
The Optimal Profile Database contains bus dynamic variables and powersplit	The Optimal Profile Database contains the Transition Probability and Reward Matrices for different driving conditions
The powersplit and speed profile optimization are addressed using Deterministic Dynamic Programming	The powersplit and speed profile optimization are addressed using infinite horizon Stochastic Dynamic Programming

Table 5.4: Comparison of DDP based and SDP based approaches



# ADAPTIVE CRUISE CONTROL WITH STOP&GO

---

## **Abstract**

This chapter presents an Eco Adaptive Cruise Control with Stop&Go (eACCwSG) maneuvers control strategy aiming to improve the energy economy of a HEV. The algorithm is another way to reduce energy consumption along with powersplit strategies, as it smooths speed in acceleration and deceleration phases. One more important feature of this algorithm is the safety aspect, as eACCwSG permits to maintain a safety distance in order to avoid collision and apply a smooth braking. As it was mentioned before, smooth braking ensures passengers comfort.

---

## 6.1/ INTRODUCTION

In urban environment, due to traffic conditions, traffic lights, a bus encounters frequent Stop&Go situations. This results in augmented fuel consumption during the starts phase. In this sense, the Adaptive Cruise Control with Stop&Go (eACCwSG) strategy brings the undeniable benefit.

Researches have started to explore the introduction of additional objectives to ACC, e.g., fuel economy and driver desired response. Ioannou [Ioannou et al., 2005] suggested the use of ITS technologies, including adaptive cruise control, to reduce fuel consumption of vehicles. Jonsson et al. [Jonsson et al., 2004] proposed a dynamic programming based offline control method. It reduced the fuel consumption while allowing more tracking error. The improvement of fuel consumption usually decreases the acceleration performance and lowers the tracking capability. This will lead to two problems consequently: 1) when the preceding car accelerates, larger inter-vehicular distance occurs due to the deficient acceleration performance, resulting in frequent vehicle cut-ins from adjacent lanes, 2) when the preceding vehicle decelerates, inter-vehicular distance shortens quickly and rear-end collisions happen more easily. On the contrary, if an ACC system pursues good tracking capability only, it leads to unnecessary acceleration and emergency braking, which also deteriorates the fuel economy of vehicle to some extent. A velocity control system in order to save the fuel consumption by involving traffic signal information was proposed by [Li et al., 2011]. Model predictive control scheme was used in order to control the velocity predicting states of the vehicle and traffic signal switching. An algorithm to judge whether a vehicle should accelerate or not when the vehicle cannot pass the traffic lights during the green phase. In the algorithm, the fuel economy was predicted using

traffic signal information. A vehicle speed and vehicle-to-vehicle distance control algorithm for vehicle stop-and-go cruise control has been proposed in [Yi et al., 2001]. Linear quadratic optimal control theory has been used to develop a vehicle speed and distance control algorithm. A desired acceleration for the vehicle has been designed on the basis of the vehicle speed and distance control algorithm. S. Kim [Kim, 2012] formulated the optimization problem to find the optimal relative distance profile during a complete stop and the optimal velocity profile during a starting motion. It suggested that once leader car resumes the motion after a full stop, the host car is not obliged to follow the leader car, instead it can follow an optimal profile.

The global control scheme, presented in Chapter 3, converts into Figure 6.1 with an eACCwSG mode on. The reference speed of the driver is adapted depending on the environment and sensor information to react to the actual state of the traffic via eACCwSG block. The Energy Management block provides a sub-optimal powersplit control law in order to reduce the energy consumption complied with the chosen methodologies criteria.

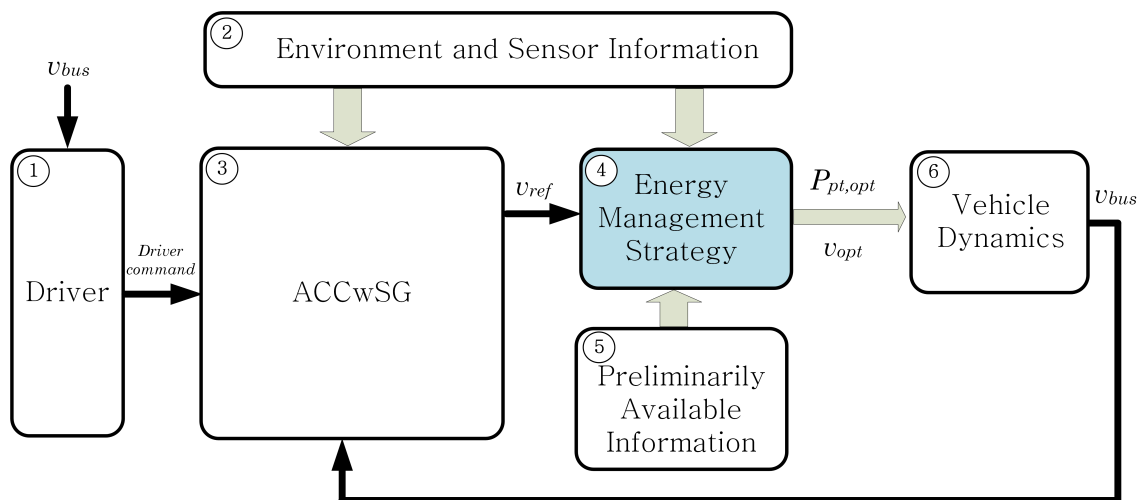


Figure 6.1: Global control scheme in eACCwSG mode on

ACC systems are now commercially available on high-end vehicles of most car manufacturers. They are introduced as one of the advanced driver-assist features that assist the driver's longitudinal control task with limited acceleration range. With reduced workload and stress during daily driving when the ACC system is turned on, the driver could focus more on other important driving tasks and thus achieve improved comfort and safety.

## 6.2/ ADAPTIVE CRUISE CONTROL WITH STOP&GO ALGORITHM

Adaptive Cruise Control with Stop&Go (eACCwSG) is a mix of vehicle capability of maintaining a user-preset speed (Cruise Control), capability of keeping a safe distance from a preceding vehicle (ACC) and capability to perform maneuvers at low speeds (Stop&Go) (cf. Figure 6.2) [Abdrakhmanov et al., 2017b].

The proposed eACCwSG parameters used for situation modeling are presented in Figure 6.3. The aim of eACCwSG is to keep the inter-vehicular distance  $d_{ref}$  while vehicles are



Figure 6.2: eACCwSG concept

moving. At the full stop of both vehicles, the constant minimal safety distance  $d_{min\ safety}$  must be respected.

It is assumed that the current distance  $d$  between the vehicles is known and obtained by the bus sensors. In order to avoid collisions with the preceding car, the bus must follow the reference speed  $v_{ref}$  which must consider the following safety requirements. The reference distance  $d_{ref}$  to maintain between the vehicles is defined as follows:

$$d_{ref} = d_{min\ safety} + d_v \quad (6.1)$$

The distance  $d_{min\ safety}$  is minimal distance to maintain at full stop of both vehicles. The distance  $d_v$  is defined as follows [Zhang et al., 2004]:

$$d_v = T_h v + h^* v^2 \quad (6.2)$$

where  $T_h = t_{dr} + t_{sensor} + t_{motor}$  a headway time which expresses the delays due to driver reaction, sensor perception, motors dynamics, respectively,  $v = v_{follower}$  is the current bus speed.

The term  $h^*$  is calculated based mostly on the braking capability of the bus and the leader vehicle:

$$h^* = \frac{1}{2} \left( \frac{1}{a_{l_{max}}} - \frac{1}{a_{f_{max}}} \right) \quad (6.3)$$

where  $a_{l_{max}}$  maximal deceleration of the leader,  $a_{f_{max}}$  maximal deceleration of the bus. To ensure the passengers comfort and the safety, it is necessary that  $a_{l_{max}} < a_{f_{max}}$  to take into account the extreme cases (e.g., preceding vehicles with emergency stop). The calculation of  $d_{ref}$  is based on the parameters given in Table 6.1.

Table 6.1: Parameter values for  $d_{ref}$  calculation

Parameter	Value
Driver reaction time $t_{dr}$	0.4 s
Sensor perception delay $t_{sensor}$	0.1 s
Motors delay $t_{motor}$	0.1 s
Bus max deceleration $a_{f_{max}}$	-1.27 m/s <sup>2</sup>
Leader max deceleration $a_{l_{max}}$	-6.87 m/s <sup>2</sup>

Two speed references proposed are in this work,  $v_{cc}$  which is an external reference set by the driver, and the reference speed  $v_{ref}$  resulting from the eACCwSG system. In the eACCwSG mode, this reference depends mostly on the speed of the leader and the current inter-vehicular distance. The expression of  $v_{ref}$  is given as follows:

$$v_{ref} = v_{leader} + k_p(d - d_{ref}) - \dot{d}_{ref} \quad (6.4)$$

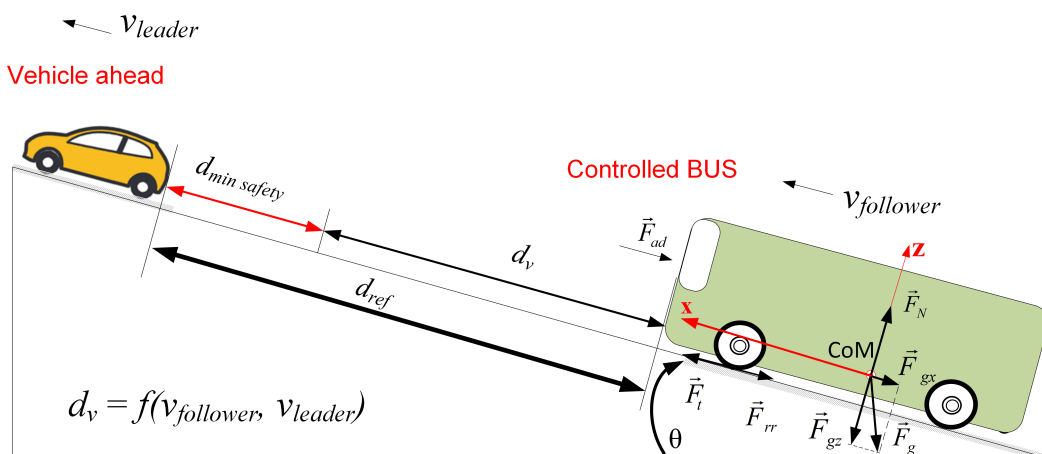


Figure 6.3: eACCwSG parameters

This expression contains the term  $d_{ref}$  (see equations 6.1 and 6.2). After derivation, we obtain the following expression for the  $\dot{d}_{ref}$ :

$$\dot{d}_{ref} = T_h a + 2h^* v a = (T_h + 2h^* v) a \quad (6.5)$$

where  $a$  bus acceleration and  $v$  bus speed. To demonstrate the convergence of this control law, the Lyapunov theory has been used. The Lyapunov function candidate is defined as follows:  $e = \frac{1}{2}(d - d_{ref})^2$ . The time derivative of  $e$ :

$$\begin{aligned} \dot{e} &= (d - d_{ref})(d - d_{ref}) \\ &= (V_{leader} - V_{ref} - \dot{d}_{ref})(d - d_{ref}) \\ &= -k_p(d - d_{ref})(d - d_{ref}) \\ &= -k_p(d - d_{ref})^2 < 0 \end{aligned} \quad (6.6)$$

According to Lyapunov synthesis, this control is asymptotically stable and converges to 0 (while  $d \neq d_{ref}$ ).

### 6.3/ SIMULATION RESULTS

This section is dedicated to the simulation results of the developed eACCwSG strategy for the Businova in urban environment.

This section shows the results of efficiency of the eACCwSG strategy. The strategy is tested for several scenarios in order to demonstrate its validity. Firstly, some extreme punctual missions have been tested, afterwards a realistic urban driving cycles have been applied to validate the algorithm.

The minimal safety distance is set to 10 m, and the cruise speed  $v_{cc} = 40$  km/h.

#### 6.3.1/ URBAN ENVIRONMENT FLOW

Urban environment flow is characterized by the frequent leader speed fluctuations. Figure 6.4 shows that despite the high leader speed fluctuation, the controlled vehicle

has a smooth speed profile. Once the cruise speed is achieved the bus control system switches to Cruise Control mode.

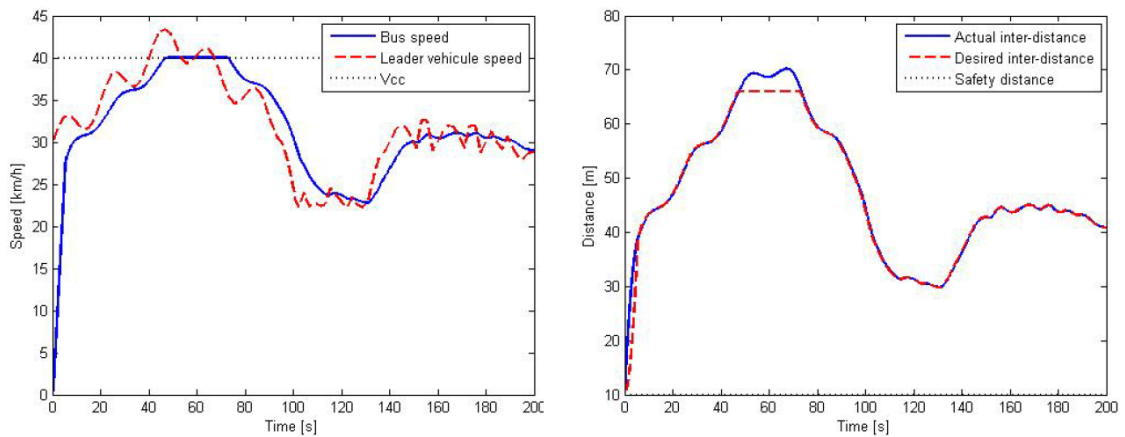


Figure 6.4: ACCwSG in an urban environment flow

### 6.3.2/ CONGESTED ENVIRONMENT WITH FREQUENT STOPS

Figure 6.5 demonstrates that even in case where the bus encounters frequent starts and stops, the bus ACCwSG controller manages to keep a safe inter vehicular distance.

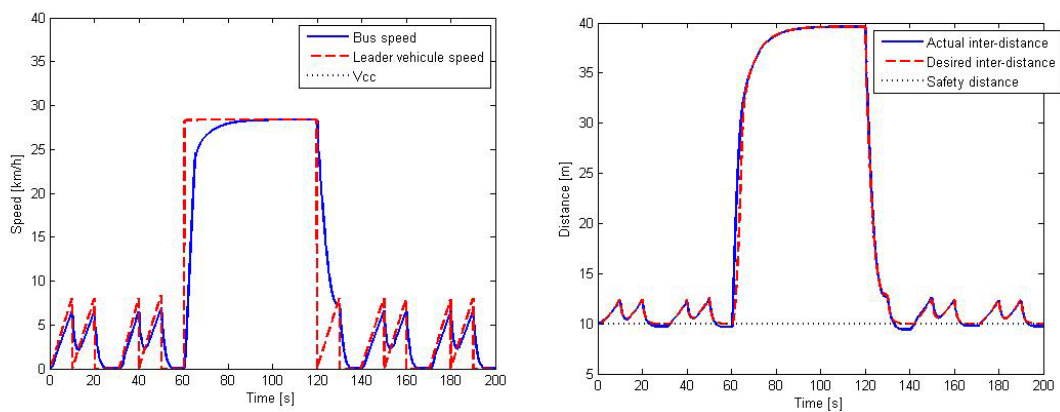


Figure 6.5: eACCwSG congested environment with frequent stops

### 6.3.3/ UNRESTRICTED ENVIRONMENT FLOW WITH LEADER'S SPEED FREQUENT VARIATION

This scenario demonstrates that despite, at some extent, inadequate behavior of a leader car (cf. Figure 6.6), the bus controller supplies a smooth acceleration while keeping an inter vehicular distance above the minimal safety distance. .

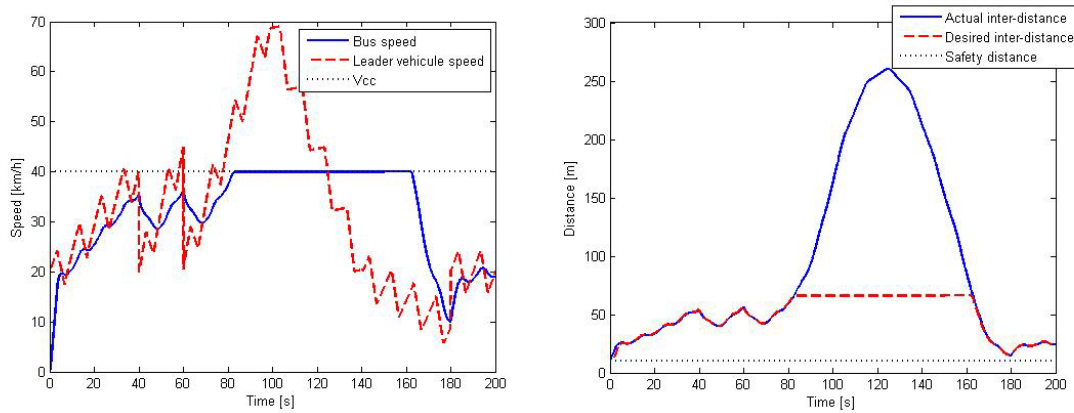


Figure 6.6: eACCwSG in unrestricted environment flow with leader's speed frequent variation

The minimal safety distance is set to 5 m, and the cruise speed  $v_{cc} = 40$  km/h. The tested scenarios show the efficiency and the robustness of the developed eACCwSG controller. Speed smoothness ensures the passenger's comfort.

#### 6.3.4/ NEDC DRIVING CYCLE

NEDC stands for New European Driving Cycle. This cycle is characterized by long constant-speed phases. We can see that the BUS follows perfectly the leader vehicle but acceleration and braking phases are smoother as we can see in the Figure 6.7. When the leader vehicle exceeds 40 km/h, the BUS switches to Cruise Control mode and maintains the value, logically the distance  $d$  between two vehicles increases. When the front vehicle starts braking, the bus starts braking when  $d = d_{ref}$ .

#### 6.3.5/ ART URBAN DRIVING CYCLE

Art Urban driving cycle is characterized by frequent starts and stops in a dense urban conditions. Figure 6.8 shows that the BUS follows the leader vehicle at the safe distance that permits to brake smoothly.

### 6.4/ DISCUSSION

The proposed eACCwSG have compared to a ACC algorithm presented in the paper of [Shakouri et al., 2014]. To compare the two methods, SDP based energy management presented in the **Chapter 5** has been fixed. The energy comparison is presented in the table 6.2. The simulation results show that the energy consumption is reduced down to 11%. This is due to the smoother speed profile during acceleration and braking phases. However, due to the assumption of a high braking capacity of the leader vehicle the safety distance is quite high, and the bus risks to be overtaken by another vehicle. As it has been

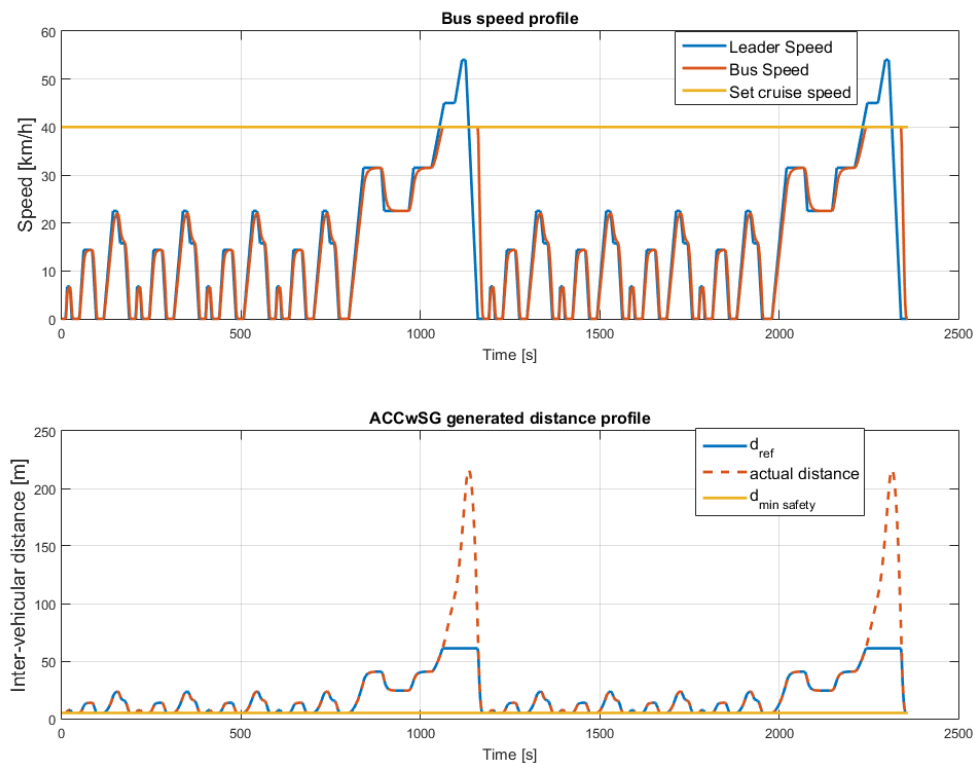


Figure 6.7: Leader vehicle follows NEDC driving cycle

mentioned before there is always a compromise between a generated safety distance and the braking applied.

Table 6.2: Comparison of the eACCwSG (I) w.r.t. ACC (II) [Shakouri et al., 2014] strategies.

Dr. Cycle	$\Delta SOC$ [%]			Fuel [l]			Energy [kWh]		Diff. [%]
	I	II	Diff. [%]	I	II	Diff. [%]	I	II	
ArtUrban	2.15	2.21	-3.3	0.60	0.66	-9.1	7.04	7.74	-9.01
NEDC	4.60	4.66	-1.3	0.15	0.18	-17.2	3.65	4.25	-14.2

In terms of energy efficiency, an optimization and smoothing of speed profile gives an additional advantage to energy management strategy. For an urban bus that often meets Stop&Go situations, a smoother acceleration and deceleration phases can significantly reduce the energy consumption.

Human driver, depending on its driving behavior, can increase the energy consumption up to 19% [Dunkle Werner, 2013]. Therefore, a driver assistance systems can help to avoid overconsumption of the energy, especially during acceleration phases. However, although the algorithm is adapted to calculate a safety distance to ensure a smoother braking, it is very important to give priority to a driving in case of emergency brake. This could happen, for example, when maintains a large inter vehicular distance and then a car from another lane takes over.

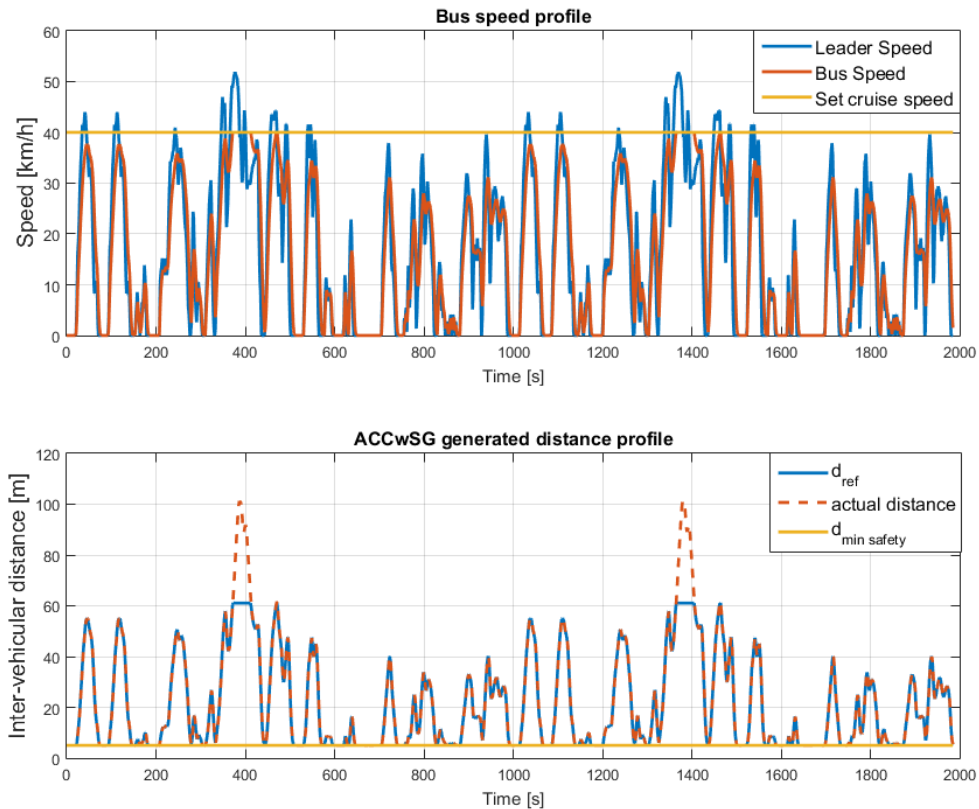


Figure 6.8: Leader vehicle follows Art Urban driving cycle

The subject is a part of Intelligent Vehicles systems along with the efficiency energy management in a hybrid powertrain. Combined these features can bring an undeniable advantage in terms of fuel economy, gas emissions and safety.

## 6.5/ CONCLUSION

This section described an Adaptive Cruise Control with Stop&Go (eACCwSG) maneuvers control strategy aiming to improve the energy economy of a HEV. The contribution of this PhD thesis compared to another ACC and Stop&Go algorithms is a fusion of both and its adaptation depending on the driving zone. The algorithm is another way to reduce energy consumption along with powersplit strategies, as it smooths speed in acceleration and deceleration phases. One more important feature of this algorithm is the safety aspect, as eACCwSG permits to maintain a safety distance in order to avoid collision and apply a smooth braking. Introduction of the BUS acceleration limits for calculation of an inter vehicular distance permits to ensure passengers comfort by smooth braking, which is another contribution compared to reviewed literature.

# GENERAL CONCLUSION AND FUTURE WORKS

## GENERAL CONCLUSION

The main subject of the given PhD thesis is an energy optimization in a complex series-parallel hybrid powertrain of the BUS. Such kind of hybrid systems should deliver an efficient powersplit by means of its Energy Management Strategy. The hybrid control system should create an efficient strategy of coordinating the flow of energy between the heat engine, battery, electrical and hydraulic motors (cf. **Chapter 3**). Intelligent EMS should provide smooth operation avoiding unpleasant jerks, shudders and shakes of the vehicle velocity. The obtained strategy is thus related to a multi-objective optimization problem.

With this aim in the **Chapter 3** a global control architecture has been proposed (cf. Figure 3.1) to tackle these problems. With regard to the proposed global control architecture, global energy can be optimized by:

- applying an efficient energy management strategy. An efficient powersplit permits to distribute optimally the energy demand to perform a trip and to maintain a sufficient battery charge to complete the mission,
- applying a relevant speed, especially during acceleration phase. Speed profile can come either from the driver (in manual mode) or from the eACCwSG block in case of urban environment (Stop&Go) or highway (ACC),

**Chapter 4** emphasizes in details the proposed Deterministic Dynamic Programming based approach. A simultaneous speed and powersplit optimization algorithm has been first proposed for a given trip (constrained by the traveled distance and time limit). This algorithm turned out to be highly time consuming so it cannot be used in real-time. To overcome this drawback, an Optimal Profiles Database based on DP (OPD-DP) has been constructed. It contains elementary optimal speed profiles and related powersplit for different bus masses, road slopes, speeds and accelerations. As only finite number of values can be stored in the OPD-DP, different multi-dimensional interpolation methods have been proposed to make use of the database in real-time application.

The strategy proposed in the **Chapter 5** results from the previous approach and extends it by considering a stochastic nature of the driving and the traffic conditions. A Stochastic

Dynamic Programming technique is used to simultaneously generate an optimal speed profile and related powersplit strategy. The cost function is calculated by taking into account the state propagation, making use of Transition Probability Matrices. For that purpose, the driver's power demand is modeled as a Markov Chain. The formulated energy optimization problem, being intrinsically multi-objective problem, has been transformed into several single-objective ones with constraints using an  $\epsilon$ -constraint method to determine a set of optimal solutions (the Pareto Front).

Another technique linked to the stochastic domain, is the Stochastic MPC (cf. section 5.2). It has been designed to decrease the energy consumption of the bus in the presence of uncertainties. An original control architecture that combines an eco Adaptive Cruise Control with Stop&Go (eACCwSG) manoeuvres and predictive stochastic energy management strategy has been proposed for the studied HEV. The Stochastic MPC problem has been formulated so that it reduces the fuel consumption and smooths engine's power change rate.

**Chapter 6** presented the Eco Adaptive Cruise Control with Stop&Go (eACCwSG) manoeuvres strategy, aiming to improve the energy economy and provide passengers' comfort, has been developed. The algorithm takes into account the deceleration capacity of the bus to generate the safety distanced to maintain, therefore soft braking is guaranteed for the passengers' comfort. Smoothing the acceleration phases impact the passengers' comfort at the vehicle start and also contribute to the global energy optimization.

## FUTURE WORKS

This thesis allows to explore and to extend several research in the following hybrid vehicles domain:

### ENERGY MANAGEMENT OPTIMIZATION TAKING INTO ACCOUNT BATTERY AGING

The developed EMS consider a short term impact for the battery, thus, the battery is discharged as uniformly as possible. The further development could consist in:

- Battery aging model to estimate the efficiency of the EMS in a longterm prospective,
- Battery Management Strategy to avoid overheating and battery damage.

### EFFICIENT REGENERATIVE BRAKING STRATEGY

In this PhD thesis the part of Regenerative braking has not been addressed profoundly. A simple strategy has been used to simulate an electric regenerative braking.

- Efficient Regenerative Braking (ERB) is linked to a reliable battery model and represents a part of the Global EMS. An ERB maximizes the efficiency of the global EMS,
- During braking optimally distribute a regenerated energy between battery and hydraulic accumulators, minimizing the losses.

## EFFICIENT DRIVING INDICATOR

Each driver has different style of driving, which can aggravate the energy consumption. Efficient Driving Indicator (EDI) should be created to show to a driver how he should behave to save the energy. Also this EDI can measure the efficiency of the eACCwSG in a congested area:

- Efficient Driving Indicator will show how efficient is the vehicle performance,
- EDI will be composed of different indicators: acceleration smoothness, balance energy consumed/regenerated, passengers comfort, respecting the timetable, etc.

## SMART CITY: EFFICIENT RECHARGE OF THE BUS NETWORK

The Businova contains a huge electric battery which is a main source of the energy. The EMS applied are classified as *charge-depletion* strategies (contrary to *charge-sustaining EMS*), as we drain the battery to its  $SOC_{min}$  in the end of the day. The recharging is carried out during the night in the depot. That is why it is important:

- To develop an efficient Battery Recharging Strategy of the Bus Network, avoiding a voltage drop, energy overconsumption, etc.
- Enlarge the idea: create a multiple spots of recharge and their interaction depending on the hour, line charge, traffic data, etc.



## ANNEXES



# A

## INTRODUCTION TO MARKOV DECISION PROCESSES

A Markov chain is a stochastic model describing a sequence of possible events in which the probability of each event depends only on the state attained in the previous event. The Markov decision process (MDP) consists of decision epochs, states, actions, rewards, and transition probabilities. Choosing an action in a state generates a reward and determines the state at the next decision epoch through a transition probability function. Decision makers seek policies which are optimal in some sense.

### DECISION EPOCHS

Decisions are made at points of time referred to as *decision epochs*. A set of decision epochs can be either discrete or continuum. When discrete, decisions are made at all decision epochs. In discrete time problems, time is divided into *periods* or *stages*.

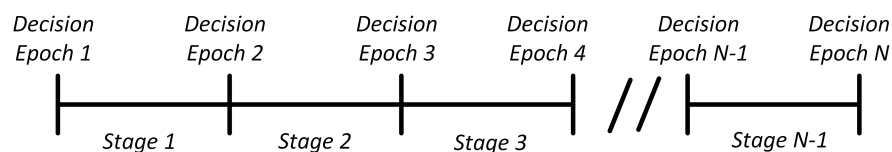


Figure A.1: Illustration of epochs and stages (periods)

Stochastic Models are formulated so that a decision epoch corresponds to the beginning of a period (cf. Figure A.1). The set of decision epochs ( $T \equiv \{1, 2, \dots, N\}$ ) is either finite for  $N < \infty$  and decision problems are called *finite horizon* problems, or infinite for  $N \leq \infty$  and decision problems are called *infinite horizon* problems.

### STATE AND ACTION SETS

At each decision epoch, the system occupies a *state*. We denote a set of possible system states by  $S$ . If, at some decision epoch, the decision maker observes the system in state

$s \in S$ , he may choose action  $a$  from a set of allowable actions in state  $s, A_s$ . Here we assume that  $S$  and  $A_s$  are *discrete* (finite) (cf. Figure A.2).

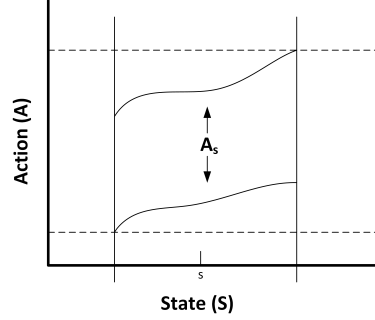


Figure A.2: Illustration of states and actions

Actions may be chosen either randomly or deterministically. Choosing actions randomly means selecting a probability distribution  $q(\cdot) \in Pr(A_s)$ , in which case  $a$  is selected with probability  $q(a)$ . Eliminate probability distributions correspond to deterministic action choice.

## REWARDS AND TRANSITION PROBABILITIES

As a result of choosing action  $a \in A_s$  in state  $s$  at decision epoch  $t$ ,

1. the decision maker receives a reward,  $r_t(s, a)$ , and
2. the system state at the next decision epoch is determined by the probability distribution  $p_t(\cdot|s, a)$ .

When the reward depends on the state of the system at the next decision epoch, we let  $r_t(s, a, j)$  denote the value at time  $t$  of the reward received when the state of the system at decision epoch  $t$  is  $s$ , action  $a \in A_s$  is selected, and the system occupies state  $j$  at decision epoch  $t + 1$ . Its expected value at decision epoch  $t$  maybe evaluated by calculating:

$$r_t(s, a) = \sum_{j \in S} r_t(s, a, j) p_t(j|s, a) \quad (\text{A.1})$$

where  $p_t(j|s, a)$  non-negative function, called *transition probability function*, which denotes the probability that the system is in state  $j \in S$  at time  $t + 1$  when the decision maker chooses action  $a \in A_s$  in state  $s$  at time  $t$ .

It is assumed that

$$\sum_{j \in S} p_t(j|s, a) = 1 \quad (\text{A.2})$$

In finite horizon Markov Decision processes, no decision is made at decision epoch  $N$ . Consequently, the reward at this time point is only a function of the state. It is denoted by  $r_N(s)$  and referred to as a *salvage value* or *scrap value*.

Thus, a Markov decision process can be referred by a collection of the following objects:

$$\{T, S, A_s, p_t(\cdot|s, a), r_t(s, a)\}$$

## DECISION RULES

A *decision rule* prescribes a procedure for action selection in each state at a specified decision epoch. Decision rules range in general from deterministic Markovian to randomized history dependent, depending on how they incorporate past information and how they select actions.

Markovian decision rules are functions  $d_t : S \rightarrow A_s$ , which specify the action choice when the system occupies state  $s$  at decision epoch  $t$ . For each  $s \in S$ ,  $d_t(s) \in A_s$ . This decision rule is called *Markovian* (memoryless) because it depends on previous system states and actions only through the current state of the system, and *deterministic* because it chooses an action with certainty.

## POLICIES

A *policy*, *contingency plan*, *plan*, or *strategy* specifies the decision rule to be used at all decision epoch. A policy  $\pi$  is a sequence of decision rules, i.e.  $\pi = (d_1, d_2, \dots, d_{N-1})$ .

A policy is called *stationary* if  $d_t = d$  for all  $t \in T$ . Stationary deterministic policies are referred to as *pure* policies and are fundamental to theory of infinite horizon Markov decision processes.



# BIBLIOGRAPHY

- [Abdrakhmanov et al., 2017a] Abdrakhmanov, R., et Adouane, L. (2017a). **Dynamic programming resolution and database knowledge for online predictive energy management of hybrid vehicles**. In *International Conference on Informatics in Control, Automation and Robotics (ICINCO)*, Madrid-Spain.
- [Abdrakhmanov et al., 2017b] Abdrakhmanov, R., et Adouane, L. (2017b). **Efficient acc with stop&go maneuvers for hybrid vehicle with online sub-optimal energy management**. In *IEEE 11th International Workshop on Robot Motion and Control (RoMoCo)*, Wasowo-Poland.
- [Abdrakhmanov et al., 2017c] Abdrakhmanov, R., et Adouane, L. (2017c). **Energy management and powersplit for hybrid electric bus using dp-based optimal profiles database**. In *IEEE Vehicle Power and Propulsion Conference (VPPC)*, Belfort-France.
- [Abdrakhmanov et al., 2018] Abdrakhmanov, R., et Adouane, L. (2018). **Stochastic dp based on trained database for sub-optimal energy management of hybrid electric vehicles**. *Lecture Notes in Electrical Engineering*.
- [Acarman et al., 2006] Acarman, T., Liu, Y., et Ozguner, U. (2006). **Intelligent cruise control stop and go with and without communication**. In *American Control Conference, 2006*, pages 6–pp. IEEE.
- [Akhegaonkar et al., 2016] Akhegaonkar, S., Nouveliere, L., Glaser, S., et Holzmann, F. (2016). **Smart and green acc: Energy and safety optimization strategies for evs**. *IEEE Transactions on Systems, Man, and Cybernetics: Systems*.
- [Angkititrakul et al., 2012] Angkititrakul, P., Miyajima, C., et Takeda, K. (2012). **An improved driver-behavior model with combined individual and general driving characteristics**. In *Intelligent Vehicles Symposium (IV), 2012 IEEE*, pages 426–431. IEEE.
- [Assanis et al., 2000] Assanis, D. N., Filipi, Z., Gravante, S., Grohnke, D., Gui, X., Louca, L., Rideout, G., Stein, J., et Wang, Y. (2000). **Validation and use of simulink integrated, high fidelity, engine-in-vehicle simulation of the international class vi truck**. Technical Report, SAE Technical Paper.
- [Astrom et al., 2009] Astrom, K. J., et Murray, R. M. (2009). **Feedback systems**. John Wiley & Sons, Ltd.
- [Bailey, 2018] Bailey, R. (2018). **Hybrid Vehicles**. <https://www.utc.edu/college-engineering-computer-science/research-centers/cete/hybrid.php>. [Online; accessed 08-January-2018].
- [Barkenbus, 2010] Barkenbus, J. N. (2010). **Eco-driving: An overlooked climate change initiative**. *Energy Policy*, 38(2):762–769.

- [Barlow et al., 2009] Barlow, T. J., Latham, S., McCrae, I., et Boulter, P. (2009). **A reference book of driving cycles for use in the measurement of road vehicle emissions.** *TRL Published Project Report*.
- [Bengler et al., 2014] Bengler, K., Dietmayer, K., Farber, B., Maurer, M., Stiller, C., et Winner, H. (2014). **Three decades of driver assistance systems: Review and future perspectives.** *IEEE Intelligent Transportation Systems Magazine*, 6(4):6–22.
- [Bera et al., 2012] Bera, T. K., Samantaray, A. K., Merzouki, R., et Ould-Bouamama, B. (2012). **Bond graph modeling of an over-actuated intelligent autonomous vehicle with decoupled steering wheel.** In *Robotics and Biomimetics (ROBIO), 2012 IEEE International Conference on*, pages 624–629. IEEE.
- [Bertsekas, 1995] Bertsekas, D. P. (1995). **Dynamic programming and optimal control**, volume 1. Athena Scientific Belmont, MA.
- [Bichi et al., 2010] Bichi, M., Ripaccioli, G., Di Cairano, S., Bernardini, D., Bemporad, A., et Kolmanovsky, I. V. (2010). **Stochastic model predictive control with driver behavior learning for improved powertrain control.** In *Decision and Control (CDC), 2010 49th IEEE Conference on*, pages 6077–6082. Atlanta, USA.
- [Biswas et al., 2006] Biswas, S., Tatchikou, R., et Dion, F. (2006). **Vehicle-to-vehicle wireless communication protocols for enhancing highway traffic safety.** *IEEE communications magazine*, 44(1):74–82.
- [Bondy et al., 1976] Bondy, J. A., et Murty, U. S. R. (1976). **Graph theory with applications**, volume 290. Citeseer.
- [Borutzky, 2009] Borutzky, W. (2009). **Bond graph methodology: development and analysis of multidisciplinary dynamic system models.** Springer Science & Business Media.
- [Broussely et al., 2005] Broussely, M., Biensan, P., Bonhomme, F., Blanchard, P., Herreyre, S., Nechev, K., et Staniewicz, R. (2005). **Main aging mechanisms in li ion batteries.** *Journal of power sources*, 146(1):90–96.
- [Bu et al., 2014] Bu, F., et Chan, C.-Y. (2014). **Adaptive and cooperative cruise control.** In Eskandarian, A., editor, *Handbook of intelligent vehicles*, chapter 9, pages 192–206. Springer.
- [Calef et al., 2007] Calef, D., et Goble, R. (2007). **The allure of technology: How france and california promoted electric and hybrid vehicles to reduce urban air pollution.** *Policy sciences*, 40(1):1–34.
- [Cervantes, 2014] Cervantes, I. (2014). **Energy management and optimization.** In Emadi, A., editor, *Advanced electric drive vehicles*, chapter 17, pages 558–585. CRC Press.
- [Chan, 2007] Chan, C. C. (2007). **The state of the art of electric, hybrid, and fuel cell vehicles.** *Proceedings of the IEEE*, 95(4):704–718.
- [Chen et al., 2014a] Chen, B.-C., Wu, Y.-Y., et Tsai, H.-C. (2014a). **Design and analysis of power management strategy for range extended electric vehicle using dynamic programming.** *Applied Energy*, 113:1764–1774.

- [Chen et al., 2014b] Chen, Z., Mi, C. C., Xu, J., Gong, X., et You, C. (2014b). **Energy management for a power-split plug-in hybrid electric vehicle based on dynamic programming and neural networks.** *Vehicular Technology, IEEE Transactions on*, 63(4):1567–1580.
- [Cheng et al., 2013] Cheng, Q., Nouveliere, L., et Orfila, O. (2013). **A new eco-driving assistance system for a light vehicle: Energy management and speed optimization.** In *Intelligent Vehicles Symposium (IV), 2013 IEEE*, pages 1434–1439. IEEE.
- [Choi et al., 2002] Choi, S. S., et Lim, H. S. (2002). **Factors that affect cycle-life and possible degradation mechanisms of a li-ion cell based on licoo 2.** *Journal of Power Sources*, 111(1):130–136.
- [Ci et al., 2007] Ci, S., Zhang, J., Sharif, H., et Alahmad, M. (2007). **A novel design of adaptive reconfigurable multicell battery for power-aware embedded networked sensing systems.** In *Global Telecommunications Conference, 2007. GLOBECOM'07. IEEE*, pages 1043–1047. IEEE.
- [Coelingh et al., 2010] Coelingh, E., Eidehall, A., et Bengtsson, M. (2010). **Collision warning with full auto brake and pedestrian detection-a practical example of automatic emergency braking.** In *Intelligent Transportation Systems (ITSC), 2010 13th International IEEE Conference on*, pages 155–160. IEEE.
- [Covert et al., 2016] Covert, T., Greenstone, M., et Knittel, C. R. (2016). **Will we ever stop using fossil fuels?** *Journal of Economic Perspectives*, 30(1):117–38.
- [Curry, 2017] Curry, C. (2017). **Lithium-ion battery costs and market.** Technical Report, Bloomer New Energy Finance.
- [Dagan et al., 2004] Dagan, E., Mano, O., Stein, G. P., et Shashua, A. (2004). **Forward collision warning with a single camera.** In *Intelligent Vehicles Symposium, 2004 IEEE*, pages 37–42. IEEE.
- [Dahmane et al., 2018] Dahmane, Y., Adouane, L., et Abdrakhmanov, R. (2018). **Stochastic mpc for optimal energy management strategy of hybrid vehicle performing acc with stop& go maneuvers.** In *15th IFAC Symposium on Control in Transportation Systems (CTS 2018)*, Savona-Italy.
- [De Nunzio et al., 2016] De Nunzio, G., De Wit, C. C., Moulin, P., et Di Domenico, D. (2016). **Eco-driving in urban traffic networks using traffic signals information.** *International Journal of Robust and Nonlinear Control*, 26(6):1307–1324.
- [D.Guillespie, 1992] D.Guillespie, T. (1992). **Fundamentals of vehicle dynamics.** Society of Automotive Engineers.
- [Dib et al., 2012] Dib, W., Chasse, A., Di Domenico, D., Moulin, P., et Sciarretta, A. (2012). **Evaluation of the energy efficiency of a fleet of electric vehicle for eco-driving application.** *Oil & Gas Science and Technology—Revue d'IFP Energies nouvelles*, 67(4):589–599.
- [Dib et al., 2014] Dib, W., Chasse, A., Moulin, P., Sciarretta, A., et Corde, G. (2014). **Optimal energy management for an electric vehicle in eco-driving applications.** *Control Engineering Practice*, 29:299–307.

- [Dunkle Werner, 2013] Dunkle Werner, K. (2013). **Driver behavior and fuel efficiency**. PhD thesis.
- [Ehsani et al., 2005] Ehsani, M., Gao, Y., Gay, S. E., et Emadi, A. (2005). **Modern Electric, Hybrid Electric, and Fuel Cell Vehicles**. CRC PRESS.
- [Elbert et al., 2015] Elbert, P., Widmer, M., Gisler, H.-J., et Onder, C. (2015). **Stochastic dynamic programming for the energy management of a serial hybrid electric bus**. *International Journal of Vehicle Design*, 69(1-4):88–112.
- [Emadi, 2014] Emadi, A. (2014). **Advanced electric drive vehicles**. CRC Press.
- [Eskandarian, 2014a] Eskandarian, A. (2014a). **Fundamentals of driver assistance**. In Eskandarian, A., editor, *Handbook of intelligent vehicles*, chapter 19, pages 493–531. Springer.
- [Eskandarian, 2014b] Eskandarian, A. (2014b). **Introduction to intelligent vehicles**. In Eskandarian, A., editor, *Handbook of intelligent vehicles*, chapter 1, pages 1–13. Springer.
- [Fang et al., 2011] Fang, L., Qin, S., Xu, G., Li, T., et Zhu, K. (2011). **Simultaneous optimization for hybrid electric vehicle parameters based on multi-objective genetic algorithms**. *Energies*, 4(3):532–544.
- [Guemri et al., 2014] Guemri, M., Neffati, A., Caux, S., et Ngueveu, S. U. (2014). **Management of distributed power in hybrid vehicles based on dp or fuzzy logic**. *Optimization and Engineering*, 15(4):993–1012.
- [Guzzella et al., 2007] Guzzella, L., Sciarretta, A., et others (2007). **Vehicle propulsion systems**, volume 1. Springer.
- [Haimes, 1971] Haimes, Y. Y. (1971). **On a bicriterion formulation of the problems of integrated system identification and system optimization**. *IEEE transactions on systems, man, and cybernetics*, 1(3):296–297.
- [He et al., 2013] He, Y., Yan, X., Wu, C., Chu, D., et Peng, L. (2013). **Effects of driver's unsafe acceleration behaviors on passengers' comfort for coach buses**. In *ICTIS 2013@ Improving Multimodal Transportation Systems-Information, Safety, and Integration*, pages 1649–1655. ASCE.
- [Hellström et al., 2009] Hellström, E., Ivarsson, M., slund, J., et Nielsen, L. (2009). **Look-ahead control for heavy trucks to minimize trip time and fuel consumption**. *Control Engineering Practice*, 17(2):245–254.
- [Hemi et al., 2015] Hemi, H., Ghouili, J., et Cheriti, A. (2015). **Combination of markov chain and optimal control solved by pontryagin's minimum principle for a fuel cell/supercapacitor vehicle**. *Energy Conversion and Management*, 91:387–393.
- [Heppeler et al., 2016] Heppeler, G., Sonntag, M., Wohlhaupter, U., et Sawodny, O. (2016). **Predictive planning of optimal velocity and state of charge trajectories for hybrid electric vehicles**. *Control Engineering Practice*.
- [Hofman et al., 2007] Hofman, T., Steinbuch, M., Van Druten, R., et Serrarens, A. (2007). **Rule-based energy management strategies for hybrid vehicles**. *International Journal of Electric and Hybrid Vehicles*, 1(1):71–94.

- [Huang et al., 2011] Huang, X., Tan, Y., et He, X. (2011). **An intelligent multifeature statistical approach for the discrimination of driving conditions of a hybrid electric vehicle.** *IEEE Transactions on Intelligent Transportation Systems*, 12(2):453–465.
- [Ioannou et al., 2005] Ioannou, P. A., et Stefanovic, M. (2005). **Evaluation of acc vehicles in mixed traffic: Lane change effects and sensitivity analysis.** *IEEE Transactions on Intelligent Transportation Systems*, 6(1):79–89.
- [Jiang et al., 2014] Jiang, W., Yang, Y., et Suntharalingam, P. (2014). **All-electric vehicles and range-extended electric vehicles.** In Emadi, A., editor, *Advanced electric drive vehicles*, chapter 15, pages 491–515. CRC Press.
- [Johannesson et al., 2007] Johannesson, L., Asbogard, M., et Egardt, B. (2007). **Assessing the potential of predictive control for hybrid vehicle powertrains using stochastic dynamic programming.** *IEEE Transactions on Intelligent Transportation Systems*, 8(1):71–83.
- [Jones, 2001] Jones, W. D. (2001). **Keeping cars from crashing.** *IEEE spectrum*, 38(9):40–45.
- [Jonsson et al., 2004] Jonsson, J., et Jansson, Z. (2004). **Fuel optimized predictive following in low speed conditions.** *IFAC Proceedings Volumes*, 37(22):119–124.
- [Jula et al., 2000] Jula, H., Kosmatopoulos, E. B., et Ioannou, P. A. (2000). **Collision avoidance analysis for lane changing and merging.** *IEEE Transactions on vehicular technology*, 49(6):2295–2308.
- [J.Y.Wong, 2008] J.Y.Wong (2008). **The theory of ground vehicles.** John Wiley & Sons.
- [Kamal et al., 2017] Kamal, E., Adouane, L., Abdrakhmanov, R., et Ouddah, N. (2017). **Hierarchical and adaptive neuro-fuzzy control for intelligent energy management in hybrid electric vehicles.** In *IFAC World Congress*, Toulouse-France.
- [Karden et al., 2007] Karden, E., Ploumen, S., Fricke, B., Miller, T., et Snyder, K. (2007). **Energy storage devices for future hybrid electric vehicles.** *Journal of Power Sources*, 168(1):2–11.
- [Karnopp et al., 1968] Karnopp, D., et Rosenberg, R. C. (1968). **Analysis and simulation of multiport systems: The bond graph approach to physical system dynamics.**
- [Kim, 2012] Kim, S. (2012). **Design of the adaptive cruise control systems: An optimal control approach.** PhD dissertation, University of California, Berkeley.
- [Kim et al., 2009] Kim, T. S., Manzie, C., et Sharma, R. (2009). **Model predictive control of velocity and torque split in a parallel hybrid vehicle.** In *Systems, Man and Cybernetics, 2009. SMC 2009. IEEE International Conference on*, pages 2014–2019. IEEE.
- [Kirchner et al., 2014] Kirchner, M., Schubert, P., et Haas, C. T. (2014). **Characterisation of real-world bus acceleration and deceleration signals.** *Journal of Signal and Information Processing*, 5(01):8.

- [Kitayama et al., 2015a] Kitayama, S., Saikyo, M., Nishio, Y., et Tsutsumi, K. (2015a). **Torque control strategy and optimization for fuel consumption and emission reduction in parallel hybrid electric vehicles.** *Structural and Multidisciplinary Optimization*, 52(3):595–611.
- [Kitayama et al., 2015b] Kitayama, S., Saikyo, M., Nishio, Y., et Tsutsumi, K. (2015b). **Torque control strategy and optimization for fuel consumption and emission reduction in parallel hybrid electric vehicles.** *Structural and Multidisciplinary Optimization*, 52(3):595–611.
- [Klein, 2004] Klein, M. (2004). **A specific heat ratio model and compression ratio estimation.** Division of Vehicular Systems, Department of Electrical Engineering, Linköping University.
- [Larminie et al., 2003] Larminie, J., et Lowry, J. (2003). **Electrical Vehicle Technology Explained.** John Wiley & Sons, Ltd.
- [Larsson et al., 2009] Larsson, H., et Ericsson, E. (2009). **The effects of an acceleration advisory tool in vehicles for reduced fuel consumption and emissions.** *Transportation Research Part D: Transport and Environment*, 14(2):141–146.
- [Larsson et al., 2015] Larsson, V., Johannesson, L., et Egardt, B. (2015). **Analytic solutions to the dynamic programming subproblem in hybrid vehicle energy management.** *IEEE Transactions on Vehicular Technology*, 64(4):1458–1467.
- [LaValle, 2006] LaValle, S. M. (2006). **Planning algorithms.** Cambridge university press.
- [Li et al., 2015] Li, L., Yang, C., Zhang, Y., Zhang, L., et Song, J. (2015). **Correctional dp-based energy management strategy of plug-in hybrid electric bus for city-bus route.** *IEEE Transactions on Vehicular Technology*, 64(7):2792–2803.
- [Li et al., 2011] Li, S., Li, K., Rajamani, R., et Wang, J. (2011). **Model predictive multi-objective vehicular adaptive cruise control.** *IEEE Transactions on Control Systems Technology*, 19(3):556–566.
- [Lin et al., 2004] Lin, C.-C., Peng, H., et Grizzle, J. (2004). **A stochastic control strategy for hybrid electric vehicles.** In *American Control Conference, 2004. Proceedings of the 2004*, volume 5, pages 4710–4715. IEEE.
- [Luu, 2011] Luu, H. (2011). **Développement de méthodes de réduction de la consommation en carburant d'un véhicule dans un contexte de sécurité et de confort: un compromis entre économie et écologie.** PhD thesis, Thèse doct. Université d'Evry Val d'Essonne.
- [Martinez et al., 2007] Martinez, J.-J., et Canudas-de Wit, C. (2007). **A safe longitudinal control for adaptive cruise control and stop-and-go scenarios.** *IEEE Transactions on control systems technology*, 15(2):246–258.
- [Maurer, 2014] Maurer, M. (2014). **Forward collision warning and avoidance.** In Eskandarian, A., editor, *Handbook of intelligent vehicles*, chapter 25, pages 659–683. Springer.
- [Milanés et al., 2012] Milanés, V., Villagrà, J., Godoy, J., et González, C. (2012). **Comparing fuzzy and intelligent pi controllers in stop-and-go manoeuvres.** *IEEE Transactions on Control Systems Technology*, 20(3):770–778.

- [Ming, 1997] Ming, Q. (1997). **Sliding mode controller design for abs system**. PhD thesis, Virginia Tech.
- [Mollenhauer et al., 2010] Mollenhauer, K., et Tschöke, H. (2010). **Handbook of Diesel Engines**. Springer.
- [Murphey, 2008a] Murphey, Y. (2008a). **Intelligent vehicle power management: An overview**. In *Computational Intelligence in Automotive Applications*, pages 169–190. Springer Berlin Heidelberg.
- [Murphey, 2008b] Murphey, Y. L. (2008b). **Intelligent vehicle power management: An overview**. In *Computational Intelligence in Automotive Applications*, pages 169–190. Springer.
- [Musardo et al., 2005] Musardo, C., Rizzoni, G., Guezennec, Y., et Staccia, B. (2005). **A-ecms: An adaptive algorithm for hybrid electric vehicle energy management**. *European Journal of Control*, 11(4):509–524.
- [Ouddah et al., 2018] Ouddah, N., Adouane, L., et Abdrakhmanov, R. (2018). **From offline to adaptive online energy management strategy of hybrid vehicle using pontryagin's minimum principle**. *International Journal of Automotive Technology*, 19(3):571–584.
- [Ouddah et al., 2017] Ouddah, N., Adouane, L., Abdrakhmanov, R., et Kamal, E. (2017). **Optimal energy management strategy of plug-in hybrid electric bus in urban conditions**. In *International Conference on Informatics in Control, Automation and Robotics (ICINCO)*, Madrid-Spain.
- [Ozatay et al., 2014a] Ozatay, E., Onori, S., Wollaeger, J., Ozguner, U., Rizzoni, G., Filev, D., Michelini, J., et Di Cairano, S. (2014a). **Cloud-based velocity profile optimization for everyday driving: A dynamic-programming-based solution**. *Intelligent Transportation Systems, IEEE Transactions on*, 15(6):2491–2505.
- [Ozatay et al., 2014b] Ozatay, E., Ozguner, U., Michelini, J., et Filev, D. (2014b). **Analytical solution to the minimum energy consumption based velocity profile optimization problem with variable road grade**. In *World Congress*, volume 19, pages 7541–7546.
- [Panday et al., 2014] Panday, A., et Bansal, H. O. (2014). **A review of optimal energy management strategies for hybrid electric vehicle**. *International Journal of Vehicular Technology*, 2014.
- [Paynter, 1961] Paynter, H. (1961). **Analysis and design of engineering systems**.
- [Pei et al., 2013] Pei, D., et Leamy, M. J. (2013). **Dynamic programming-informed equivalent cost minimization control strategies for hybrid-electric vehicles**. *Journal of Dynamic Systems, Measurement, and Control*, 135(5):051013.
- [Puterman, 2014] Puterman, M. L. (2014). **Markov decision processes: discrete stochastic dynamic programming**. John Wiley & Sons.
- [Rakha et al., 2011] Rakha, H., et Kamalanathsharma, R. K. (2011). **Eco-driving at signalized intersections using v2i communication**. In *Intelligent Transportation Systems (ITSC), 2011 14th International IEEE Conference on*, pages 341–346. IEEE.

- [Ripaccioli et al., 2010] Ripaccioli, G., Bernardini, D., Di Cairano, S., Bemporad, A., et Kolmanovsky, I. (2010). **A stochastic model predictive control approach for series hybrid electric vehicle power management.** In *American Control Conference (ACC), 2010*, pages 5844–5849. IEEE.
- [Romaus et al., 2010] Romaus, C., Gathmann, K., et Böcker, J. (2010). **Optimal energy management for a hybrid energy storage system for electric vehicles based on stochastic dynamic programming.** In *Vehicle Power and Propulsion Conference (VPPC), 2010 IEEE*, pages 1–6. IEEE.
- [Rousseau, 2008] Rousseau, G. (2008). **Véhicule hybride et commande optimale.** PhD thesis, École Nationale Supérieure des Mines de Paris.
- [Saerens et al., 2013] Saerens, B., Rakha, H., Diehl, M., et Van den Bulck, E. (2013). **A methodology for assessing eco-cruise control for passenger vehicles.** *Transportation research part D: transport and environment*, 19:20–27.
- [Salmasi, 2007] Salmasi, F. R. (2007). **Control strategies for hybrid electric vehicles: Evolution, classification, comparison, and future trends.** *IEEE Transactions on vehicular technology*, 56(5):2393–2404.
- [Schaltz, 2011] Schaltz, E. (2011). **Electrical vehicle design and modeling.** INTECH Open Access Publisher.
- [Schouten et al., 2002] Schouten, N. J., Salman, M., Kheir, N., et others (2002). **Fuzzy logic control for parallel hybrid vehicles.** *Control Systems Technology, IEEE Transactions on*, 10(3):460–468.
- [Shakouri et al., 2014] Shakouri, P., Czczot, J., et Ordys, A. (2014). **Simulation validation of three nonlinear model-based controllers in the adaptive cruise control system.** *Journal of Intelligent & Robotic Systems*, pages 1–23.
- [Shen et al., 2015] Shen, D., Bensch, V., et Müller, S. (2015). **Model predictive energy management for a range extender hybrid vehicle using map information.** *IFAC-PapersOnLine*, 48(15):263–270.
- [Simpson et al., 2006] Simpson, A., et others (2006). **Cost-benefit analysis of plug-in hybrid electric vehicle technology.** Citeseer.
- [Sivak et al., 2012] Sivak, M., et Schoettle, B. (2012). **Eco-driving: Strategic, tactical, and operational decisions of the driver that influence vehicle fuel economy.** *Transport Policy*, 22:96–99.
- [Song et al., 2015] Song, Z., Hofmann, H., Li, J., Han, X., et Ouyang, M. (2015). **Optimization for a hybrid energy storage system in electric vehicles using dynamic programming approach.** *Applied Energy*, 139:151–162.
- [Sun et al., 2015a] Sun, C., Hu, X., Moura, S. J., et Sun, F. (2015a). **Velocity predictors for predictive energy management in hybrid electric vehicles.** *Control Systems Technology, IEEE Transactions on*, 23(3):1197–1204.
- [Sun et al., 2015b] Sun, C., Sun, F., Hu, X., Hedrick, J. K., et Moura, S. (2015b). **Integrating traffic velocity data into predictive energy management of plug-in hybrid electric vehicles.** In *American Control Conference (ACC), 2015*, pages 3267–3272. IEEE.

- [Suntharalingam et al., 2014] Suntharalingam, P., Yang, Y., et Jiang, W. (2014). **Hybrid electric vehicles**. In Emadi, A., editor, *Advanced electric drive vehicles*, chapter 12, pages 411–437. CRC Press.
- [Tang et al., 2015] Tang, L., Rizzoni, G., et Onori, S. (2015). **Energy management strategy for hevs including battery life optimization**. *IEEE Transactions on Transportation Electrification*, 1(3):211–222.
- [Tate et al., 2008] Tate, E., Harpster, M. O., et Savagian, P. J. (2008). **The electrification of the automobile: from conventional hybrid, to plug-in hybrids, to extended-range electric vehicles**. *SAE international journal of passenger cars-electronic and electrical systems*, 1(2008-01-0458):156–166.
- [Thoma et al., 1976] Thoma, J., et Perelson, A. S. (1976). **Introduction to bond graphs and their applications**. *IEEE Transactions on Systems, Man, and Cybernetics*, (11):797–798.
- [Tian et al., 2017] Tian, H., Wang, X., Lu, Z., Huang, Y., et Tian, G. (2017). **Adaptive fuzzy logic energy management strategy based on reasonable soc reference curve for online control of plug-in hybrid electric city bus**. *IEEE Transactions on Intelligent Transportation Systems*.
- [Tokekar et al., 2014] Tokekar, P., Karnad, N., et Isler, V. (2014). **Energy-optimal trajectory planning for car-like robots**. *Autonomous Robots*, 37(3):279–300.
- [Tulpule et al., 2009] Tulpule, P., Marano, V., et Rizzoni, G. (2009). **Effects of different phev control strategies on vehicle performance**. In *American Control Conference, 2009. ACC'09.*, pages 3950–3955. IEEE.
- [van Dixhoorn, 1980] van Dixhoorn, J. J. (1980). **Bond graphs and the challenge of a unified modelling theory of physical systems**. *Progress in Modelling & Simulation*, pages 207–245.
- [Van Keulen et al., 2010a] Van Keulen, T., de Jager, B., Foster, D., et Steinbuch, M. (2010a). **Velocity trajectory optimization in hybrid electric trucks**. In *Proceedings of the 2010 American Control Conference*, pages 5074–5079. IEEE.
- [Van Keulen et al., 2010b] Van Keulen, T., de Jager, B., Kessels, J., et Steinbuch, M. (2010b). **Energy management in hybrid electric vehicles: Benefit of prediction**. *IFAC Proceedings Volumes*, 43(7):264–269.
- [Venhovens et al., 2000] Venhovens, P., Naab, K., et Adiprasito, B. (2000). **Stop and go cruise control**. In *Seoul 2000 FISITA World Automotive Congress*, Seoul-South Korea.
- [Wada et al., 2011] Wada, T., Yoshimura, K., Doi, S.-i., Youhata, H., et Tomiyama, K. (2011). **Proposal of an eco-driving assist system adaptive to driver's skill**. In *Intelligent Transportation Systems (ITSC), 2011 14th International IEEE Conference on*, pages 1880–1885. IEEE.
- [White, 1982] White, H. (1982). **Maximum likelihood estimation of misspecified models**. *Econometrica: Journal of the Econometric Society*, pages 1–25.
- [Wirasingha et al., 2011] Wirasingha, S. G., et Emadi, A. (2011). **Classification and review of control strategies for plug-in hybrid electric vehicles**. *IEEE Transactions on vehicular technology*, 60(1):111–122.

- [Wouk, 1997] Wouk, V. (1997). **Hybrid electric vehicles**. *Scientific American*, 277(4):70–74.
- [Xu et al., 2011] Xu, G., Li, W., Xu, K., et Song, Z. (2011). **An intelligent regenerative braking strategy for electric vehicles**. *Energies*, 4(9):1461–1477.
- [Yan, 2014] Yan, F. (2014). **Internal combustion engines**. In Emadi, A., editor, *Advanced electric drive vehicles*, chapter 3, pages 27–42. CRC Press.
- [Yi et al., 2001] Yi, K., Hong, J., et Kwon, Y. (2001). **A vehicle control algorithm for stop-and-go cruise control**. *Proceedings of the Institution of Mechanical Engineers, Part D: Journal of Automobile Engineering*, 215(10):1099–1115.
- [Yu et al., 2015] Yu, K., Yang, J., et Yamaguchi, D. (2015). **Model predictive control for hybrid vehicle ecological driving using traffic signal and road slope information**. *Control theory and technology*, 13(1):17–28.
- [Yu et al., 2010] Yu, X., Shen, T., Li, G., et Hikiri, K. (2010). **Regenerative braking torque estimation and control approaches for a hybrid electric truck**. In *American Control Conference (ACC), 2010*, pages 5832–5837. IEEE.
- [Zeng, 2009] Zeng, X. (2009). **Improving the Energy Density of Hydraulic Hybrid Vehicle (HHV) and Evaluating Plug-in HHV**. PhD thesis, University of Toledo.
- [Zeng et al., 2017] Zeng, X., et Wang, J. (2017). **A stochastic driver pedal behavior model incorporating road information**. *IEEE Transactions on Human-Machine Systems*.
- [Zhang et al., 2004] Zhang, J., et Ioannou, P. (2004). **Integrated roadway/adaptive cruise control system: Safety, performance, environmental and near term deployment considerations**. *California Partners for Advanced Transit and Highways (PATH)*.
- [Zhang et al., 2014] Zhang, Y., Jiao, X., Li, L., Yang, C., Zhang, L., et Song, J. (2014). **A hybrid dynamic programming-rule based algorithm for real-time energy optimization of plug-in hybrid electric bus**. *Science China Technological Sciences*, 57(12):2542–2550.
- [Zhu et al., 2004] Zhu, Y., Chen, Y., Tian, G., Wu, H., et Chen, Q. (2004). **A four-step method to design an energy management strategy for hybrid vehicles**. In *American Control Conference, 2004. Proceedings of the 2004*, volume 1, pages 156–161. IEEE.



**Title: Sub-optimal Energy Management Architecture for Intelligent Hybrid Electric Bus: Deterministic vs. Stochastic DP strategy in Urban Conditions**

**Keywords:** Hybrid Electric Vehicle, Energy Management Strategy, Dynamic Programming based optimization, Stochastic Dynamic Programming, Stochastic MPC, Multi-Dimensional Database, ACC with Stop&Go.

**Abstract:**

This PhD thesis proposes Energy Management Strategies conceived for a hybrid electrical urban bus. The hybrid control system should create an efficient strategy of coordinating the flow of energy between the heat engine, battery, electrical and hydraulic motors. Firstly, a Deterministic Dynamic Programming (DDP) based approach has been proposed: simultaneous speed and powersplit optimization algorithm for a given trip (constrained by the traveled distance and time limit). This algorithm turned out to be highly time consuming so it cannot be used in real-time. To overcome this drawback, an Optimal Profiles Database based on DP (OPD-DP) has been constructed for real-time application. Afterwards, a Stochastic Dynamic Programming (SDP) technique is used to simultaneously generate an optimal speed profile and related powersplit strategy.

This approach takes into account a stochastic nature of the driving behavior and urban conditions. The formulated energy optimization problem, being intrinsically multi-objective problem, has been transformed into several single-objective ones with constraints using an  $\epsilon$ -constraint method to determine a set of optimal solutions (the Pareto Front). In urban environment, due to traffic conditions, traffic lights, a bus encounters frequent Stop&Go situations. This results in increased energy consumption during the starts. In this sense, a relevant Eco Adaptive Cruise Control with Stop&Go (eACCwSG) strategy brings the undeniable benefit. The algorithm smooths speed profile during acceleration and braking phases. One more important feature of this algorithm is the safety aspect, as eACCwSG permits to maintain a safety distance in order to avoid collision and apply a smooth braking. As it was mentioned before, smooth braking ensures passengers comfort.

**Titre : Architecture de gestion de l'énergie sous-optimale pour les bus électriques hybrides intelligents : stratégie basée DP déterministe versus stratégie basée DP stochastique en milieu urbain**

**Mots-clé :** Véhicule électrique hybride, Gestion de l'énergie, Programmation dynamique, Programmation dynamique stochastique, MPC stochastique, Base de données multidimensionnelle, ACC avec Stop&Go.

**Résumé :**

Cette thèse propose des stratégies de gestion de l'énergie conçues pour un bus urbain électrique hybride. Le système de commande hybride devrait créer une stratégie efficace de coordination du flux d'énergie entre le moteur thermique, la batterie, les moteurs électriques et hydrauliques. Tout d'abord, une approche basée sur la programmation dynamique déterministe (DDP) a été proposée : algorithme d'optimisation simultanée de la vitesse et de la puissance pour un trajet donné (limité par la distance parcourue et le temps de parcours). Cet algorithme s'avère être gourmand en temps de calcul, il n'a pas été donc possible de l'utiliser en temps réel. Pour remédier à cet inconvénient, une base de données de profils optimaux basée sur DP (OPD-DP) a été construite pour une application en temps réel. Ensuite, une technique de programmation dynamique stochastique (SDP) a été utilisée pour générer simultanément et d'une manière optimale un profil approprié de la vitesse du Bus ainsi que sa stratégie de partage de puissance correspondante. Cette approche prend en compte à la fois la nature stochastique du comportement de conduite et

les conditions de circulations urbaines (soumises à de multiples aléas). Le problème d'optimisation énergétique formulé, en tant que problème intrinsèquement multi-objectif, a été transformé en plusieurs problèmes à objectif unique avec contraintes utilisant une méthode  $\epsilon$ -constraint afin de déterminer un ensemble de solutions optimales (le front de Pareto).

En milieu urbain, en raison des conditions de circulation, des feux de circulation, un bus rencontre fréquemment des situations Stop&Go. Cela se traduit par une consommation d'énergie accrue lors notamment des démarrages. En ce sens, une stratégie de régulation de vitesse adaptative adaptée avec Stop&Go (eACCwSG) apporte un avantage indéniable. L'algorithme lisse le profil de vitesse pendant les phases d'accélération et de freinage du Bus. Une autre caractéristique importante de cet algorithme est l'aspect sécurité, étant donné que l'ACCwSG permet de maintenir une distance de sécurité afin d'éviter les collisions et d'appliquer un freinage en douceur. Comme il a été mentionné précédemment, un freinage en douceur assure le confort des passagers.